Sheffield Hallam University

A Sheffield Hallam University thesis

Large-Scale Method for Identifying the Relationships between Racket Properties and Playing Characteristics

Helen Elizabeth Karditsas

A thesis submitted in partial fulfilment of the requirements of Sheffield Hallam University for the degree of Doctor of Philosophy

June 2020

Collaborating Organisation: International Tennis Federation

Candidate Declaration

I hereby declare that:

1. I have not been enrolled for another award of the University, or other academic or professional organisation, whilst undertaking my research degree.

2. None of the material contained in the thesis has been used in any other submission for an academic award.

3. I am aware of and understand the University's policy on plagiarism and certify that this thesis is my own work. The use of all published or other sources of material consulted have been properly and fully acknowledged.

4. The work undertaken towards the thesis has been conducted in accordance with the SHU Principles of Integrity in Research and the SHU Research Ethics Policy.

5. The word count of the thesis is 35,027.

Name	Helen Elizabeth Karditsas
Award	PhD
Date of Submission	June 2020
Faculty	Health and wellbeing
Director of Studies	Simon Goodwill

I. Abstract

The application of advanced engineering in tennis has seen vast changes in playing styles, racket materials and racket design. Although previous researchers have investigated the effects of racket properties during and post ball-racket impacts, the studies focused on limited variation within racket properties. As regulators of the game, the International Tennis Federation monitor racket performance, however, standard laboratory test methods do not exist. The establishment of appropriate testing standards would further the understanding of the effect of racket properties, or racket property combinations, whilst reducing discrepancies between studies. This work aims to identify racket properties resulting in distinct behavioural characteristics through the development of a test protocol accurately simulating different forehand conditions found within the field of play.

Classification of the raw player testing data, previously collected from the 2006 Wimbledon Qualifying tournament, identified the characteristics of three specific forehand shots used within the field of play. The forehand shots were identified as either topspin or slice, each possessing different defining characteristics. The results from the player shot classification, five impact positions varying along the longitudinal and transverse axis, and a restrictive torque value representative of hand grip were used in the development of a laboratory test protocol capable of realistically and accurately simulating different forehand shots.

Using the developed test protocol for a typical topspin and slice forehand, a total of 39 rackets of varying properties and property combinations, were repeatedly impacted at the relative impact positions. A three-dimensional analysis, through the use of two Phantom High-Speed video cameras, recorded the experimental outputs within a fully calibrated control volume.

Reducing the complexity of the data, the experimental outputs were interpreted using clustering techniques, identifying clusters of rackets sharing similar behavioural characteristics. A total of four clusters of distinct behavioural characteristics were identified for both the topspin and slice forehand. Analysis of these clusters revealed that rackets of diverse property combinations can produce similar behavioural characteristics, indicating the importance of varying racket property combinations in this area of research.

The relationships between the behavioural clusters and subsequent racket properties were identified using multinomial logistic regression. (MNLR). Investigations revealed a complex dynamic relationship between racket properties and racket behaviour, such that racket behaviour, or performance, is dependent on its physical properties as both individual and interacting entities and are specific to shot type. Therefore, to gain a complete understanding regarding the effects of racket properties on the nature of the game, investigations consider the combined effects of racket properties and their relationship(s) to specific shot types found within the field of play.

Keywords: rackets, forehands, impact testing, clustering, multinomial logistic regression

II. Acknowledgements

I would like to thank my supervisors Dr Simon Goodwill, Dr Simon Choppin and Dr John Kelley for their advice and guidance throughout the duration of the project.

I am also very appreciative to the International Tennis Federation for supporting this project and would like to thank Jamie Capel-Davis and James Spurr for their additional support.

My extended thanks go to all the members of the Centre for Sports Engineering Research, both past and present, whose friendships and support have been invaluable.

I would also like to thank my family (especially Maria Karditsa) for the constant support, love and patience they have provided me throughout the PhD.

My final thanks go to Terry Senior, for being such a wonderful, reassuring and supportive person. I am very grateful to have had the opportunity to have learnt from him.

III.   Contents

IV. List of Figures

V.   List of Tables

VI.   Nomenclature

ACOR   Apparent coefficient of restitution

COM   Centre of mass

COP   Centre of percussion

COR   Coefficient of restitution

DFA   Discriminant function analysis

DLT   Direct linear transformation

FE   Finite element

FEA   Finite element analysis

fps   Frames per second

GSC   Geometric stringbed centre

ITF   International Tennis Federation

MNLR   Multinomial logistic regression

MOI   Moment of inertia

NP   Node point

PC   Principal component

PCA   Principal component analysis

RDC   Racket diagnostic centre

Roman Letters

d   Perpendicular distance from the axis to the line of the action force (mm)

F_1, F_2, F_3, F_4	Applied forces (N)
I_p	Twistweight
I_s	Swingweight
$M_1 \ M_2 \ M_3 \ M_4$	Moment force (Nm)
r	Pearson's Correlation
R	Distance of impact from the x-axis (m)
S	Distance of impact from the y-axis (m)
T	Distance of impact from the z-axis (m)
(U, V)	Image coordinates
V_{Imo}	Resultant impact velocity (m/s)
V_m	Vector mean
V_x, V_y, V_z	Relative component velocities (m/s)
V_{xr}, V_{yr}, V_{zr}	Racket component velocities (m/s)
V_{xb}, V_{yb}, V_{zb}	Ball component velocities (m/s)

Greek Letters

α	Inbound playing angle relative to normal (˚)
$α_2$	Rebound playing angle relative to normal (˚)
β	Inbound offset angle relative to the perpendicular (˚)
$β_2$	Rebound offset angle relative to the perpendicular (˚)
μ	Coefficient of friction
τ	Torque (Nm)

ω_b Ball spin (rad/s)

ω_{xr}, ω_{yr}, ω_{zr} Angular racket velocities (rad/s)

Tennis rackets are typically developed in the non-SI world to which the units used will be stated first followed by appended SI units in brackets throughout this thesis.

Αφιερώνω αυτήν την πτυχιακή στον αρχικό Δρ Καρδίτσα και στην μαμά μου για την υποστήριξη των ονείρων μας

1 Introduction

This thesis outlines a research project investigating the relationship between racket properties and rebound ball characteristics. The project involves a laboratory test methodology simulating distinct forehand shots found within the field of play and a number of rackets possessing a range of racket properties.

1.1 *Study Motivation*

The International Tennis Federation (ITF) is the world governing body of tennis and aims to protect the nature of the game through the establishment of rules and regulations (Coe, 2000).

Through the application of enhanced manufacturing techniques, tennis rackets have not only increased in dimension but have also been modified with lighter, stiffer materials (Miller, 2007). In fact, until the introduction of grommets in the 1960s, metal was not considered a practical alternative to wood and until the late 1980s hollow extruded aluminium and magnesium alloys were the material of choice for the marketed rackets. In 1975 Howard Head developed the aluminium Prince Oversize racket (Head, 1975). With a 50% larger strung area, this racket had a larger 'sweet spot' and such was the design that the game of tennis was effected, prompting the ITF to establish the first rules and regulations regarding the tennis racket in 1981 (Haake et al., 2007). These rules and regulations state:

"The racket shall not exceed 73.7 cm (29.0 inches) in overall length, and 31.7 cm (12.5 inches) in overall width. The hitting surface shall not exceed 39.4 cm (15.5 inches) in overall length, when measured parallel to the longitudinal axis of the handle, and 29.2 cm (11.5 inches) in overall width, when measured perpendicular to the longitudinal axis of the handle" ITF (2017a).

Although the established rules and regulations were a direct response to the effects of Howard Head's innovation, advanced manufacturing applications still provide the ability to push the boundaries of racket innovation. In order to

help the ITF successfully regulate the sport, researchers have investigated the rebound characteristics of a tennis ball, using high-quality quantitative data.

Much of the conducted investigative work focused on the impact between a ball and a racket within laboratory environments. In order to conduct such experiments effectively, efficiently and reliably, knowledge regarding test parameters is vital. Test parameters must be representative of those found within the field of play to ensure results are applicable to 'real world' conditions. Although player testing data, collected at the 2006 Wimbledon Qualifying Tournament (Choppin, 2008), provides great insight into ball and racket kinematics found within the field of play, there are no indications regarding the racket kinematics of specific forehand shots. Categorisation of the forehand data, into groups of similar shot conditions, will provide for realistic simulation of different forehand shots within a laboratory-based environment.

Realistic shot conditions can be simulated by altering the resultant inbound ball velocity, the impact position on the racket face and the relative angle between the inbound ball and racket face. However, with no test standards, many investigations have been conducted with resultant inbound ball velocities and relative angles not representative of realistic shot conditions. Similarly, many investigations have also been limited to the results of one tennis racket with specific properties. Quantifying the behavioural characteristics (rebound ball spin, rebound resultant velocity, rebound playing angle and rebound offset angle) as a result of different racket properties for realistic forehand conditions would further advance knowledge regarding the influences of the rackets' combined properties on the rebound characteristics of a tennis ball (racket behaviour). Such knowledge would aid the ITF to effectively monitor and assess the effects of equipment development, thus preserving the balance between technology and tradition.

1.2 *Aims and Objectives*

The aim of this project was to ascertain the relationships between racket properties and distinct behavioural characteristics, for specific typical forehand shots.

The following objectives shall be met to achieve this aim:

1. Critically analyse existing literature in the field of ball to racket impacts relevant to this project.

2. Determine the racket kinematics associated with specific forehand shots, using data collected from the practice courts at the 2006 Wimbledon Qualifying Tournament.

3. Develop a test protocol, accurately and realistically simulating specific forehand shots in a laboratory-based environment.

4. Distinguish clusters of rackets possessing similar behavioural characteristics for each given forehand simulation.

5. Identify the fundamental relationships between racket properties and behavioural characteristics for each given forehand simulation.

2 Literature Review

2.1 *Introduction*

One of the earliest accounts of scientific research into the world of tennis was conducted in 1877 (Rayleigh, 1877). Since then, research into the understanding of interactions between a tennis ball and a tennis racket has greatly expanded, producing a large volume of literature on the physics of tennis. This research provides vital information to the ITF, contributing to the governance and regulation of the sport. However, interest in tennis as a scientific pursuit increased with the development of the Prince Oversize racket (Head, 1975). Such was its design that it altered the nature of the game, prompting the ITF to establish the first rules and regulations regarding the tennis racket in 1981 (Haake et al., 2007). Although the established rules and regulations were a direct response to the effects of Howard Head's innovation, advanced manufacturing applications still provide the ability to push the boundaries regarding racket innovation.

The major challenge of protecting the nature of tennis is ensuring an in-depth understanding of the full effects that racket property and property combinations have on the post-impact ball trajectory.

This study is an investigation into the impact between a tennis ball and a tennis racket for realistic forehand simulations. This chapter aims to critically analyse the current literature with respect to the intended study. This chapter starts with an investigation into the fundamental equipment of tennis (the ball, the stringbed and the racket), then moves onto the analysis of the simulation of realistic shot conditions in a laboratory environment for ball-racket testing. The final sections will look at earlier analysis of ball-racket impacts and the tools of use for this study.

2.2 *The Ball and the Stringbed*

2.2.1 **The Ball**

To ensure consistency and to regulate the sport, all balls must be approved by the ITF (ITF, 2017b). This involves the ball passing a series of tests including measurements of mass, size and bounce height. Within the 2000s three types of tennis balls were introduced, each possessing different pace ratings; Type 3, Type 2 and Type 1 tennis balls. Designed with a 6% larger diameter, the type 3 tennis ball, also referred to as the slow tennis ball, was designed to decelerate more as the ball travels through the air. A type 2 tennis ball, also referred to as the medium tennis ball, shares the same specifications as the balls prior to the 2000s. Finally the Type 1 tennis ball, also referred to as the fast tennis ball, was designed to be harder and bounce lower than that of type 2 or type 3 tennis balls. Prior to testing for approval, the balls must be acclimatised for 24 hours, at $20 \pm 2\,^{\circ}\text{C}$ and $60 \pm 5\%$ relative humidity and then compressed (ITF, 2017b).

When using tennis balls within a laboratory testing, it is essential that the ball properties remain as homogenous as possible. Miller & Messner (2003) studied the effect of wear on the coefficient of restitution (COR) (rebound ball velocity divided by inbound ball velocity) values through firing tennis balls at a solid surface at 20 and 40 m/s. To simulate wear, tennis balls were impacted at $15\,^{\circ}$ on a rough block at a resultant inbound velocity of 20 m/s. The COR of balls were measured after 50, 100 and 150 and 300 impacts. At a resultant inbound velocity of 20 m/s, little difference was observed in the COR for balls having impacted 50, 100 and 150 times. A difference was only noticed for balls of 300 repeated impacts. However, at 40 m/s a difference in COR was observed after the ball had undergone 50 to 100 impacts. In competitive play, the balls are changed every 9 games, with a total of 6 balls in play at one time. Miller argues that it cannot be assumed that 1 or 2 balls could have undergone approximately 100 impacts, therefore exhibiting different characteristics at higher velocities. To ensure consistency and realistic representation within future testing results, wearing of the ball is a parameter that must be deliberated, for which impacts should be kept below 50.

2.2.2 **The Stringbed**

In the early stages of lawn tennis, strings were manufactured from sheep intestine or serosa. Following WW2, sheep intestines were replaced by those of cows (ITF, 2018). The comparatively high cost and low durability of natural gut led to the development of strings formed from synthetic materials (Haines, 1993). Synthetic strings are usually manufactured from polyester, nylon, Kevlar or combinations of these materials, each possessing different properties.

Cross, Lindsey, & Andruczyk (2000) analysed the dynamic properties of 90 different strings. The stress/strain behaviour was monitored by attaching a load cell to a single string, which is attached to a tensioning rig. The string was preloaded at 60 lbs (267 N) tension. On a pivot, a 4.5 kg hammer was swung at the string. The inbound hammer velocity was measured at 2.63 m/s, whilst the rebound hammer velocity was measured at -2.5 m/s. Cross found that unlike the synthetic string, the stiffness of natural gut did not increase during impact. These results support the finding of Cadler et al. (1987). Cross et al. (2000) also monitored the creep of the strings, over time. This was achieved by loading a single string statically for a period of time and measuring the tension loss. The findings showed that some strings lost tension rapidly, such that in a matter of hours the stringbed tension can significantly decrease. Results also showed that after 100 s, the string tension and log(time) plot to have a linear relationship. Whilst the study produced by Cadler may reflect the behaviour of a strung racket better, through string isolation Cross was able to identify individual parameters. In doing so, Cross was able to eliminate many variables present in a complex interwoven stringbed.

Coaching knowledge advises strings to be tensioned at high values to increase control and at low values to increase power. Goodwill, Douglas, Miller, & Haake (2006) analysed the spin generation properties of nylon and polyester strings. Thirty identical rackets were strung at 60 lbs (267 N) tension with various nylon and polyester strings. Prior to testing the stiffness of the strings were measured and recorded to compare experimental results. The nylon and polyester strings had a measured stiffness between 150 - 220 and 230 -300 lb/in respectively (26-39 and 40-53 N/mm respectively). Balls were

fired at the string bed at an angle of 40° and 60° from the perpendicular and with a backspin rate of 100 and 400 rad/s. Results found that at impacts of 40° and 60° the polyester string generated more rebound spin and less rebound spin respectively. Such results were accredited to the stiffness and lateral deformation of the stringbed. For impacts of 40°, the stiffer polyester stringbed exhibited lower deformation and more spin generation through rolling. However, at 60° the polyester stringbed was similar to that of a rigid surface, causing the ball to slip throughout impact and thus generate less spin. The impact angles used within this study, however, are not representative of those found within the field of play which ranges from 14 to 33° (Choppin, 2008). It can, therefore, be concluded that the results of such extreme angles are not relevant to the real world.

Cross (2003) stated that when a steel ball bounces off the stringbed, the height and speed of the bounce is not affected by the stringbed tension. Regardless of stringbed tension, such results are due to the lack of deformation of the steel ball and thus results in the stringbed absorbing almost all of the energy from the impact. Leigh & Lui (1992) observed the bounce height of a pool ball when dropped onto the stringbed of a head clamped racket. The pool ball rebounded to 95% of its original dropping height. This demonstrates that the stringbed loses very little energy in deformation, thus making the stringbed very efficient.

2.3 *The Racket*

2.3.1 Tennis Racket History

Initially, lawn tennis rackets were manufactured by a single piece of ash, boiled and bent into the shape of a keyhole whilst still hot. As lawn tennis grew in popularity, manufacturers started using the latest materials and production techniques, moving away from small workshops to mass production. The 1930s saw the launch of the first multi-ply racket, the Dunlop Maxply, which was in production for the next 50 years. It was not until the 1960s that metal was seen as an alternative to wood, due to the difficulty in stringing a metal tennis racket. With the inclusion of grommets this issue was overcome and allowed

manufacturers to develop tennis rackets formed of metal (ITF, 2018). In 1975 Howard Head invented the Prince Oversize racket, manufactured from aluminium. The racket head was made 10 % wider, increasing the size of the rackets 'sweet spot' (discussed in Section 3.3.2) and reducing the twisting in the hand as a result of off-centre impacts (Haake, 2018; Head, 1975). The impact of this design, in fact, prompted the first rule change, regarding the racket, by the International Tennis Federation. Prior to 1981, any material could be used to construct a tennis racket of any shape or size. Currently, as stated by the (ITF, 2017a), the rules stand as follows:

'The frame of the racket shall not exceed 29.0 inches (73.7 cm) in overall length, including the handle. The frame of the racket shall not exceed 12.5 inches (31.7 cm) in overall width. The hitting surface shall not exceed 15.5 inches (39.4 cm) in overall length, and 11.5 inches (29.2 cm) in overall width.'

Currently, the majority of modern tennis rackets consist of composite lay-ups, allowing materials to be precisely placed for optimum weight distribution and stiffness. Modern rackets are lighter and stiffer, than the wooden or metal rackets were, and come in a variety of masses and sizes. Figure 1 shows an example of an early tennis racket, a traditional laminated racket and a modern composite tennis racket.

Figure 1 - Racket Examples through the Ages: Early Racket (Left), Traditional Laminated Racket (Centre) and Modern Composite Racket (Right)

Taraborrelli et al. (2019) investigated the development of the tennis racket, through the use of racket measurements and material classifications for

525 samples. Racket measurements included geometric, inertial and dynamic properties and the number of strings. In agreement to the findings of Haake et al. (2007), results showed that rackets predating 1970 were predominantly wood and were characterised by head areas below 0.05 m^2, masses greater than 350 g and racket natural frequencies below 120 Hz. Taraborrelli et al. also stated that rackets, postdating 1980, were found to be made from fibre-polymer composites possessing larger head sizes, lower masses and higher natural frequencies in comparison to their predecessors. Using principal component analysis (PCA), to reduce the dimensionality of the number of variables, indicated that the variances observed in the measured racket properties to be significantly affected by material. It was concluded that early rackets were constrained by the limitations of wood, and with the move to composites allowed for the observed increase in head size and natural frequency. Composite rackets offer limited damping and further advancements to the tennis racket could come from automated production using materials possessing higher damping.

2.3.2 Sweet Spots

The sweet spot is a well-known term commonly referred to in published and marketing research. There is no set definition for this term due to the various claims as to its position on the racket face and what job the sweet spot actually does. The term sweet spot started to become a commonly used term, within tennis, after the development of the Prince Oversize racket by Howard Head in 1974.

Brody (1979) originally defined the sweet spot as the centre of percussion (COP). The COP is the point on the racket face where an impact will produce no reactive shock at the pivot; in this case the player's wrist. Brody also presented that the distance of the COP can be calculated from the rackets centre of mass (COM):

$$b = \frac{I}{a\,M} \qquad\qquad\qquad\qquad\qquad\qquad\qquad\qquad \textbf{[1]}$$

where I is the moment of inertia, a is the location where the racket is gripped, and M is the mass of the racket.

It can be seen by Equation 1 that the COP is not only dependent on the mass and moment of inertia of the racket but is also dependent on where the racket is gripped.

Hatze (1998) argued against such an analysis due to its simplicity. Hatze (1994) had earlier presented that during play a tennis player is more likely to hit the racket's node point. The impact locations of nine tennis players were recorded using high-speed video and a probability density function calculated according to the results. The results found that 80% of the recorded impacts were located at a region centred on the node point of the racket face. Although players aim to strike the ball at the racket's node point, players do so with little success for every impact thus resulting in impact location scatter. These results are in agreement with Choppin (2008) and Choppin et al. (2011). Player data from the 2006 Wimbledon Qualifying Tournament, recorded by Choppin (2008), provides great insight into the range of ball-racket impact parameters found within the field of play.

Brody (1981) described the node point according to the first mode of vibration. An impact upon the node point will excite the particular mode of vibration to which it corresponds. The first mode of vibration in tennis racket is larger than any higher mode, leading Brody to conclude that a player will not experience any vibration at the hand upon striking the ball. Brody (1995) confirmed the significance of the node point as a sweet spot through the measurement of the of handle vibrations. Striking the stringbed at various locations along the longitudinal axis, vibrations were measured through the use of a piezoelectric transducer placed on the racket handle. Figure 2 shows the measured handle vibrations at various impacts along the racket's longitudinal axis. Results identified the node point to be close to the centre of the stringbed.
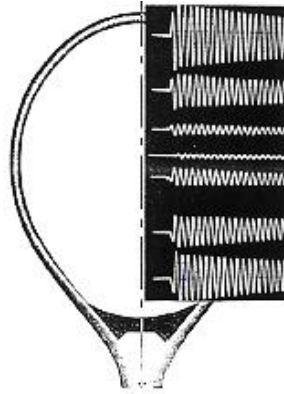
Figure 2 - Measured Handle Vibrations at Various Impact Location along the Racket's Longitudinal Axis (Brody 1981)

The third sweet spot was defined by Head (1975). This sweet spot is considered to be the point on the racket stringbed which results in the highest rebound ball velocity. Head argued that this sweet spot would be found at the area on the racket stringbed with a high apparent coefficient of restitution value. ACOR values are measured from ball velocity alone, thus resulting in such values to be relevant in cases of a stationary racket being struck by a moving ball; to which such conditions are never experienced during competitive play. Whilst Cross (1997) acknowledged the existence of such a point on the racket, he also acknowledged the existence of a point on the racket face for which rebound ball velocity would be zero. This point was referred to as the dead spot of the racket, for which its location is illustrated in Figure 3. Brody and Roetert (2004) expressed that the dead spot can also act as a sweet spot on the racket. When impacting a stationary tennis racket at its dead spot the ball stops and the racket quickly recoils. However, for conditions of a stationary tennis ball and a moving tennis racket, the reverse is true; the racket stops and the ball accelerates. This condition can be found during a serve. At the peak of the ball toss, the ball is effectively stationary and with the amount of racket movement towards the ball, higher velocities are found towards the tip. Cross (1997), therefore, stated that the dead spot should be exploited during the serve when the ball is at its peak and the tip of the racket possesses considerably higher velocities.

Choppin (2013) investigated the nature of the power point in tennis. Originally defined by Head (1975), the power point is an impact location which

maximises rebound ball velocity. A series of static racket impact tests and a surface polynomial fitting model were used to simulate four different shot types: a laboratory shot, a flat shot, an average shot and a wristy shot. Increasing the amounts of angular velocity, the 'power point' for each shot was identified. Through the use of a rigid body model, the ideal point was defined for each shot type. The ideal point is the point which theoretically produces maximum rebound ball velocity. Comparison of theory with experiment indicated that the closer the ideal point is to the racket node point, the smaller the difference between the ideal point position and the location of the maximum rebound ball velocity.

From this analysis, it is apparent that the sweet spot identifies the point on the racket face which results in maximum rebound ball velocity or minimum discomfort to the player's hand. The relative position of each discussed sweet spot is shown in Figure 3, as taken from Kotze, Mitchell, & Rothberg (2000).
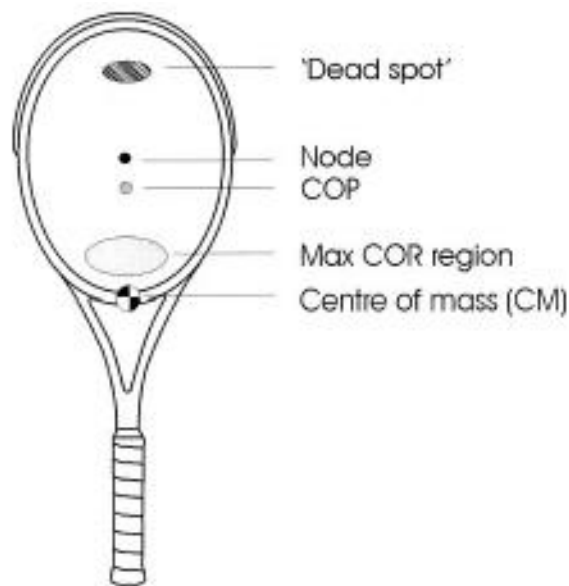
Figure 3 - The Relative Locations of the Discussed Sweet Spots (Choppin 2008)

2.4 *Effects of Racket Properties*

2.4.1 **Mass and Balance Point**

Haake et al. (2007) outlined the progression of racket properties such as mass, balance point, fundamental frequency and racket head sizes using 150 tennis rackets from 1870 to 2007. Results found that the natural frequency of

tennis rackets had increased since 1870, whilst the mass of tennis rackets had decreased. Such changes are a result of advancements in both the manufacturing process and the materials in use. The largest changes in racket frequency and mass can be seen to have occurred after the 1970s.
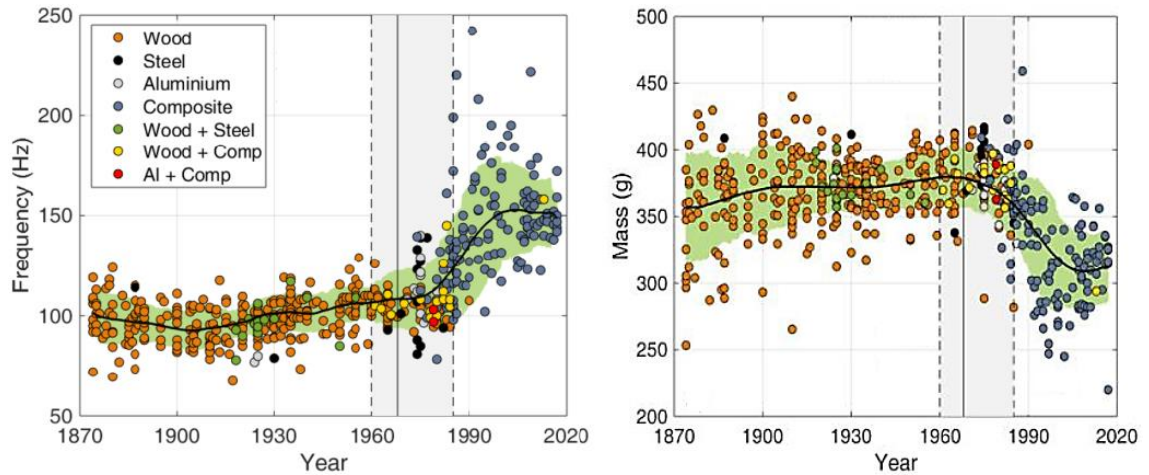
Figure 4 - Racket Property Changes from 1870-2020 for a) Frequency and b) Mass (Taraborrelli et al., 2019a)

Spurr & Downing (2007) investigated the relationship between racket 'power' and fundamental frequency. The fundamental frequencies of 47 rackets were obtained, ranging between 130 - 180 Hz. These results are in agreement with those obtained by Haake et al. (2007). Using the ITF power machine, three stringbed locations were used to simulate an impact. The ITF power machine measures the power of a tennis racket. The machine simulates a player's serve and speed gates are used to measure the post-impact ball velocity (Goodwill, Haake, & Miller, 2007). The impact locations were 75 mm (tip), 150 mm (centre) and 225 mm (throat) from the tip of the racket. The velocity of the racket was defined at the location on the stringbed which has a radius of 700 mm from the pivot point (Goodwill, Haake, et al., 2007). Thus, the resultant velocity between the racket and the ball would be highest for impacts towards the tip and lowest for those at the throat. The overall results showed no correlation between fundamental frequency and the rebound ball velocity for impacts along the longitudinal axis. This is in agreement with Haake et al.'s (2007) conclusion, that racket stiffness has only a small effect on the speed of serve. Haake et al. concluded that a rackets mass and balance point has a larger effect on the speed of serve. Testing a selection of rackets with a wider range in properties,

resulting in a wider range of natural frequencies, may result in a stronger correlation with power.

Allen (2009) and Allen et al. (2011) investigated the effects of mass, balance point and structural stiffness on a forehand shot. Impacts were simulated at six different locations upon the string-bed, an impact angle of 20° and with an inbound velocity and spin of 35 m/s and 300 rad/s respectively. Results indicated that racket mass has a relatively high influence on the rebound ball characteristics. As the mass of the racket went from low to high, rebound ball velocity increased considerably for all six impact positions. More specifically, the difference in rebound ball velocity was found to be approximately 3.5 m/s, for all impact locations between the heaviest and lightest tested rackets. Though a decrease in racket mass resulted in a decrease in rebound ball spin, it resulted in an increase in rebound angle in both the horizontal and longitudinal axis. Findings also indicate that the use of a head-heavy racket will result in a faster rebound velocity, larger rebound spin rates and acuter rebound angles in both the horizontal and longitudinal axis. For impacts occurring at the Geometric String Centre (GSC), a head-heavy racket is likely to result in higher rebound ball velocities and spin rates than a head-light racket possessing the same mass.

2.4.2 Frame Stiffness

Frame stiffness can be altered through the use of stiffer materials or changes in its geometry. A racket's resonant frequency of vibration is a function of its structural stiffness, as well as mass distribution (Cross, 1999). Haake et al. (2007) analysed the fundamental frequency of rackets from 1870 to 2007 and reported frequency values of approximately 80 to 120 Hz for pre-1970 rackets, whereas modern rackets were found to have frequency values of 100 to 180 Hz. Haake et al. (2007) also reported the respective change in mass as frequency increased. Thus, the evolution of rackets, from wood to composite, resulted in lighter and stiffer rackets.

Allen et al. (2009) found frame stiffness, for impacts at and around the node point, to have virtually no effect on ball rebound characteristics. This is due to limited or no excitement of the fundamental mode of vibration, for

impacts at or close to the node point of the racket. However, for impacts away from the node, more specifically closer to the tip of the racket, stiffer rackets are found to experience lower vibrational energy losses; where the racket's effective mass is found to be greatest (Goodwill and Haake, 2003; Allen et al., 2009; Cross and Nathan, 2009).

Allen et al. (2011) applied finite element techniques to investigate the effects of frame stiffness on a spinning ball for oblique impacts. The findings showed a 9% increase in ball rebound velocity going from rackets with low stiffness to high stiffness (96 Hz and 253 Hz respectively). This included impacts up to 85 mm from the stringbed centre. Although an increase in ball rebound velocity was reported, stiffness was found to have no clear effects on rebound angle or spin of the ball.

A racket with greater stiffness can increase rebound ball velocity (Cross, 2000) and accuracy (Bower & Sinclair, 1999); defined as the initial angle of the rebound ball relative to the intended target (Allen et al., 2016). However, elite players aim to strike the node point or close to the node point during a groundstroke, due to the reduction of vibrations felt to the hand and/or reductions of clipping the racket frame. As a result, the effects of frame stiffness are small on groundstrokes but are greater for serves which are typically struck away from the node and towards the tip of the racket.

2.4.3 Inertial Properties

The inertial properties of a racket are important due to their effect on shot performance and their interaction with stroke mechanics. Transverse moment of inertia, also known as 'swingweight'(I_s), is the resistance to rotation of the racket about an axis through the grip. A racket's swingweight simply refers to the difficulty in swinging the racket. For a given force, a racket with low swingweight will have greater acceleration than a racket with high swingweight. Polar moment of inertia, also known as 'twistweight' (I_p), is the resistance to rotation of the frame about its longitudinal axis. A racket with a greater polar moment of inertia will have greater resistance to angular rotation of the frame about its longitudinal axis. Polar moment of inertial is also approximately 20 times smaller than the transverse moment of inertia (Brody et al., 2002).

Cross and Nathan (2009) used data from 133 rackets, with a range of swingweights from 0.026 to 0.038 kg·m^2, and showed that ball rebound velocity increased with swingweight for perpendicular impacts 0.16 m from the racket tip. Cross (2010) also used the same impact speed and found that the error in the rebound ball angle is normally negligible, irrespective of the value of the polar moment. However, one main advantage found by Cross was as twistweight increased, ball rebound velocities also increased for normal off-axis impacts.

Allen et al. (2011) used finite element analysis to investigate the effects of racket mass and the position of the centre of mass (COM), for oblique impacts with a spinning ball. Alteration of the mass or balance point of a racket consequently alters the transverse and polar moment of inertia, therefore Allen et al. tested rackets with different swingweights and twistweights. Results found that with an increase in racket mass (from 279 g to 418 g), ball rebound velocity and spin increased by 37% and 23%, respectively. Allen et al. also investigated the effect of racket mass COM position (i.e. balance point) for oblique impacts and found that as the COM moved from 29.9 to 39.6 cm from the butt, rebound ball velocity and topspin increased by 31% and 23% respectively.

Taraborrelli et al. (2019b) assessed the accuracy of mathematical models for the transverse moment of inertia used by Allen et al. (2018), and two models of polar moment of inertia. Using 416 different rackets, this process identified the parameters influencing the moments of inertia, whilst quantifying their effects. Results showed the models to estimate, within -4 to 5 % and -11 to 12 %, the moments of inertia about the butt and longitudinal axis respectively. Though a stepwise linear regression model indicated that the mass and the location of the COM (balance point) had the largest effect on the transverse moment of inertia, overall racket length and handle length were also found to significantly influence the transverse moment of inertia. Similarly, racket head width was found to largely influence the polar moment of inertia of a racket, followed by racket mass, COM location, head length, and overall racket length. Taraborrelli et al. concluded that the MOI models can be useful tools to quickly characterise a number of diverse rackets or monitoring trends but traditional

measurement techniques are recommended for racket behavioural investigations.

2.5 *Player Testing*

When undertaking laboratory experiments, it is vital in ensuring that the conditions are representative of those found within the field of play. Player testing during match play conditions is considered to be an appropriate method of determining ball and racket kinematics.

2.5.1 Shot Characteristics

Bower and Cross (2005) investigated the effect of string tension during player testing. The players returned balls fed to them by a tennis ball machine, using three identical rackets strung at three different tensions; 40 lbs, 51 lbs and 62 lbs (178, 227 and 276 N). The mean rebound ball velocity, measured by a radar gun, was found to be 30.1 ± 2.9 and 28.9 ± 2.4 m/s for male and female tennis players respectively. Results also found that the rebound ball velocity was slightly lower for the rackets possessing a higher string tension. These findings were in agreement with previous authors conclusions (Brody et al., 2002; Cross & Lindsey, 2005; Goodwill & Haake, 2004; Haake, Carré, & Goodwill, 2003). Bower and Cross predicted the ball would leave the racket at a greater angle with respect to the racket normal, for lower strung tensions, travelling further and creating the sense of increased power. For lower stringbed tensions, player testing results identified that the greater velocities and angles resulted in more court impact locations beyond the baseline. For high stringbed tensions, more shots were found failing to clear the net.

Knudson and Blackwell (2005) measured forehand topspin groundstrokes of seven elite US players. The players were asked to simulate play, and their shots were recorded using high-speed video cameras. Upon impact, the mean racket linear velocity was found to be 24.3 ± 1.5 m/s, at an angle of 27.5 ± 3.5˚ with respect to the racket's horizontal. The mean rebound ball velocity was 29.7 ± 1.7 m/s. Although this data provides an initial insight into realistic play conditions, spin rates were not measured.

Choppin et al. (2007a, 2007b, 2008) used a pair of synchronised high-speed video cameras to capture three-dimensional (3D) movement of the tennis racket and ball. This set up was used to record players at the 2006 Wimbledon Qualifying Tournament, in which 19 players (9 male and 10 female) were recorded. Results showed impact velocities to be in the range of approximately 15 to 40 m/s, inbound ball spin to be around 230 rad/s and impact playing angles to vary between 14˚ to 33˚ (an angle relative to the racket face normal). Results also showed that players aim to strike the ball at the node point of a racket with low levels of success for every impact. The average impact position and standard deviations were found to be 549.6 ± 31.7 mm from the butt of the racket, along the racket's central axis, and 1.7 ± 26.3 mm from the central axis of the racket.

Kelley et al. (2009) measured the ball spin rates during match play at the 2007 Wimbledon Qualifying Tournament. The ball spin rates were measured both prior and post-impact for the analysis of spin rate generation from the bounce and the player. Due to weather conditions, the number of recorded usable impacts for males and females were 54 from 4 players and 152 from 10 players respectively. The mean spin off the ground for males was found to be 325 ± 127 rad/s (3104 ± 1208 rpm) and 316 ± 76 rad/s (3024 ± 721 rpm) for females.

Player testing results provide valuable insight into the range of impact characteristics found within the field of play. However, tennis is regarded as a technical sport to which both forehand and backhand groundstrokes can be executed as flat, topspin or slice groundstrokes. Clustering of the raw player testing data into sets of similar shot types would enable further development of test protocols for the simulation of different types of forehand or backhand shots. Such would be the advancement that would allow future work to investigate the effects of equipment on different shot types found within the field of play.

2.5.2 Effect of Grip

In order to assess the performance of a tennis racket, controlled repeatable tests must be conducted. Although the most realistic impact

conditions would come from player testing, it is very difficult to achieve repeatable impact positions and racket velocities. Simulating a ball-racket impact is a complex task due to the combination of various racket angles and orientations as a result of the different hitting techniques used by each individual tennis player (Choppin et al., 2007b). For an impact system reduced to a ball and racket, the interface between the racket and player must be accurately simulated. In a laboratory environment, for a stationary racket, grip can be simulated by restricting the movement around the racket handle according to a representative restrictive torque value (Choppin, 2008).

Research presented by Peebles & Norris (1998) shows that the highest torque value one can expect from a human grip is approximately 10 Nm. Although this provides a maximum value regarding resistive torque for laboratory testing, a representative value during impact conditions has not previously been stated. Though others attempted to quantify grip forces exerted by a player when striking the ball, again, no statements of equivalent torque values had been made (Knudson, 1991; Knudson & White, 1989; Savage 2006).

Baker & Putnam (1979) compared handle clamped and freely standing racket conditions. Using high-speed video, ball impacts on a stationary freely supported and handle clamped racket were recorded. Different rackets and strings were tested, for which no effects were found on the resultant rebound ball velocity under clamped conditions. However, for a freely suspended racket, a noted difference was observed when impacting off the longitudinal axis. It was concluded that the observed change in ball trajectory was due to the large rotational displacements for freely suspended racket conditions during impact.

Elliott (1982) experimentally tested the effect of grip firmness with the use of a pneumatic arm. Three levels of grip firmness were used within the experiment; light, medium and tight. A college tennis player was requested to grip a racket, equipped with force transducers, lightly, moderately and tightly; thus determining the corresponding forces for the three grip levels. Four impact locations were impacted; GSC, ± 5 cm laterally from the GSC and 5 cm transversely from the GSC with regard to the racket's longitudinal axis. For

central impacts, a 7% increase in rebound ball velocity was observed at tight grip levels compared to light grip levels. This was determined to be statistically insignificant. However, for off-axis impacts, a 20% increase in rebound ball velocity was found at tight grip levels. It was therefore concluded that the level of grip firmness insignificantly affects rebound ball velocity for impacts at the GSC, but significantly affects rebound ball velocity for impacts off the longitudinal axis.

Choppin et al. (2010) investigated the effects of grip tightness on impacts off the longitudinal axis for forehand shots in tennis. Testing was conducted using his previously developed impact test rig (Choppin, 2008). The racket mount consists of a handle clamp, limiting clutch and a universal joint. The limiting clutch was included to replicate the rotational restrictions about the longitudinal axis, as that set by a player when griping their racket. Three torque values, defined as different levels of grip tightness, were obtained and tested; 0 Nm (no grip), 7.5 Nm (firm grip) and 15 Nm (extremely tight grip). These values were obtained from 'Adultdata: The Handbook of Adult Anthropometric and Strength Measurements: Data for Design Safety' of a hand gripping an object of similar shape to that of a racket handle; a jam jar lid (Peebles & Norris, 1998). A range of inbound ball velocities, impact angles and impact positions, along both the longitudinal axis and transverse axis of the racket, were tested. The ranges of these properties were 16 to 40 m/s, 0 to 30°, 0 to 64 mm from the longitudinal axis and -100 to 115 mm from the GSC respectively. Results found that grip tightness did not affect the resulting rebound ball velocity for impacts on and off the longitudinal axis. However, it was found that gripping the racket handle with a torque above 0 Nm reduced the rebound ball angle by approximately 2° for impacts off the longitudinal axis. Relating these results to the field of play, it was concluded that a tight grip reduces the effects of off-axis impacts. Though the inbound parameters are consistent with player testing data, there was no indication of the use of inbound ball spin, whilst also limiting the off-axis impacts to one side of the racket face only.

Chadefaux et al. (2017) analysed the racket dynamic behaviour as a function of the applied grip force. This study uses five commercial rackets, of different mass, head size, length and moment of inertia. Modal analysis was

conducted when "slight", " medium" and "strong" grip conditions were applied. Using high-resolution methods (ESPRIT: estimation of signal parameters via rotational invariance techniques), modal frequencies and damping factors were obtained. Results indicate that the stronger the grip force applied, the frequencies for the first two modes decreased, whilst both the damping factors and the frequency for the first torsional mode increased. Chadefaux et al. also designed a phenomenological hand-gripped racket model, which examines the racket dynamic behaviour variations and allows for the prediction of the first modal frequency for a given racket and grip force. These results combined with the model revealed how the force applied by a player's grip can drive the racket dynamic behaviour, underlining the necessity of taking the player into account and hence, accurate simulation of a players grip in a laboratory environment to be vital.

2.6 *Data Collection of Ball to Racket Impacts*

To obtain ball velocities, spin rates and impact positions from laboratory-based impact testing, the ball and racket will need to be tracked over many impacts. The literature discusses the use of high-speed camera solutions and digitisation methods.

2.6.1 **High-Speed Camera Methods**

Videogrammetry is a useful tool for collecting data both in the field and in laboratory testing and is used within tennis research, whether two-dimensional or three-dimensional videogrammetry.

Two-dimensional analysis uses a single high-speed video camera for the recording of impacts. Though two-dimensional analysis may be advantageous for some impact scenarios, such as ball-stringbed interactions, this method limits data analysis to a single plane and also restricts investigations to ball-racket variations along the longitudinal axis.

Three-dimensional analysis uses two synchronised high-speed video cameras for the recording of ball-racket impacts. The use of three-dimensional analysis methods increases the amount of information obtained from testing, one of which is the measurement of depth. Though depth can be perceived

through the use of a single image, it cannot be measured without the use of a second image taken from a different angle. When impacting a realistically supported tennis racket, Choppin et al. (2008) suggest impacts will result in out-of-plane ball trajectories. Therefore, to accurately track the rebounding ball and to satisfy the overall objectives of this study three-dimensional analysis is necessary.

2.6.2 Camera Calibration

Three-dimensional analysis is a vital tool for data analysis of ball-racket impacts, providing a greater understanding of how the many variables in tennis can impact the game. For which, 2D coordinates of objects are extracted from the camera image and used to reconstruct the 3D location of the objects in a local coordinate system. To ensure accurate 3D reconstruction, however, the system must be calibrated.

To calibrate the cameras for three-dimensional measurement, Papadopoulos et al. (2000) and Bray et al. (2006) used direct linear transformation (DLT) method, however, Choppin (2008) used the planar method of camera calibration using a checkerboard. Both methods of camera calibration require the use of a calibration object of a known length to ensure appropriate calculation of the calibration factor. In an internal report, Neil Whyld (2004) evaluated the use of direct linear transformation method (DLT) and the use of the planar method (checkerboard) for camera calibration, through comparing the measurement of reconstructed points of known positions. It was concluded that the checkerboard method was not only more practical but also produced more accurate results than that of the DLT. The full report can be reviewed in Appendix A within the work of Choppin (2008). The checkerboard, itself, is easy to accurately construct and scale accordingly, thus ensuring points are collected throughout the entirety of the impact area.

To produce an accurate planar method of calibration, cameras are calibrated individually to provide intrinsic parameters such as focal length, principal point and pixel skewness. Using the position of the checkerboard's top corner and the known size of each checked square, the intrinsic parameters can re-project the intersection points back onto the calibration image. The re-

projection error can then be calculated from the pixel discrepancy between the intersect point detected by the software and the re-projected intersection point and plotted in image coordinates (*U, V*) for every checkerboard. In doing so an average error is calculated. The intrinsic parameters, ultimately, describe image distortions due to the lens (radial distortion) and camera (tangential distortions). Spurr (2017) evaluated the planar method of camera calibration by comparing different image distortion models correcting for radial and tangential distortion. When corrected for radial image distortion only, the evaluation established the best performing calibration models and must be considered for future calibrations to ensure the optimum parameters are used and the calibration does not fail. With this information the cameras are then calibrated as a stereo system, giving extrinsic parameters which allow for the reconstruction of three-dimensional real-world coordinates from pairs of image coordinates.

2.6.3 Image Processing

Transformation of the video recordings into a single or series of images allows for the obtaining of measurements; otherwise known as digitisation. Digitisation of image coordinates (*U, V*) is a common measurement tool used to extract valuable point information. Combined with suitable calibrations, the extracted point information or *U, V* image coordinates can be reconstructed into real-world *X, Y, Z* coordinates. This reconstruction then allows for the calculation of displacement, velocity, and acceleration.

Spurr (2017) developed an automated ball tracking algorithm to facilitate large scale data collection and digitisation. The algorithm identifies the ball using a white pixel count and tracks the movement of the ball prior to and post-impact. The ball centroids are automatically digitised, recording the image's *U, V* coordinates. Using appropriate calibrations the image coordinates can then be reconstructed into three-dimensional coordinates. The algorithm was validated by comparison to manual digitisation and found a systematic error of -0.5 pixels. Although the systematic error was found to be greater than the repeatability of manual digitisation, for ball velocity calculations the effect of the error was found to be negligible. Spurr (2017) also modified the *SpinTrack3D* algorithm (Kelley, 2011), an automated spin rate and spin axis measurement

algorithm, to correct for perspective error when measuring ball spin from images. For a given ball position, the apparent angle was calculated using the cosine rule and the axis of rotation was calculated as the perpendicular vector to the plane defined by the camera and ball centroids. The apparent spin was subtracted from the measured spin and validated using Rodrigues' rotation formula. The previously observed ball centroid measurement error was also found to have a negligible effect in the calculation of apparent spin. The accuracy of the modified algorithm was also measured and found a mean error between 0.017 and 0.025 radians for the high-spin simulation.

Prior to automated digitisation, manual digitisation had been used by researchers, capturing the ball, the racket and the stringbed movements with the use of high-speed video cameras (Cottey, 2002; Sissler, 2011). Cottey (2002) manually digitised ball centroids, whilst adding reference lines to the ball centroid, to calculate ball velocity and spin rates. Using a second camera to record ball-stringbed interactions, Cottey measured the ball contact lengths and string movements also through manual digitisation. Manual digitisation is a valid process for the measurement of necessary data, however, digitisation of multiple points through many images is a time-consuming process prone to human error. Automated image processing is an efficient and effective solution to this issue.

2.7 *Impact between a Ball and Racket*

For the assessment of racket performance, researchers have conducted ball-racket impact testing, to which the complexity and accuracy of these tests have varied. Realistic shot conditions can be created experimentally by altering the following parameters: resultant inbound ball velocity, the impact position on the racket face and the relative angle between the inbound ball and racket face.

Due to limitations in equipment, investigations were limited to perpendicular impacts occurring along the longitudinal axis only. This can be seen through the work of Brody (1997), Goodwill & Haake (2001), Goodwill (2002). Brody (1997) analysed the effect of impact location along the longitudinal axis of a freely suspended racket. Using a simple method of

analysis, Brody measured found the ACOR to be dependent on impact location, for a resultant inbound ball velocity of 20 m/s (Figure 5). The resultant rebound ball velocity was found to be its lowest at the tip of the racket and highest near the racket throat. Testing at a range of resultant velocities would have provided further insight into the relationship between ACOR, impact location and resultant inbound ball velocity.
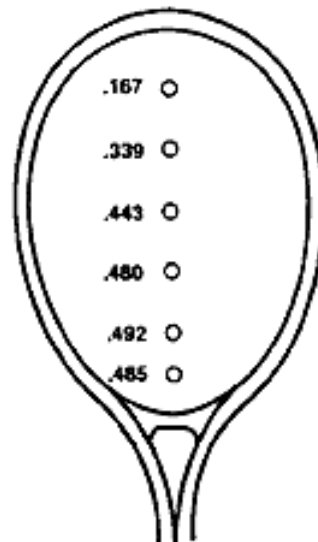
Figure 5 - Variation of ACOR with Impact Location as seen by Brody (1997)

Goodwill & Haake (2001) analysed the impact between a ball and a freely suspended tennis racket strung at 60 lbs (267 N) tension. Balls were fired perpendicularly at three distinct impact locations along the longitudinal axis; the GSC, 50 mm above and 50 mm below the GSC. The resultant inbound velocity of the balls was in the range of 14 - 32 m/s. Results identified maximum resultant rebound ball velocity at the throat region of the racket (-50mm) and minimum at the tip region. These results are in agreement of those found by Brody (1997).

Although an impact perpendicular to the racket face is a true representation of a flat tennis serve, typically in practice a player will perform an impact in which the racket is at an oblique angle to the ball when executing forehand shots (Choppin, 2008). Simulating oblique ball-racket impacts, in a laboratory environment, increases the complexity of the testing methodology. Reducing the complexity, through head clamping of the tennis racket and limiting impact locations to the GSC, researchers can investigate the mechanics

regarding the interaction between the tennis ball and the racket stringbed (Cross, 2003b; Haake, Allen, Jones, Spurr, & Goodwill, 2012; Nicolaides, Elliott, Kelley, Pinaffo, & Allen, 2013). Though this may be beneficial for ball-stringbed impact testing, this method of testing does not represent conditions found within the field of play.

Realistically simulating forehand shot conditions, for ball-racket impact testing, provides the opportunity to further the understanding regarding the interaction between a tennis ball and a tennis racket. In doing so, researchers then began ball-racket testing for oblique impacts.

Goodwill & Haake (2004) analysed an oblique impact of a tennis ball, possessing no spin, on a freely suspended tennis racket. Two string tensions were used within this study, 40 and 70 lbs (178 and 312 N) and the GSC was the only set impact location, however, there was no indication as to the measurement of the stated location. Whilst string tension was found to have no effect on the rebound spin or speed, rebound ball angle relative to the normal was found to increase with string tension. The conclusion that stringbed tension has no effect on rebound ball velocity is in direct contradiction to the previously stated common belief of a lower stringbed tension providing more power. Goodwill and Haake used a large inbound angle, relative to the stringbed normal, and thus resulting in a relatively small perpendicular velocity component. This then led to the prediction that a small inbound ball angle relative to the stringbed would result in a higher rebound ball velocity, for the lower stringbed tension. Player testing data also highlighted that the ball can have inbound spin rates of 300 - 550 rad/s prior to racket impact (Goodwill, Capel-Davis, Haake, & Miller, 2007; Kelley, 2011b). Therefore, testing would have been more representative of typical shot conditions if the ball had been fired with initial spin.

Choppin (2013) investigated the relevance of the ideal point using a series of static racket impact tests and a surface fitting model. The experimental impact tests, used to validate the model, were performed using a modified ball projection device . The racket was impacted at varying positions, incrementing from 0.06 to 0.25 m from the COM, along the longitudinal axis, in increments of

0.032m. At all impact locations, the resultant inbound ball velocity varied between 15 and 35 m/s, in increments of 5 m/s. For impact occurring above 0.2m from the COM, the BOLA launch velocity was increased to 50 m/s while maintaining 5 m/s increments. The results indicated that the closer the ideal point is to the racket node point, the smaller the difference between the ideal point and the location of the maximum resultant rebound ball velocity. Though results allowed for the simulation of different shot types, testing was limited to normal impacts along the longitudinal with no indication of inbound ball spin. Testing oblique spinning impacts would better represent different shot types found within the field of play (Choppin, 2008; Goodwill, Capel-Davis, et al., 2007; Kelley, 2011).

Though impacts were conducted obliquely, impacts along the longitudinal axis are not a true representation of forehand shots. Choppin (2008) revealed that even the best of players will occasionally hit the ball off the racket's longitudinal axis and furthered the testing methodology for the simulation of oblique impacts occurring on and off the longitudinal axis.

Choppin (2008) fired balls onto a realistically supported stationary tennis racket. The resultant inbound ball velocity was incremented four times between 20 and 40 m/s and the angle was set to 0 and approximately 30 degrees. The impact position was altered incrementally 10 times along the longitudinal axis and 6 times along the transverse axis of the racket from the centre line. It was found, for impacts occurring at the centre of the racket, that with an increase in the initial impact velocity, rebound ball velocity increased linearly. As the impact position moves from the tip of the racket towards the throat, the rebound ball velocity correspondingly increases. Though rebound ball velocity was found to be higher for impacts at the throat than at the tip, as the impact position continued to incrementally approach the throat, rebound ball velocity began to decrease. It was concluded that this was a result of high frame vibrations. Choppin also found that as the impact position moves off the longitudinal axis, rebound ball velocity was found to decrease. The inbound impact angle and rebound angle were observed to be linearly related, with a consistently larger rebound angle in comparison to the inbound angle. This was concluded to be a result of the racket's rotation during an impact.

Oblique impact testing, occurring on and off the longitudinal axis, has since been used by many other researchers whether in a laboratory environment or through the use of finite element analysis (FEA) (Allen, 2009; Allen et al., 2009, 2011a; Choppin et al., 2010; Spurr, 2017).

Allen et al. (2011) used the previously validated finite element (FE) model of a freely suspended tennis racket and strings, by Allen et al. (2009), to determine the effects of three racket properties for oblique spinning impacts. The Impacts were simulated at six different impact locations, the GSC (0,0), (0, +60), (0, -60), (+60, 0), (+60, +60) and (+60, - 60) measured in mm; shown in Figure 6. The resultant inbound ball velocity and spin were simulated at 35 m/s and 300 rad/s respectively, at an impact angle of 20˚. These inbound parameters corresponded with the groundstroke player testing data collected by Choppin et al. (2008). Clear differences were found between impacts at the tip (0, +60) and the throat (0, -60), for all six simulated rackets. The mean rebound velocity was found to have decreased, with a mean rebound angle increase (angle from the normal) for tip impacts than for the throat impacts. For impacts occurring off the longitudinal axis, rebound ball velocity was found to have decreased, rebound angle increased, whilst also observing a decrease in rebound topspin. These results are also in agreement with Choppin et al. (2010). Although it was not discussed within this study, Allen (2009) also reported the longitudinal rebound angles (rebound offset angles) for the same simulations. For impacts occurring at the GSC and (+60, 0) the longitudinal rebound angle was found to be approximately zero. For impacts occurring both on and off the longitudinal axis, at the tip and throat, the offset rebound angle was found to increase negatively and positively respectively. Though simulations were representative of a typical groundstroke, without extensive testing, necessary assumptions regarding materials and the composite lay-ups of the materials were required to reduce the complexity of the finite element analysis. Though three racket properties were varied, the racket geometry remained constant. Through the development of methodological applications, it would be possible to include more racket geometries within the FEA software library. However, modelling of the individual geometries of the rackets requires a vast amount of time and resources.
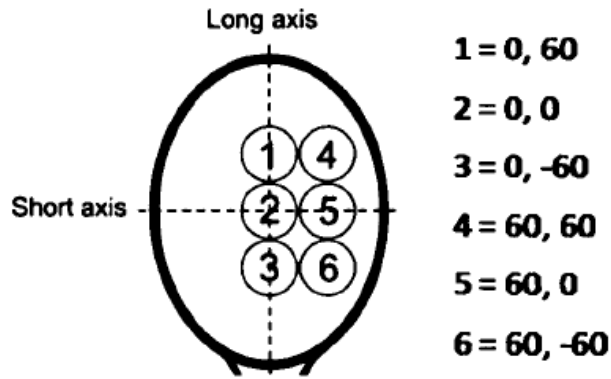
Figure 6 - Depiction of the Six Impact Locations Simulated by Allen et al. (2009)

Ball-racket impact testing has evolved from limited perpendicular impacts along the longitudinal axis to oblique impacts occurring on and off the longitudinal axis. This evolution allows for accurate and representative simulation of forehand shots in a laboratory environment, ensuring relevance of results to the 'real world'.

2.7.1 Testing Methodologies

The impact between a viscoelastic tennis ball and a tennis racket, for high impact velocities, is a complex non-linear system. A non-linear system is a system in which the change of the output is not proportional to the change of the input. More specifically, non-linear dynamic systems, such as deformation of a tennis ball during impact, describes the changes in variables over time which may appear unpredictable compared to a much simpler linear system. By acknowledging ball-racket impacts as non-linear dynamic systems we are able to determine dependent variables such as displacement, velocity, force and energy as a function of time, not only throughout the impact but also after the impact. Goodwill (2002) evaluated the linearity of ball stiffness to ball deformation for a simple visco-elastic model with one degree of freedom, for which a linear relationship had previously been assumed. However, for a time (t) of $t > 0.2$ ms, results found the value of ball stiffness to increase with impact velocity, thus implying the relationship between ball stiffness and ball deformation to be non-linear. A similar conclusion was also drawn regarding ball dampening and ball deformation; as impact velocity increased the value of ball dampening also increased. Sissler et al. (2014) also found a viscoelastic tennis

ball, consisting of a rubber core and covered in a felt material, to exhibit non-linear strain rate properties during impacts of high velocity. It is, therefore, essential when undertaking laboratory-based experiments that conditions are representative of those found within the field of play and in doing so, ensuring results are applicable to 'real world' conditions.

Realistic shot conditions can be simulated by altering the resultant inbound ball velocity, the impact position on the racket face and the relative impact angle between the inbound ball and racket face. Figure 7 illustrates the impact angle relative to the racket normal.
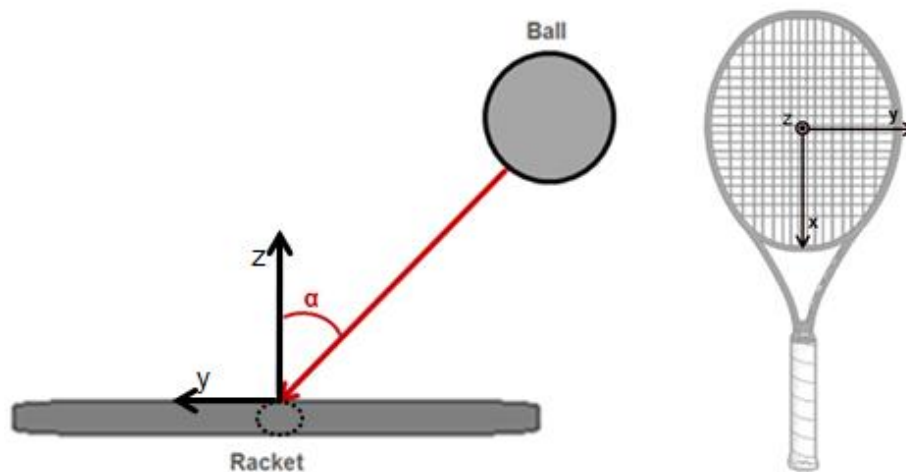
Figure 7 - Depiction of Impact Angle Relative to the Racket Normal

As discussed in Section 2.6, much work has been conducted over the years, investigating ball-racket impacts using laboratory-test methodologies. These tests are typically developed and applied by the ITF, researchers, and manufacturers, however, there are no standardised tests for the measurement of ball and tennis racket performances.

Table 1 shows a summary of the varying inbound parameters used for previous laboratory ball-racket impact testing. With no test standards, impact testing parameters are at the investigator's discretion, resulting in wide ranges and inconsistencies between conducted research.

Table 1 - Comparison of Used Laboratory Testing Methodologies from Different Publications

Author/s	Inbound Ball Velocity (m/s)	Inbound Ball Spin (rad/s)	Impact Angle to the Racket Normal (°)	Racket Head Impact Location (mm)	Number of Rackets
Goodwill & Haake (2004)	15 - 40	0	36	GSC	1
Spurr & Downing (2007)	35	n/a	0	Tip Centre Throat	47
Choppin (2008)	20 - 40	n/a	0, 30	10 Incremental impacts along longitudinal (tip - throat) 6 Incremental impacts along transverse from the centre line	1
Allen et al. (2009)	10 - 40	0	0	GSC Tip Throat Off-Centre	1
	20, 30	-500 - 100	25	GSC	
Cross and Nathan (2009)	29	n/a	0	Tip	133
Choppin et al. (2010)	16 - 40	n/a	0 - 30	0 - 64 (transverse) -100 - 115 (from GSC)	1
Haake et al. (2012)	25	0 - 400	40, 60	GSC	1
Nicolaides et al. (2013)	24	218	26	GSC	1

Choppin (2013)	15 - 35 50	n/a	0	60, 92, 124, 156, 188 220, 250 (from the COM)	1
Spurr (2017)	23, 25, 28, 30	200, 400	20	GSC (0, 0) (0, + 60) (0, - 60) (+ 60, 0) (+ 60, + 60) (+ 60, - 60)	1

Table 1 identifies that much of the previously conducted research is limited to one tennis racket of specific racket properties and for the ability to test more tennis rackets, researchers limited the number of testing parameters. Bishop (1995) described this phenomenon as '*the curse of dimensionality*'. Bishop states that as the number of parameters or dimensions, *'d'*, increases, the size of the input domain increases exponentially according to M^d, where M is the number of variations in each dimension.

Data collection in a laboratory-based environment can very quickly scale beyond reasonable and rational expectations. Therefore, to ensure representative and realistic simulation of forehand shots, on a range of rackets, for a large-scale data collection process, consideration of testing parameters and racket properties is vital.

A large-scale data collection ultimately results in a large-scale data set possessing multiple dimensions. Previous analysis has focused on modelling techniques for the prediction of racket 'behaviour' values (post-impact ball parameters) for multiple and potentially non-representative impact scenarios (Allen, 2009; Choppin, 2008; Goodwill, 2002; Spurr, 2017). However, these methods have been limited to the dimensionality of one tennis racket with specific properties. Testing a range of rackets, of varying racket properties, increases the dimensionality of the data set further than as seen by these previous researchers. Basheer & Hajmeer (2000) discussed how the use of

clustering techniques can reduce the number of dimensions of a large and complex data set, which can be applied for the clustering of racket behaviour.

Clustering analysis not only reduces dimensionality but also provides the opportunity to explore the relationships between racket behaviour and multiple racket properties and property combinations.

2.8 *Cluster Analysis*

Cluster analysis is a vital tool in Data Mining and is a multivariate technique which groups the observation variables into subsets, such that similar variables are grouped together, whilst dissimilar variables are placed in different groups. The variables are, therefore, arranged into a useful representation that characterises the sample of observations. Since the aim of cluster analysis is to discover a new set of categories, the intrinsic assessment of the new clusters and the clusters themselves are of interest (Rokach & Maimon, 2005).

Various mathematical algorithms can be used to achieve cluster analysis. These methods vastly differ in their interpretation of what constitutes a cluster and their efficiency to identify said clusters. The appropriate clustering algorithm is dependent on the individual data set and the intended use of results (Han, Kamber, & Pei, 2012; Rokach & Maimon, 2005).

Dowlan & Ball (2007) demonstrated the use of cluster analysis in sport biomechanics to accurately classify different movement phases and different styles in which an athletic hammer throw can be executed. One male elite level athlete performed five hammer throws, for which three 50 Hz cameras were used with APAS (Ariel Performance Analysis System) motion analysis system to obtain 3D displacement data on 10 points in the athlete-system; left and right shoulder, hips, heels, toes, hammer and handle. Normalised data from the athlete's best throw was used in hierarchical cluster analysis (Pearson's correlation method). The cluster analysis identified five different movement phases in the hammer throw. This analysis provided great insight into the movement of an athlete-hammer throw system that questioned the validity of the traditionally used phase theories and may permit progressive development of the athlete's movements throughout the skill.

De Cock et al. (2006) developed a foot type classification through the comparison of existing walking data to an established reference dataset for peak pressures and pressure-time integrals during jogging. Plantar pressure data was obtained from 215 healthy young adults running at 3.3 m/s over a 16.5 m running track. The track had a built-in pressure platform mounted on top of a force platform, for the measurement of peak pressures, regional impulse and relative regional impulses. Using a K-means cluster analysis, four functional foot types were suggested based on the difference in dynamic plantar pressure distribution. The four identified pressure loading patterns, combined with morphological measurements and 3D kinematic data, could aid interpretations of the functional foot behaviour and the identification of deviant foot function.

Ball & Best (2011) investigated whether two distinct swing styles, the 'front foot' style or 'reverse' style, are evident when using other clubs and whether there is consistency between the executed swing styles with the used golf club. Forty-six male golfers, of different skill levels, performed swings in a laboratory environment hitting a golf ball into a net. Ten swings were performed for each of the different clubs whilst standing on two force platforms. For each trial, a 200 Hz camera, placed perpendicularly to the intended direction of the shot, was used to measure the position of the golfer's centre of pressure, quantifying 8 different phases throughout the swing. Hierarchical cluster analysis (squared Euclidean distance method) revealed that the front and reverse style swings were evident for all clubs used and that 96% of the golfers maintained the same style of swing for all clubs. The result provided an understanding of the influences of equipment on technique, whilst also identifying the rotational strategies used by golfers.

Murray & Hunfalvay (2017) examined the visual search behaviour strategies of elite and non-elite tennis players through the use of cluster analysis. Successful performance of interceptive tasks, such as the return of serve, has been stated to be based on the players' capability to capture suitable anticipatory information prior to the approaching balls flight path. Using the Eye-Gaze Response Interface Computer Aid (ERICA), Murray & Hunfalvay were able to track the participant's eye movements and interspersed stopping point from the cornea of the eye. A total of 43 tennis players were used for the study,

21 male and 22 female, ranging in ranking status from 44th in the world to unranked. Participants were seated in front of a computer and their eyes were calibrated for the ERICA system. The participants were then asked to watch three serves as if they were to hit a return, presented in random order, whilst recording their visual search variables. Results were clustered using hierarchical cluster analysis (Wards method of Euclidean distance) and supported through the use of non-hierarchical cluster analysis (k-means). The results revealed three different clusters distinguishing visual behaviours of high, middle and low ranked players. More specifically, players of high rank demonstrated a longer mean fixation duration and lower variation of visual search in comparison to middle and low ranked players. The results demonstrated the usefulness of cluster analysis as a tool for detecting and analysing areas of interest in experimental analysis of expertise and in distinguishing visual search variables among all participants.

Phinyomark, Osis, Hettinga, & Ferber (2015) investigated the practical implications of clustering healthy runners with runners experiencing patellofemoral pain (PFP) through kinematic comparison. A principal component analysis was initially used to reduce the dimensionality of the gait waveform data and then a hierarchical cluster analysis (Wards method) was used to determine clusters of similar gait patterns. The results showed two distinct running gait patterns found with the main between-group differences. The differences found occurred in the frontal and sagittal plane knee angles, independent of age, height, weight and running speed. The comparison of the two identified groups to PFP runners, found one cluster exhibited greater peak knee abduction angle, whilst the other exhibited a reduced peak knee abduction angle. This suggested variability in gait strategies between runners and thus provided further insight and knowledge to ensure a careful selection process of injured runners when investigating their pathomechanics.

The discussed studies exhibit the benefits of clustering in sport, aiding in the identification of specific technique or behaviour characteristics driving the formation of the clusters. Identification of these clusters provided great insight and the ability to further knowledge, whether monitoring or enhancing performance, within their respective field.

The method in which the cluster analysis was conducted was through the use of either hierarchical clustering or k-means clustering. K-means is the most common method of partition clustering and is an effective and efficient method of clustering data sets with a large number of variables if the number of clusters (k) is small. However, the number of clusters, k, is an input parameter, defined by the user. An inappropriate choice of clusters can result in non-optimal cluster formations. K-means is also heavily dependent on the initial placement of the cluster centroid and with an inappropriate selection of k, will not yield the same results with each run. The key limitation of K-means is its assumption of clusters of spherical shape, which are distinguishable so that the mean converges to the cluster centroid. The clusters are, therefore, anticipated to be of similar size to ensure correct assignment of a data point to the nearest cluster centroid (Celebi, Kingravi, & Vela, 2013; Singh, Malik, & Sharma, 2011).

Hierarchical clustering is a method which aims to build a hierarchy of clusters. There are two main approaches for hierarchical clustering; agglomerative or divisive. Agglomerative methods start with each observation as its own cluster and merge each observation into clusters. Whereas, divisive methods start with all observations as one large cluster and then separates the observations successively into clusters. A prominent method of approach to hierarchical clustering is an agglomerative method of analysis (Rokach & Maimon, 2005). The merging or division of clusters is performed according to a similarity measure. Hierarchical agglomerative cluster (HAC) methods can be further divided according to the calculation methods of the similarity measure; single-link clustering, complete-link clustering and average-link clustering.

Hierarchical cluster analysis provides versatility in the method of approach and can be seen through the various approaches used within the discussed studies (Ball & Best, 2011; Dowlan & Ball, 2007; Phinyomark et al., 2015). It is this versatility which results in hierarchical clustering as the common choice of cluster analysis.

2.9 *Literature Summary*

Previous research has clearly shown racket parameters to influence rebound characteristics of the ball post-impact. Resultant rebound ball velocity has been found to be positively related to racket frame stiffness and both transverse and polar moments of inertia. Although these findings provide further knowledge into the effects of racket parameters, the investigations are limited to the lack of variation of racket parameters and parameter combinations. Therefore, it is essential to ensure a wide range of racket properties and property combinations, when undertaking investigations of ball-racket impacts to enhance the understanding of their potential effects.

Player testing data, collected at the 2006 and 2007 Wimbledon Qualifying Tournament provide great insight into the characteristics of tennis forehands found within the field play and ensure for realistic simulation within a laboratory environment. The categorisation of the raw forehand data, into groups of similar shot conditions, will not only further provide for realistic simulation of different forehand shots within a laboratory environment, but will also reduce inconsistencies between studies regarding inbound testing parameters for an average forehand shot. Player testing results have also found inconsistent impact positions upon the racket face, regardless of players aiming to strike the ball at the rackets node point, consequently, this results in impacts off the longitudinal axis. A tight grip has been found to reduce these effects compared to the same impact with no applied grip. However, the value defining a firm grip is inconsistent between studies. Therefore, grip values must also be further investigated to ensure a correct representation of the interface between the racket and the player.

Ball to racket impacts have been limited to either perpendicular impacts along the longitudinal axis of a tennis racket, oblique impacts not representative of realistic playing conditions or oblique impacts limited to one tennis racket. Although perpendicular impacts accurately represent tennis serves, due to the complexity regarding ball slip and roll during oblique impacts and the non-linearity of ball-racket impacts, impact conditions such as these cannot be used to represent realistic forehand conditions. Therefore, it is essential to ensure all

simulated forehands are representative of those found within the field of play and can be achieved through the use of player testing data. Laboratory testing of oblique impacts have also been limited to one racket of specific racket properties. Previous research has clearly shown racket properties to influence rebound characteristics of the ball when impacted. Resultant rebound ball velocity has been found to be positively related to racket frame stiffness and both transverse and polar moments of inertia. To advance knowledge regarding the effects of racket properties, testing must be conducted on a variety of rackets possessing a range of properties and property combinations, whilst also ensuring accurate representation and laboratory simulation of typical forehand shots found within the field of play.

Cluster analysis can be utilised to identify discrete clusters within large and complex data sets. Such methods are dependent only on the number of cells in each dimension in the quantized space and aim to find groups of variables of high similarity. Hierarchical clustering is a method commonly used within sports and can be used to identify distinct groups of similar racket behaviour, to find potential connections to racket properties or property combinations. Whilst, this method of analysis is adaptable to changes and can identify useful features when distinguishing clusters, it lacks the ability to differentiate relevant and irrelevant variables. Therefore, reducing the dimensionality associated with testing a large number of input variables, it is possible to increase knowledge regarding the influence of racket properties on ball rebound velocity and angle, for ball-racket impacts.

3 Laboratory Testing - Specific Forehand Shot Characteristics

3.1 *Introduction*

The literature review confirmed the importance of ball-racket impact testing methods in determining how a ball and racket perform when impacted within the field of play. In order to achieve this accurately, test parameters must be representative of a typical shot. Recorded player data from the 2006 Wimbledon Qualifying Tournament (Choppin, 2008) provides valuable insight into the range of ball-racket impact parameters found within the field of play. However, a forehand shot can be further categorised as either a flat, topspin or slice forehand, to which the data provides no indications as to the kinematic characteristics for these different forehand shots. It is possible to identify the racket kinematics of specific forehand shots through the implementation of data reduction and clustering techniques.

The identification of these kinematic characteristics will allow for the development of a more constrained laboratory test protocol, whilst also having the ability to accurately simulate different forehand shots in a laboratory environment.

3.2 *Aim*

This chapter aims to identify racket kinematics associated with specific forehand shots found within the field of play, to be used for the development of a large-scale laboratory test methodology.

3.3 *2006 Wimbledon Qualifying Tournament Data*

It is essential when undertaking laboratory-based experiments that conditions are representative of those found within the field of play and in doing so, ensuring results are applicable to 'real world' conditions. Player testing data collected by Choppin (2008) at the 2006 Wimbledon Qualifying Tournament

solely focused on the movements of the racket and ball prior to and post-impact providing essential information for representative laboratory simulation.

The player testing data was collected on a standard outdoor practice tennis court, due to the rules and regulations of competitive play (ITF, 2019). To capture the three-dimensional movements of the tennis racket and ball, a pair of synchronised high-speed video cameras recorded all impacts within a 2 x 2 x 2 m calibrated volume positioned centrally along the outdoor practice court baseline. Ensuring representation of realistic impact conditions it was imperative that the players were not influenced by the testing in any manner; therefore no requests were made to the players in terms of shot type, stance or even position on the court. To extract the three-dimensional racket movement from the recorded videos, specifically marked points on the racket were used to define the racket face plane and the ball was tracked as a single point in space. With this information, it was possible to track racket velocity, ball velocity, impact location and all associated angular velocities. The results of this data collection can be found within Choppin (2008).

A total of 108 shots from 19 male and female tennis players, 13 of which were internationally ranked were recorded. Out of the 108 recorded forehand shots, 72 were completed by male tennis players and only 36 were completed by female tennis players. Due to the limited number of recorded female player testing data, further analysis was fulfilled using the male player testing data only.

When defining shot characteristics it is useful to define them according to a global or local frame of reference. A global reference frame refers to a fixed coordinate axes system within 3D space, aligned according to the user's preference. A local frame of reference is aligned to objects that are moving throughout the 3D space. As impact testing within a laboratory environment consists of an initially stationary tennis racket and moving tennis ball, the coordinate axis system can be fixed within the global frame of reference aligned to the racket's GSC. The defined coordinate axes system is shown in Figure 8 and will be used throughout this thesis.
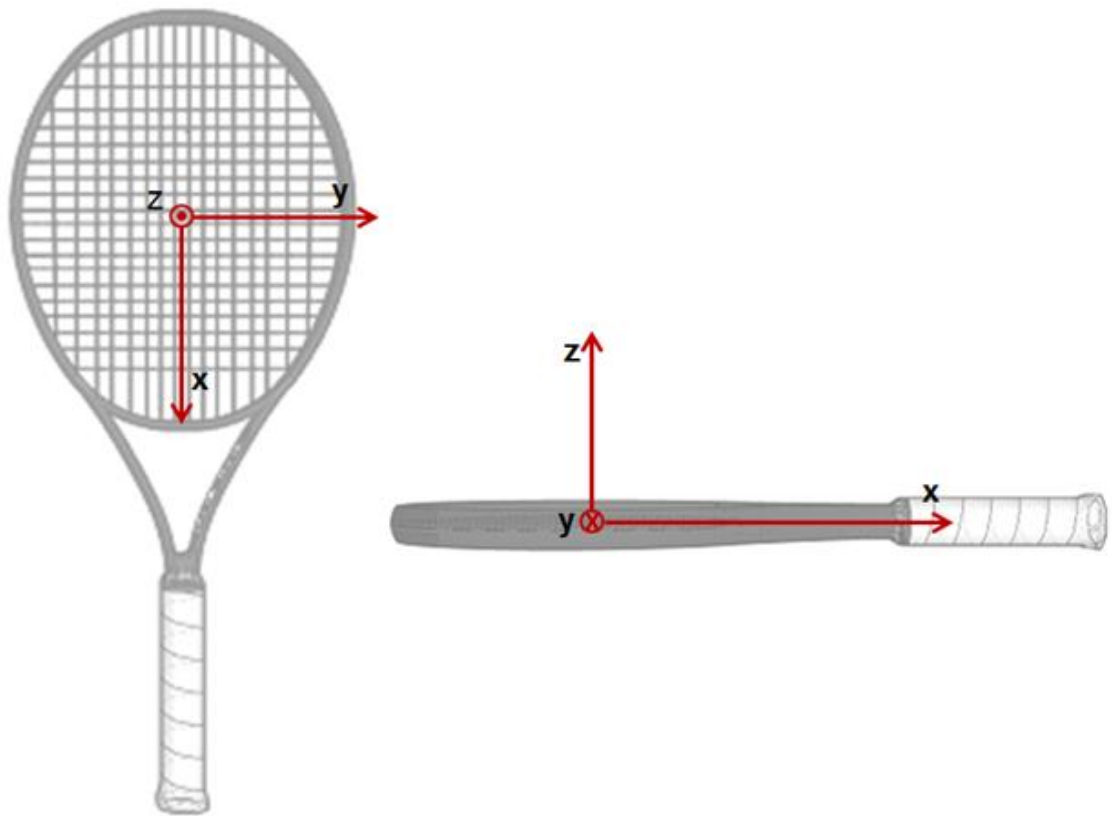
Figure 8 - Orientation of the Fixed Global Axes Coordinate System

The raw player testing data, discussed within Section 3.3, recorded a total of 72 forehand shots, completed by 9 male participants. For each recorded impact the associated linear and angular components were set to the fixed global axis system, illustrated in Figure 8.

Identified within the male participants was a single left-handed player. To ensure consistency within the dataset, the racket velocities (both linear and angular), for this participant, were rotated 180° about the fixed global x-axis.

3.4 *Orientation of Impact*

A vital component when defining shot characteristics is the orientation of the racket with the ball upon impact. With respect to the fixed global coordinate system, this orientation can be calculated using the recorded ball and racket component velocities.

To calculate the orientation, the ball (V_{xb}, V_{yb}, V_{zb}) and racket (V_{xr}, V_{yr}, V_{zr}) component velocities are first resolved into single relative component

velocities (V_x, V_y, V_z). Figure 9 (a) shows a two dimensional illustration of the component velocities for the ball and racket whereas Figure 9 (b) illustrates the resolved relative velocity components with respect to the fixed global axis. The relative velocity components, V_x, V_y, V_z, are defined by the following equations:

$$V_x = V_{xb} - V_{xr}$$ [2]

$$V_y = V_{yb} - V_{yr}$$ [3]

$$V_z = V_{zb} - V_{zr}$$ [4]

The resultant of the resolved relative component velocities is then defined by:

$$V_{Resultant} = \sqrt{V_x^2 + V_y^2 + V_z^2}$$ [5]
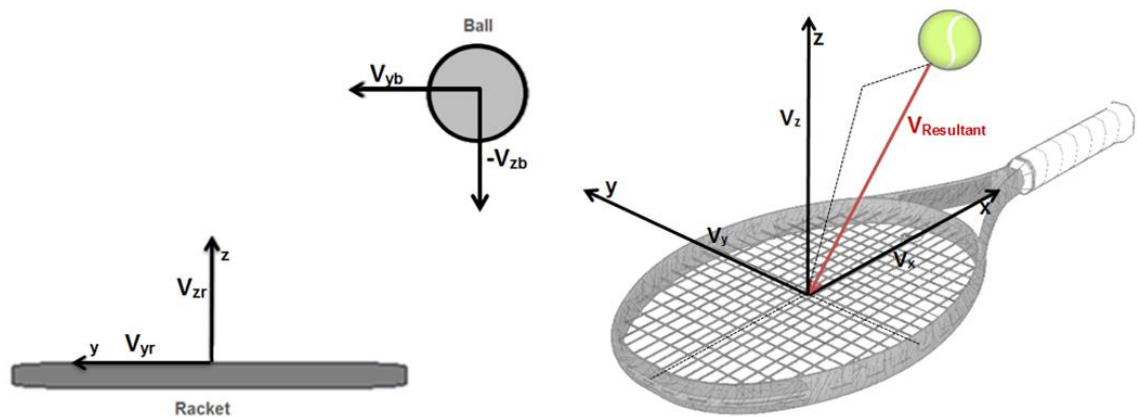
Figure 9 - a) Two Dimensional Illustration of the Ball and Racket Component Velocities and Resultant Velocity, b) Three Dimensional Illustration of the Resolved Relative Velocity in the Fixed Global Frame of Reference

For each recorded impact, the resolved relative velocity components will be used to calculate the orientation of the racket with the ball upon impact.

3.4.1 Inbound Playing Angle (α)

The inbound playing angle (α) is the angle at which the ball impacts the racket face relative the normal (z-axis). Figure 10 illustrates the inbound playing angle with reference to the defined coordinate system and the relative velocity components.
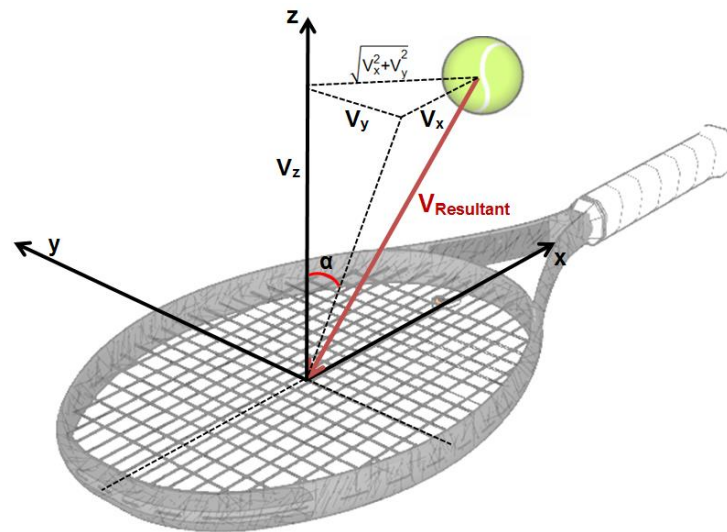
Figure 10 - Schematic of the Inbound Playing Angle and Relative Velocities Used for Calculation

Inbound playing angle was calculated using the relative component velocities along the y and z-axis as shown by Equation 6. Results of the inbound playing angles can be found in Appendix A.

$$\alpha = \tan^{-1}\left(\frac{V_y}{V_z}\right) \tag{6}$$

3.4.2 Inbound Offset Angle (β)

Through the assumption that relative velocity along the global x-axis is negligible previous research has limited the calculation of racket orientation to one angle relative to the racket face normal (inbound playing angle). However, the raw player testing data shows values of relative velocities, along the x-axis, which cannot be considered negligible, and thus the calculation of on 'offset angle' must be accounted for.

The inbound offset angle (β) acknowledges the trajectory of the tennis ball which does not directly follow an oblique and perpendicular path to the racket face. Figure 11 illustrates the inbound offset angle with reference to the racket face and the relative velocity components.
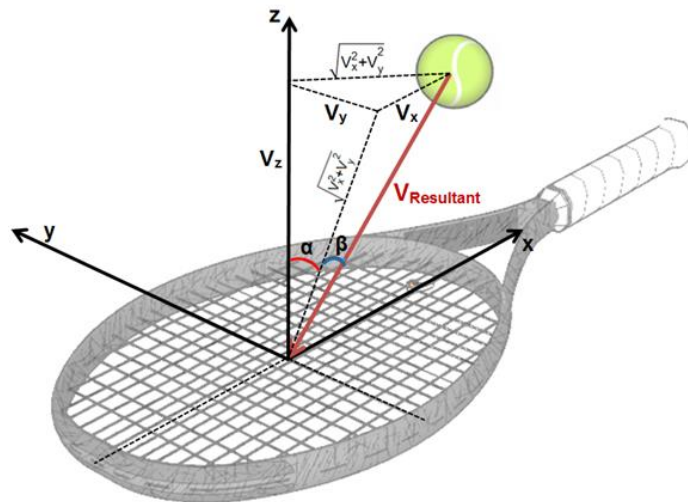
Figure 11 - Schematic of the Inbound Offset Angle and Relative Velocities Used for Calculation

The inbound offset angle is calculated using the relative velocities along the x, y and z-axis. The equation used for the calculation is shown in Equation 7. Results of the calculated inbound offset angles can also be found in Appendix A.

$$\beta = \tan^{-1}\left(\frac{V_x}{\sqrt{V_y^2+V_z^2}}\right) \qquad\qquad [7]$$

3.5 *Specific Forehand Shot Classification*

Tennis is a sport with a large number of varying inbound parameters. Through the identification of the racket kinematics of specific forehand shots, it is possible to reduce the variation; allowing for large-scale impact testing, whilst also ensuring representative inbound parameters.

To establish the racket kinematics relevant to specific forehand shot types found within the field of play, the following analysis was conducted using the recorded 2006 Wimbledon Qualifying tournament set to the fixed global axis coordinate system and the calculated racket orientations.

3.5.1 Principal Component Analysis

Principal Component Analysis (PCA) is a multivariate statistical technique which reduces the number of dimensions of complex and high-dimensional data, whilst retaining underlying correlations and patterns otherwise masked by the large volume of data (Karamizadeh et al., 2013; Wold, Esbensen, & Geladi, 1987). PCA achieves dimension reduction through the use of orthogonal linear transformations of the input variables and geometrically projects the data to a new coordinate system of lower dimensions called principal components (PC).

The PCA input variables were based on the assumption that forehand 'form' would remain consistent regardless of the incoming ball and surroundings (United States Tennis Association & United States Lawn Tennis Association, 2004) and are as follows:

1. Inbound Playing Angle (α)
2. Inbound Offset Angle (β)
3. Racket Angular Velocity in the x-axis (ω_{xr})
4. Racket Angular Velocity in the y-axis (ω_{yr})
5. Racket Angular Velocity in the z-axis (ω_{zr})
6. Racket Linear Velocity in the x-axis (V_{xr})
7. Racket Linear Velocity in the y-axis (V_{yr})
8. Racket Linear Velocity in the z-axis (V_{zr})
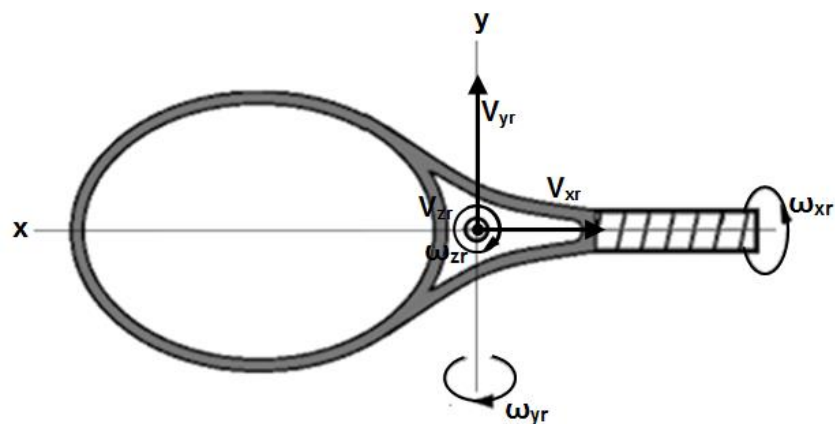
Figure 12 - Depiction of Forehand Parameters on a Tennis Racket

To ensure the extraction of important data features and information, PC's beyond the first must be considered. Through the use of a scree plot, the PCA conducted reported that PC1 and PC2 accounted for 56 % and 23 % of the variance of the data respectively. Figure 13 shows a scree plot illustrating the cumulative variance explained by the PC's, showing PC1 and PC2 to account for a total of 79 % of the variance explained.
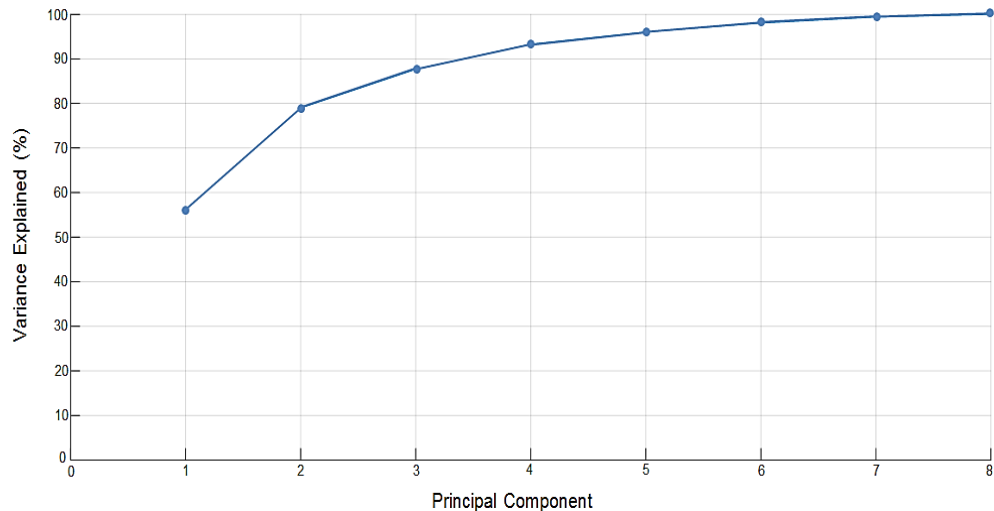
Figure 13 - Scree Plot of the Cumulative Variance Explained by the PC's

These two principal components were further investigated using bivariate Pearson's correlation (r). PC1 was found to have the best correlation with inbound playing angle (r = 0.952, $p < 0.001$), followed by racket angular velocity in the z-axis (r = - 0.920, $p < 0.001$) and racket linear velocity in the y-axis (r = -0.890, $p < 0.001$). Therefore the largest variation, captured by PC1, could be explained by differences in inbound playing angle, as well as racket angular velocity in the z-axis and racket linear velocity in the y-axis. Similarly, a bivariate Pearson's correlation was conducted on all inbound variables with PC2, inbound offset angle was found to have the largest correlation coefficient (r = 0.989, $p < 0.001$). PC2 could, therefore, be explained by the variation of inbound offset angle.
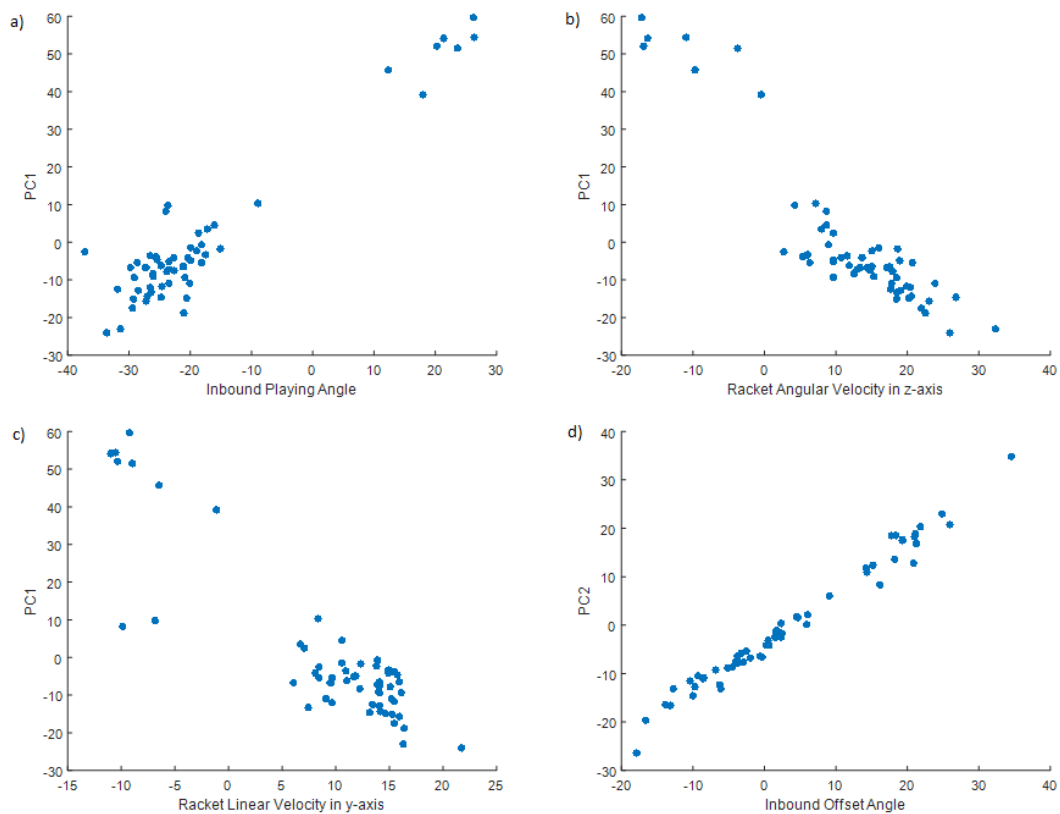
Figure 14 - Results of PCA: a) PC1 vs Inbound Playing Angle, b) PC1 vs Racket Angular Velocity in the z-axis, c) PC1 vs Racket Linear Velocity in the y-axis and d) PC2 vs Inbound Offset Angle

3.5.2 Specific Forehand Shot Characteristics

A cluster analysis was conducted using PC1 and PC2 results, for the identification of specific forehand shots. Results identified 3 distinct clusters, each possessing different racket kinematics. Each cluster was individually investigated for the removal of outliers by utilising Box and Whisker plots. Figure 15 shows the result of the Box and Whisker plots of PC1 and PC2 for each cluster, indicating a total of 4 outliers.
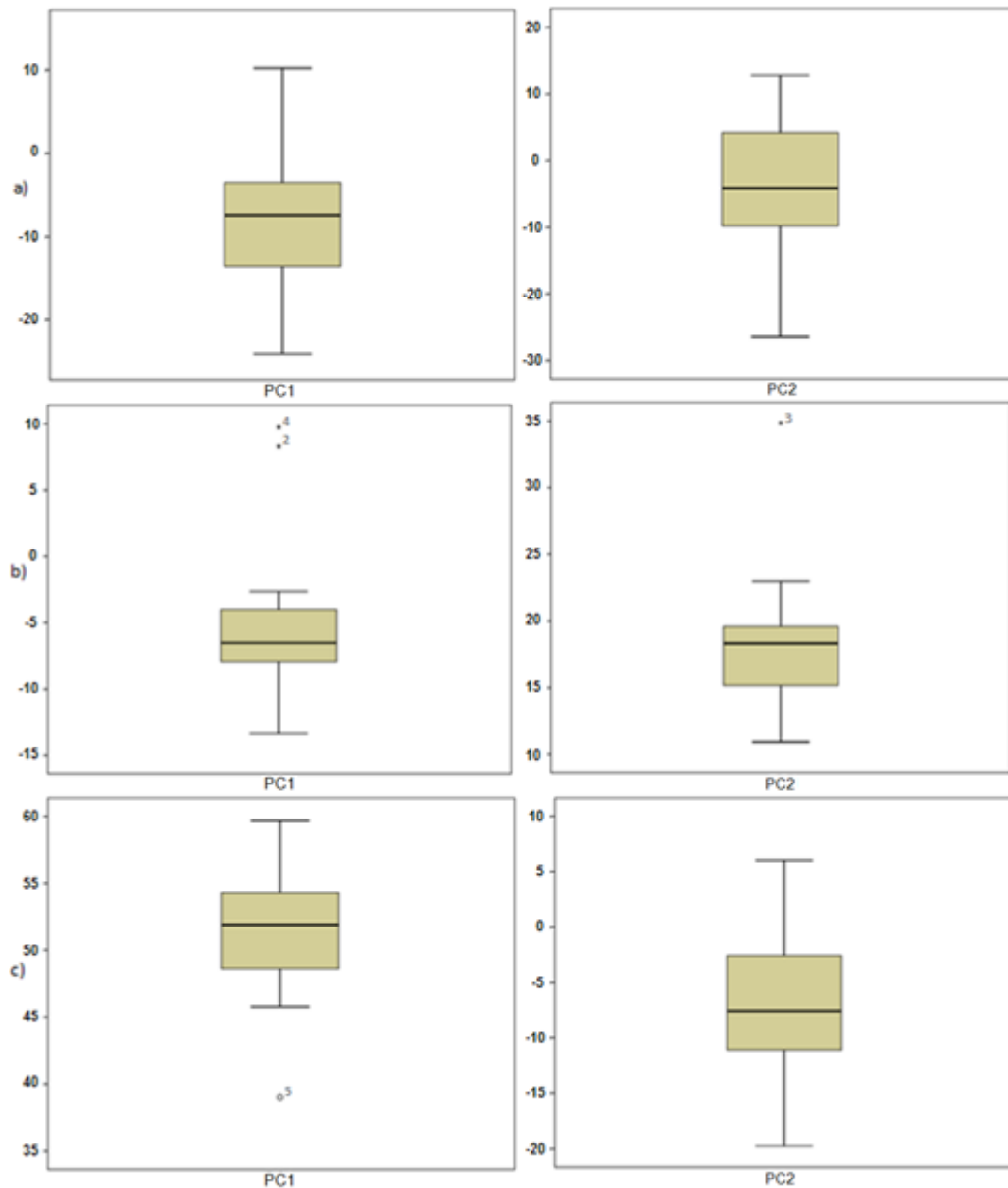
Figure 15 - Box and Whisker Plots Identifying Outliers of PC1 and PC2 for a) Forehand Shot 1, b) Forehand Shot 2 and c) Forehand Shot 3

The removal of outliers reduces the variability of the clusters and thus creates a higher degree of shot characteristic consistency. The final cluster results, using PC1 and PC2, are shown in Figure 16.
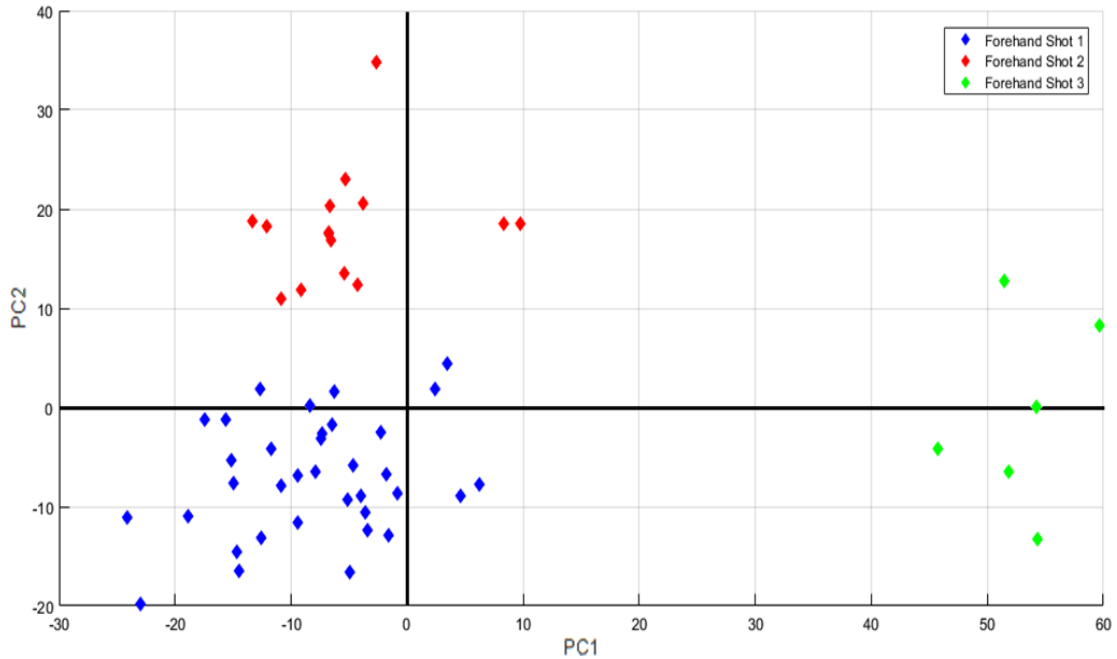
Figure 16 - Results of PC1 and PC2 with Indication of the 3 Identified Clusters

In order to identify the real-world characteristics of the revealed forehand shots, data reconstruction was conducted using the PC scores, eigenvectors and the vector means (V_m) obtained throughout the principal component analysis.

PCA Reconstruction = PC Scores · Eigenvectors$'$ + V_m **[8]**

The deviation between the original data and the reconstructed data is called the reconstruction error. The reconstruction error is inversely proportional to the total variance of the PCA space and therefore, a total of 5 PC's, accounting for approximately 97 % of the explained variance, was used to reconstruct the data to ensure minimal loss of data and reconstruction error. Table 2, Table 3 and Table 4 show the different characteristics defining each of the forehand shots.

Forehand Shot 1

Table 2 - Defining Average and Standard Deviation Characteristics Forehand Shot 1

	Inbound Playing Angle	Inbound Offset Angle	Angular Velocity rad/s			Linear Velocity m/s		
	°	°	x	y	z	x	y	z
Mean	-24	-0.4	6	32	15	-2	13	22
Standard Deviation	4.4	6.6	8.7	6.3	7.6	4.4	8.4	3.9

Forehand Shot 2

Table 3 - Defining Average and Standard Deviation Characteristics Forehand Shot 2

	Inbound Playing Angle	Inbound Offset Angle	Angular Velocity rad/s			Linear Velocity m/s		
	°	°	x	y	z	x	y	z
Mean	-26	21	10	28	14	-6	10	22
Standard Deviation	5.0	5.3	7.9	1	5.9	3.5	9.2	4.6

Forehand Shot 3

Table 4 - Defining Average and Standard Deviation Characteristics Forehand Shot 3

	Inbound Playing Angle	Inbound Offset Angle	Angular Velocity rad/s			Linear Velocity m/s		
	°	°	x	y	z	x	y	z
Mean	21	0.6	-4	21	-11	1	-8	17
Standard Deviation	4.9	12.1	3.6	4.4	6.6	4.6	3.5	2.2

3.6 *Discussion*

Player testing during match play conditions is considered to be an appropriate method of determining ball and racket kinematics. However, ecological dynamics rationalises that as long as training simulations are representative of those found within demanding competitive performance environments, practice conditions are also a viable method of determining ball and racket kinematics (Seifert & Davids, 2016). Therefore, the player testing data collected at the 2006 Wimbledon Qualifying tournament, by Choppin (2008), provides the means to ensure laboratory testing of typical forehand conditions found within the field of play.

PCA and cluster analysis quantify and simplify complex relationships among the racket kinematic parameters. PCA was conducted to reduce the dimensionality of the number of measured racket kinematic parameters, whilst preserving as much information (variance) as possible. PC1 and PC2 accumulated for more than 70 % of the data variance and were used to conduct the cluster analysis. Clustering of the PC's results, rather than the raw data, improves the extraction of cluster structure through PC extraction of key data features (Brownstein, Khodursky, Ben-Hur, & Guyon, 2003; Xue, Lee, Wakeham, & Armstrong, 2011). Though cluster analysis of all eight PC's would account for the whole data variation, the scree plot accompanied with Figure 16, indicate that extraction of crucial information of data has been accomplished by PC1 and PC2. The following six PC's can, therefore, be assumed negligible on cluster structure.

The two principal components (PCs), accounting for the most data variance, were then further analysed. Bivariate Pearson's correlation was conducted on PC1 and PC2 to identify which of the measured parameters best correlated to them. In terms of correlation coefficients where r > 0.7. PC1 was found to be highly correlated to inbound playing angle, racket angular velocity in the z-axis and racket linear velocity in the y-axis. The largest variation can, therefore, be explained by the differences found in these three parameters. Comparison of the cluster characteristics of the correlated racket kinematic parameters, PC1

can be assumed to reveal the variance of racket kinematics differentiating between a typical topspin and typical slice forehand shot. The negative inbound playing angle, a characteristic of forehand shot 1 and 2, signifies a closed racket face and is generally associated with the completion of a topspin forehand. A topspin forehand requires fast racket head speeds and fairly steep racket paths through impact, due to the difficulty to reverse the spin of the ball (Knudson, 2006). A positive inbound playing angle, a characteristic of forehand shot 3, signifies an open racket face and is generally associated with the completion of a forehand slice shot. PC2 is highly correlated to only the inbound offset angle and, thus, the variance can be explained by the differences observed in the inbound offset angle. When comparing the cluster characteristics of inbound offset angle, PC2 can be assumed to reveal the variance of racket kinematics differentiating between topspin forehand shot 1 and topspin forehand shot 2.

Forehand shot 1 and forehand shot 2, as previously mentioned, are identified as two different typical forehand shots found within the field of play, differentiated by inbound offset angle. As previously described the inbound offset angle acknowledges a non-perpendicular oblique ball trajectory to the racket face. Assuming the player is located upon the tennis court baseline, this difference is depicted in Figure 17 and can be assumed to be the result of the player's aim to change the path of the tennis ball post impact. The identified increase in angular and linear velocity about and along the x-axis, for forehand shot 2, can be a result of the player 'wrapping' the racket around the ball to aid the change in rebound ball trajectory. Although some similarities of racket kinematics can be seen between topspin forehand 1 and topspin forehand 2, it is the combining of the inbound offset angle and angular velocities which define the nature and purpose of these forehands within the field of play.
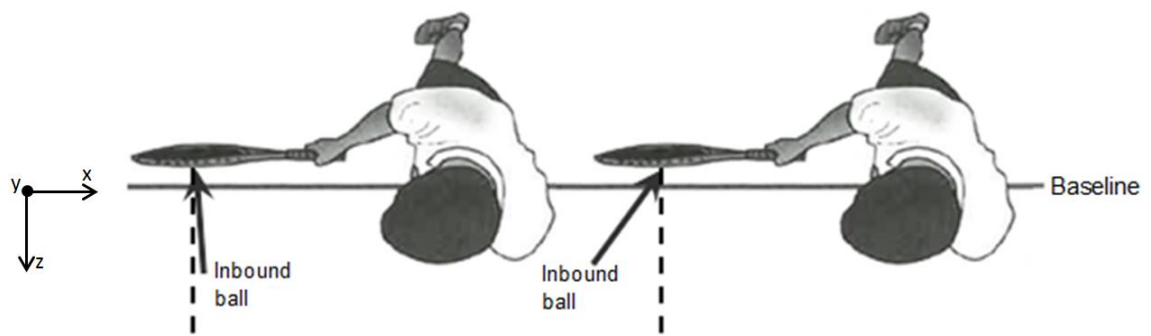
**Figure 17 - Schematic of the Inbound Offset Angle for Forehand Shot 1 and Forehand
Shot 2 Respectively**

Although Knudson and Blackwell (2005) did not record the inbound offset
angle for typical forehand shots, the inbound playing angle and the racket's
resultant linear velocity were, however, recorded. For which, forehand shot 2
can be seen to possess similar values to those found by Knudson and
Blackwell, indicating the potential of similar execution of shot type from the
recorded players, regardless of offset angle. Forehand shot 1, however,
possess a lower mean playing angle and larger mean resultant linear velocity to
that cited by Knudson and Blackwell. These differences in values could be due
to the differences regarding the nature of the testing conditions, the players skill
level, ball height contact or simply the type of shots which have been executed
by the recorded players.

3.7 *Conclusion*

This chapter describes the methodology used to determine the defining
characteristics of specific forehand shots found within the field of play. The
previously collected player testing data collected at the 2006 Wimbledon
Qualifying Tournament provided great insight into the characteristics of
forehand racket kinematics, but with no indication of the characteristics of racket
forehand movements for specific forehand shots.

A PCA was used to reduce the dimensionality of the data, into a set of
two PC's accounting for most of the information of the data set. Cluster analysis,
using the two PC's accounting for 79 % of the variation within the data, revealed
3 distinct clusters of forehands.

Use of the first 5 PC's ensured minimal data loss for the reconstruction of the data back into real-world values. Each cluster possessed different averaged racket kinematics and are defined as either a typical topspin (forehand shot 1 and 2) or slice (forehand shot 3).

The findings and results of this chapter will be used to further develop a test protocol capable of accurately and realistically simulating specific forehand shots within a laboratory environment.

4 Laboratory Testing - Apparatus and Methodology Development

4.1 *Introduction*

In order to assess the performance of a tennis racket, controlled repeatable tests must be conducted on a range of tennis rackets of varying properties and property combinations. The previous chapter identified the racket kinematics of typical forehand shots, which will be applied for the development of a laboratory-based test protocol.

To ensure accurate forehand simulation the following parameters were considered: the calculated translational inbound velocity and relative inbound playing angle for each laboratory simulation of specific forehand shots, and the impact positions along the longitudinal and transverse axes of a stationary tennis racket. Although a stationary racket prohibits racket movement during testing, both the three-dimensional angular and linear kinematics of the racket are accounted for within the calculation of the resultant inbound ball velocity. When reducing the impact system to a ball and a racket, it is also vital that the interface between the racket and player's hand is correctly simulated.

The inherent variabilities of the laboratory apparatus were also examined to ensure an efficient and effective data collection process. This analysis investigated the repeatability of the laboratory apparatus that was used.

4.2 *Aim*

This chapter aims to design a large-scale laboratory-based test protocol which measures inbound and rebound parameters of a ball impacting a stationary racket.

4.3 *Experimental Apparatus*

The experimental apparatus must facilitate large-scale data collection and ensure realistic test conditions, representative of those found within the field of play. This requires an impact test rig capable of achieving oblique,

spinning impacts for varying positions upon the racket stringbed. Such
conditions must also be attainable on a number of varying tennis rackets.

4.3.1 Impact Test Rig

The impact test rig consists of a ball projection device, BOLA (BOLA,
2017), and the racket mount, shown in Figure 18. The ball projection device is
used to fire tennis balls onto the racket stringbed and must reliably set the
tennis ball's trajectory to hit the desired location on the racket's face. The racket
mount not only allows for the change of impact position but also restricts the
movement around the racket handle according to a limiting torque value.
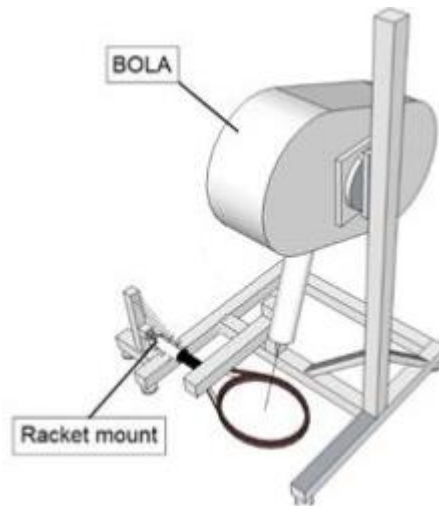
Figure 18 - A Schematic of the Impact Test Rig (Spurr, 2017)

BOLA

The BOLA had previously been modified with the attachment of an
aluminium barrel, to the front of the BOLA to increase the accuracy and
repeatability of the ball trajectory (Choppin, 2008). The addition of the barrel
allows for reliable triggering of the cameras, with the placement of a light gate
trigger at its tip.

The BOLA can launch the tennis ball at a range of resultant velocities,
spin rates and trajectories, allowing for a variety of inbound conditions to be
tested. The BOLA generates different spins around a single axis using two large
spinning wheels.

The BOLA had previously been attached to a vertical 'spine', central to four vertical struts, running down to the ground. A 20 kg weight was added onto the frame of the impact test rig to ensure solidity and insignificant movement to the BOLA and strut upon ball launch.

Racket Mount

The racket handle clamp designed and developed by Choppin (2008) serves two main purposes, firstly it provides the racket support and secondly, it generates resistance to racket rotation along the longitudinal axis to simulate the effects of a tennis player's grip.

The racket mount compromises of a universal joint to relieve stresses within the racket preventing breakages upon impact and Cross+Morse M40 Torque Limiting Clutch (Cross+Morse, 2017) to restrict the rotational movement. Figure 19 shows a schematic of the racket handle clamp. The racket cannot translate in the mount but can rotate freely about the x, y and z axes, at a point a few centimetres above the racket butt, thus restricting the racket movement to three degrees of freedom. One degree of freedom, however, is torque restricted (rotations about the longitudinal x-axis) and thus simulating a tennis player's grip.
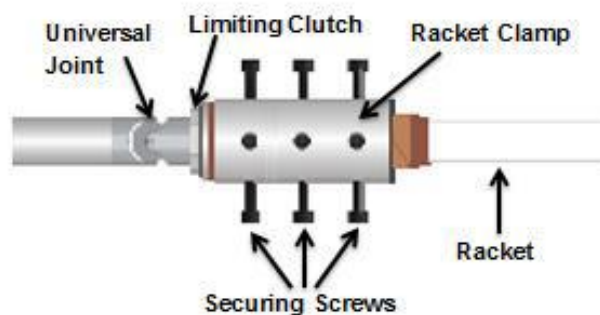
Figure 19 - Racket Mount with Torque Limiter Simulating Human Grip Developed by Choppin (2008)

The limiting clutch, with a capacity of 3 - 15 Nm, restricts the rotational movement using a leather pad kept under constant pressure between two conical springs. The force exerted by conical springs can be altered by tightening or loosening a restraining nut, and thus, allowing for the desired level

of torque. The torque is locked into position until exceeded, causing the clutch to slip.

Using an extension spring, the racket handle clamp is attached to the impact test rig, whilst also using a restraining bar, to hold the racket horizontally (Spurr, 2017). The restraining bar was used to prevent the spring from pulling the racket above the horizontal. The racket mount, a combination of the racket handle clamp and extension spring attached to a vertical post, is depicted in Figure 20.
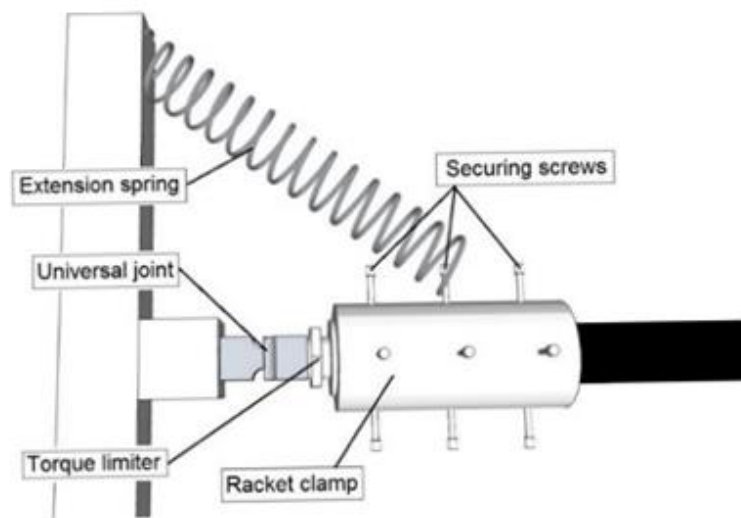
Figure 20 - A Side View of the Racket Mount (Spurr, 2017)

In a laboratory environment, the racket is kept stationary whilst a ball is projected onto the racket face. As discussed in Chapter 4, three forehand shots were identified, however, due to limitations regarding the racket handle clamping mechanism, only two of the identified three forehand shots can realistically be simulated in a laboratory environment. As previously discussed the clamping mechanism restricts linear movement along the x, y and z axes, thus compromising the racket's response to impacts possessing inbound offset angles, shown in Figure 21. Although this limitation affects the ability to accurately and realistically simulate forehand shot 2, it does not affect the ability to accurately and realistically simulate forehand shots 1 and 3 (topspin and slice), assuming inbound offset angle is negligible.
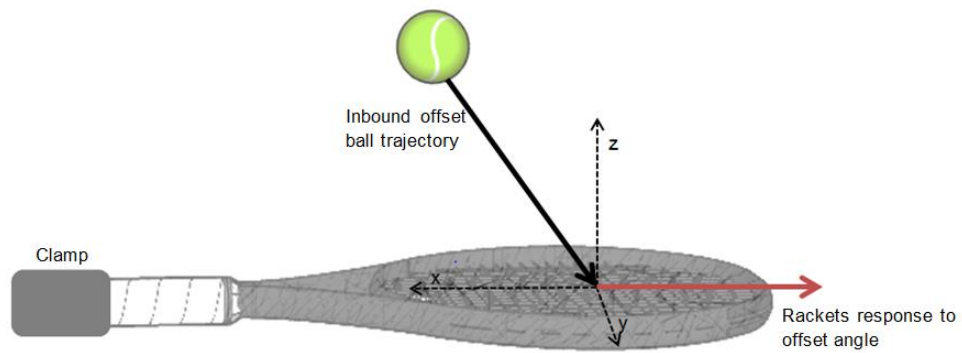
Figure 21 - Racket Response to Inbound Offset Angle Impacts

4.3.2 **Racket Selection**

The ITF possess a vast library of tennis rackets ranging in properties, year of production and even prototype rackets. Figure 22 shows the range of each racket property for every tennis racket within the ITF racket library.

In an ideal world, all 321 tennis rackets would be tested, however, this is an unattainable target. To ensure a spread of racket property combinations, the selection process initially involved the removal of all racket repetitions found within the ITF racket library. The removal of racket repetitions refers to the removal of any potential racket model duplicates and rackets possessing identical property combinations, thus leaving rackets of diverse property combinations for selection. Following the removal of repetitions, the selection process then involved individually removing rackets whilst assessing their removal effect on the spread, range and normality of each racket property. Rackets were individually removed until it was no longer possible to achieve the same spread, range and normality trend as those observed for the total 321 rackets.

Through this selection process, a total of 39 tennis rackets, of diverse properties, were selected to undergo testing. The ranges and normality of the properties, for the selected 39 rackets, are shown through the use of histograms by Figure 23 and can be compared to Figure 22 showing the ranges and normality of all the rackets. The mean and standard deviations for all the

rackets and the selected rackets can be found in Table 5, whilst the properties for each selected racket can be found in Appendix B.
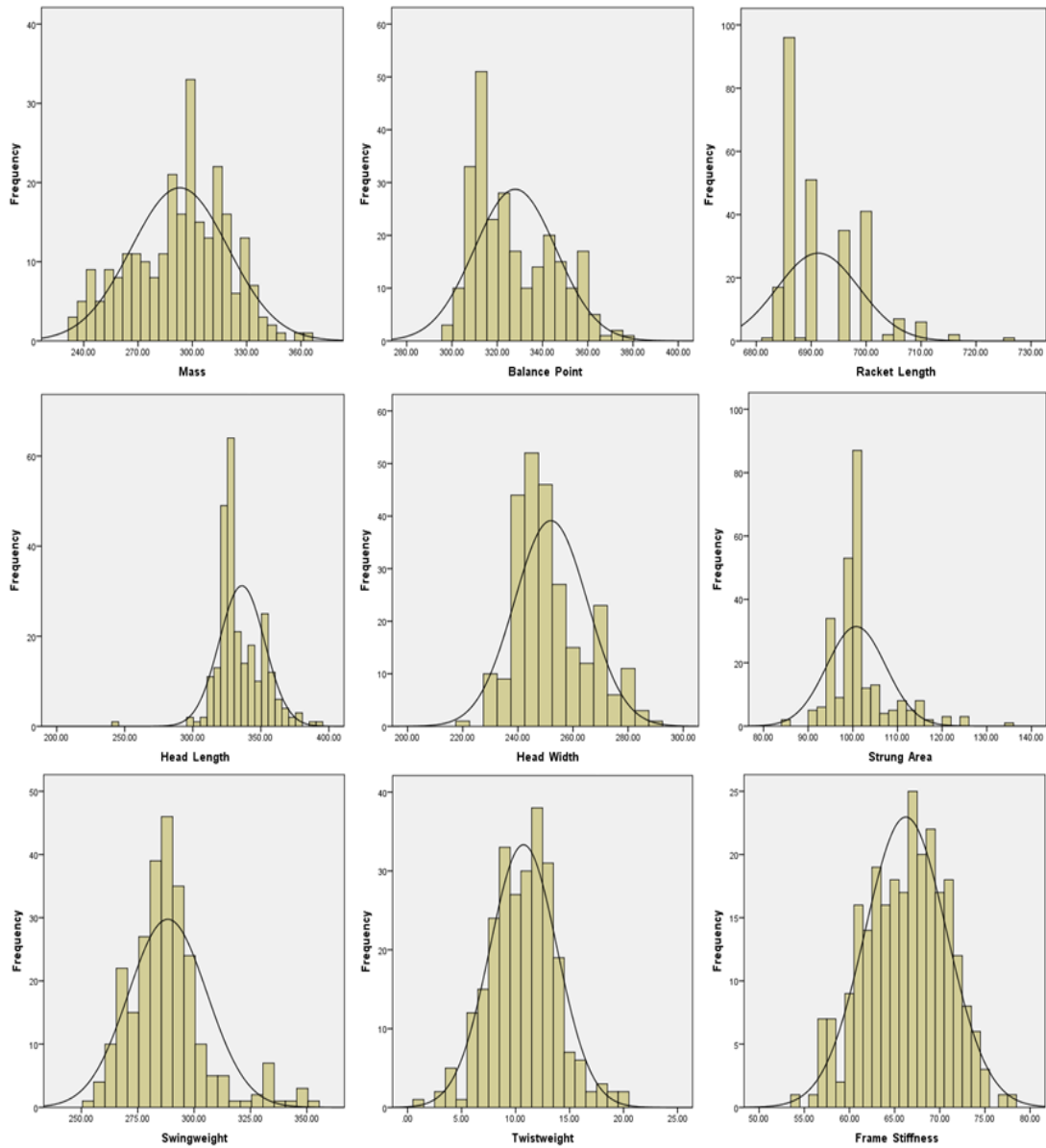
Figure 22 - Range of Each Racket Property for all 321 Rackets found within the ITF Racket Library
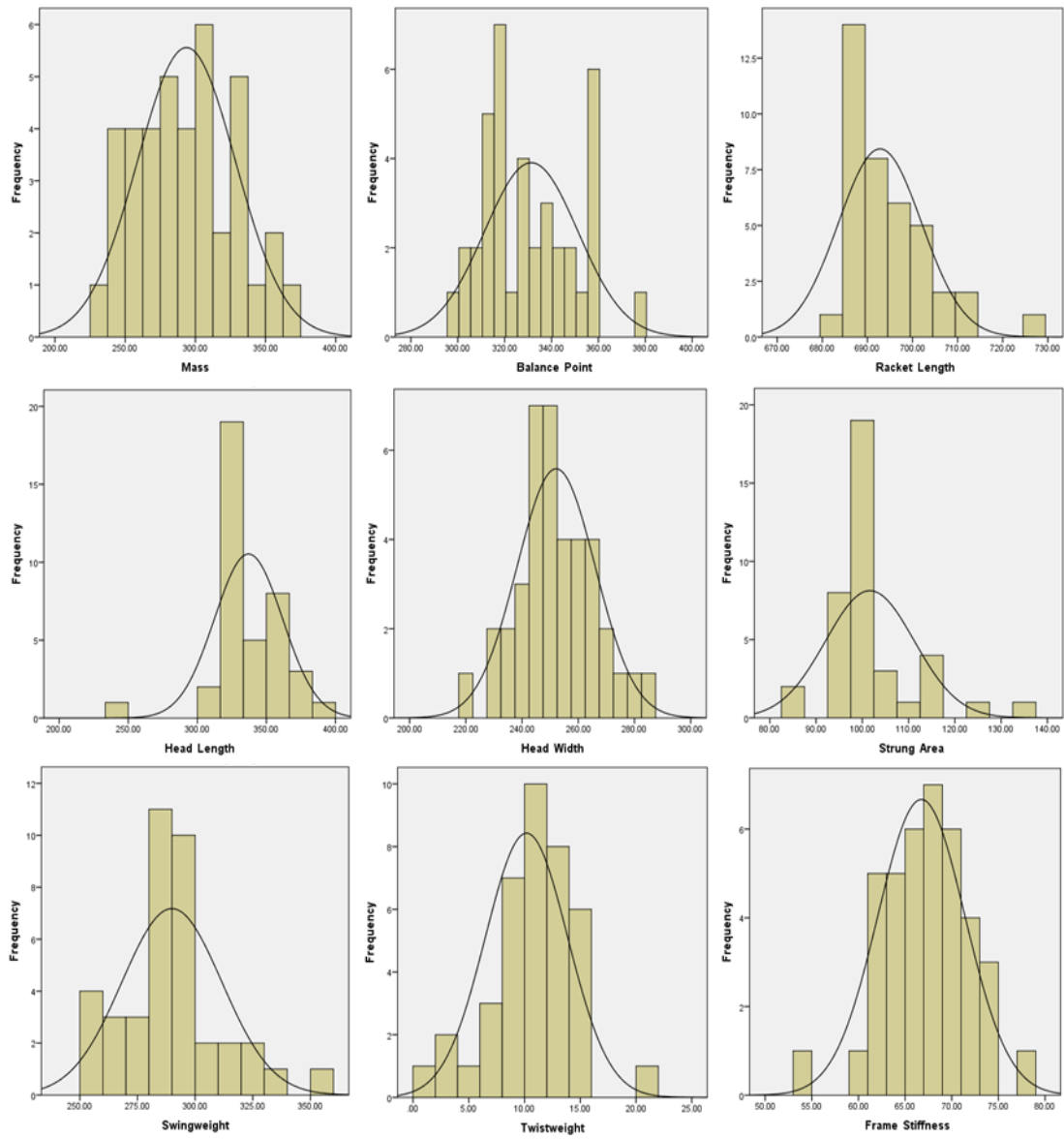
Figure 23 - Range of Each Racket Property for the Selected 39 Tennis Rackets

Table 5 - The Property Means and Standard Deviations for All and Selected Rackets

Racket Property	All Rackets (N = 321)	Selected Rackets (N = 39)
Mass (g)	293 ± 27	294 ± 35
Balance Point (mm)	328 ± 18	331 ± 20
Racket Length (mm)	691 ± 8	693 ± 9
Head Length (mm)	336 ± 17	337 ± 25
Head Width (mm)	252 ± 13	252 ± 14
Strung Area (in^2)	101 ± 7	102 ± 10
Swingweight (RDC)	288 ± 17	290 ± 22
Twistweight (RDC)	11 ± 3	10 ± 4
Frame Stiffness (RDC)	66 ± 5	67 ± 5

The Babolat racket diagnostics centre (RDC) is a machine which measures swingweight, twistweight and frame stiffness of a racket, providing results in RDC units. Though stated as RDC units, as results were obtained from the machine itself, both swingweight and twistweight are in fact given in kg·cm^2 units. Frame stiffness, however, is measured by the machine as a proprietary racket stiffness rating and stated as RDC units.

The Babolat RDC is an effective method to measure swingweight and twistweight of a tennis racket, however, previous research has found the accuracy of the machine to be subject to drift in the electronic components, especially for measurements of extreme values (Spurr et al. 2014). Such inaccuracies can be seen within the measured results of twistweight, to which some values were stated as 0 RDC reducing the fidelity of the data. Therefore,

caution must be taken when assessing the effects of twistweight on rebound characteristics.

4.4   *Simulating Realistic Forehand Conditions*

Realistic forehand shots can be simulated in a laboratory environment by changing the impact position and relative orientation of the racket and inbound ball. Player testing data and the results produced by the PCA, discussed in Chapter 3, ensures impact conditions representative of forehand shot found within the field of play.

4.4.1 Impact Position

Impact position is defined as the initial point of contact between the tennis ball and the racket strings. Whilst ensuring accurate forehand simulation within a laboratory environment, it is vital that this test parameter is truly representative of that found within the field of play.

Choppin (2008) and Hatze (1994) found that all players consistently aim to hit the ball toward the racket's node point, irrespective of the shot type they are playing. Although a player could generate a greater ball velocity hitting the ball toward the racket's throat (Choppin, 2008), it has been assumed that players learn to repeatedly aim for the node point due to the lack of vibration upon impact providing a better response at the player's hand in terms of racket feel.

With the aid of such results, it was concluded that the node point (NP) be the ideal impact position for laboratory forehand simulation, illustrated in Figure 24.
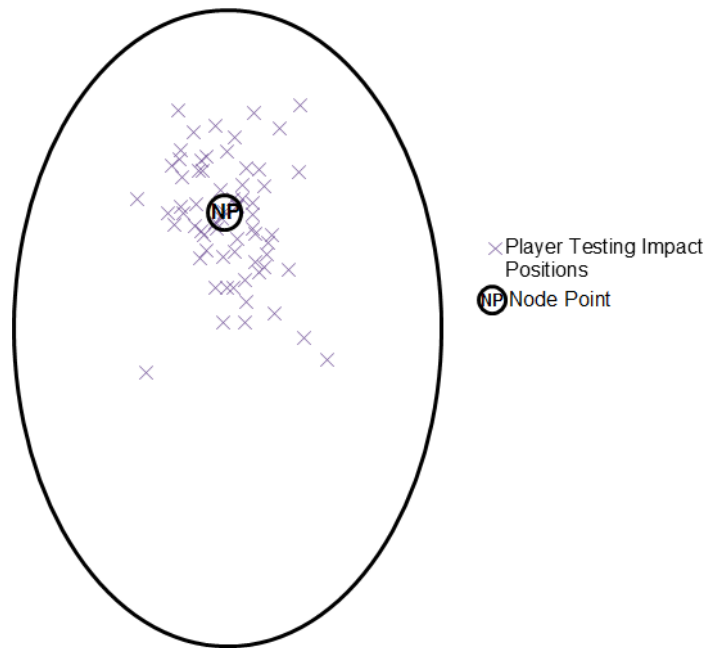
Figure 24 - The Node Point Illustrated Using a Tennis Racket of Average Dimensions in Relation to the Player Testing Data

Although player testing results have found the desire to hit the ball at the racket's node point, results have also revealed low levels of success for every impact. More specifically, many players have been found to hit the ball considerably off the centre line of the racket (Choppin, 2008), portrayed by Figure 24. Therefore, additional impact positions must also be varied along both the longitudinal (x-axis) and transverse axes (y-axis) of the racket.

Spurr (2017) quantified the inherent variability of the test apparatus and test objects to ensure an efficient and sufficient testing procedure. A total of 422 ball-racket impacts were recorded, relative to the geometric string centre (GSC), to quantify the inherent variability of the BOLA. Results identified a root mean squared error of 0.011m and 0.031m of the transverse and longitudinal axis respectively.

Using the results quantified by Spurr (2017) and Choppin (2008), whilst taking into consideration the geometry of the previously selected rackets to reduce the risk of the ball-racket frame impacts, an additional 4 impact positions were selected. With reference to the node point (0, 0 mm), the additional impact positions are as follows: 1 (+60, 0 mm), 2 (-60, 0 mm), 3 (0, +60 mm),

4 (0, -60 mm). The five impact positions are illustrated in Figure 25, with the provision of a tennis racket consisting of average dimensions.
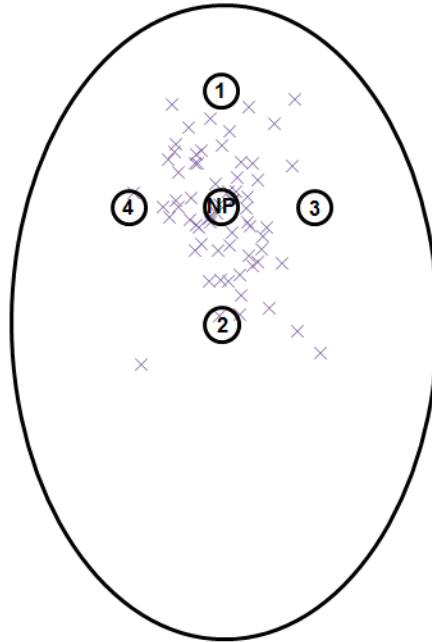
Figure 25 - All Impact Positions Illustrated Using a Tennis Racket of Average Dimensions, with Reference to the Player Testing Data

The relevant impact positions for all selected rackets, measured from each of the racket's butt, can be found in Appendix C.

4.4.2 Forehand Simulation

Player testing results, used by the PCA in Chapter 3, are those of a moving ball and racket both with their own respective velocities. Brody (1997) exhibited a simple change in reference frame provides the potential to recreate impact conditions by firing a moving tennis ball onto a stationary tennis racket.

The PCA results, discussed in Chapter 3, identified three different forehand shots, two of which are feasible for laboratory simulation; a typical slice and topspin forehand. Creating more succinct clusters of forehand shots for laboratory simulation, box and whisker plots were conducted for each inbound parameter for the removal of outliers. For the topspin forehand, a total of 5 outliers were identified within the parameters of angular velocity about the y axis and linear velocities along x and z axes. Similarly, for the slice forehand, a

total of 2 outliers were identified within the parameters of linear velocities along the x and y axes. Table 6 shows the final results of the average racket components of linear and angular velocities for both a slice and topspin forehand. These components are also illustrated in Figure 26 and Figure 27.

Table 6 - Averaged Pre-Impact Component Linear and Angular Velocities, at a Racket's COM, for a Slice and Topspin Forehand

	Angular Velocity (rad/s)			Linear Velocity (m/s)		
	ω_{xr}	ω_{yr}	ω_{zr}	V_{xr}	V_{yr}	V_{zr}
Topspin Forehand	8.0	32.4	17.1	-3.8	7.2	18.6
Slice Forehand	3.5	21.2	-11.9	0.8	-6.2	16.9

To replicate representative forehand conditions in a laboratory environment, a relative resultant inbound ball velocity must be calculated. This calculation must also include the average inbound ball component velocities. Table 7 shows the average inbound component velocities of a tennis ball measured by Choppin (2008) at the 2006 Wimbledon Qualifying Tournament.

Table 7 - Average Inbound Component Velocities of a Tennis Ball

	Linear Velocity (m/s)		
	V_{xb}	V_{yb}	V_{zb}
Ball Velocity	-9.3	-0.6	1.1

The resultant inbound ball velocity is resolved from the relative x, y and z component linear velocities (V_x, V_y and V_z) using Pythagoras' Theorem, as shown in Figure 26.
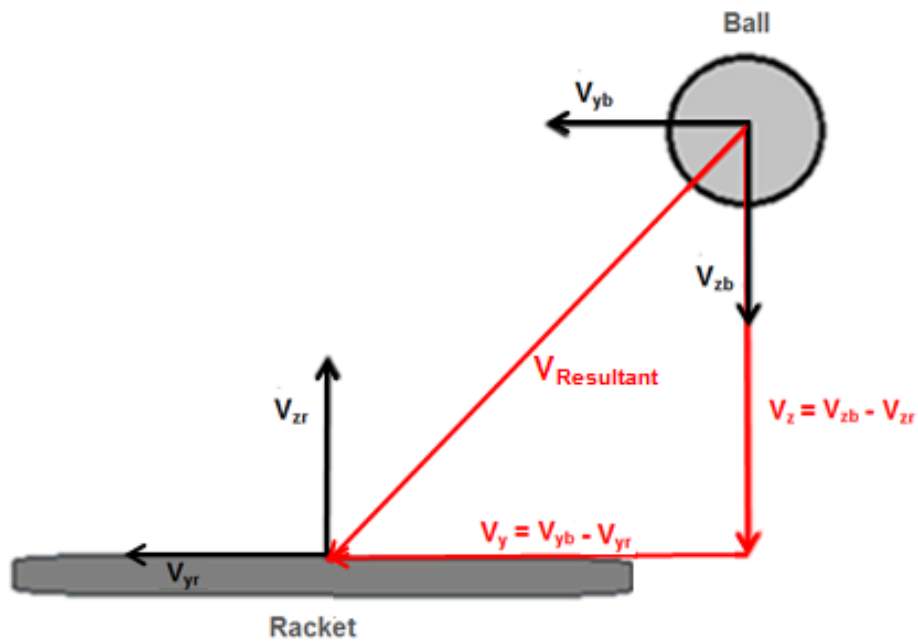
Figure 26 - Two Dimensional Illustration of the Use of Pythagoras' Theorem for Calculation

Relative to the impact position on the racket face, V_x, V_y and V_z are resolved from the racket's and ball's resultant linear velocities in the x, y and z axes and the racket's x, y and z angular velocities. The resultant inbound ball velocity is defined and calculated by Equation 9.

$$V_{imp}=\sqrt{(V_{xr}+V_{xb}+S\omega_{yr})^2+(V_{yr}+V_{yb}+T\omega_{zr})^2+(V_{zr}+V_{zb}+R\omega_{xr})^2} \qquad [9]$$

where S is the distance of the impact from the y-axis, T is the distance of the impact from the z-axis and R is the distance of the impact from the x-axis; depicted by Figure 27.
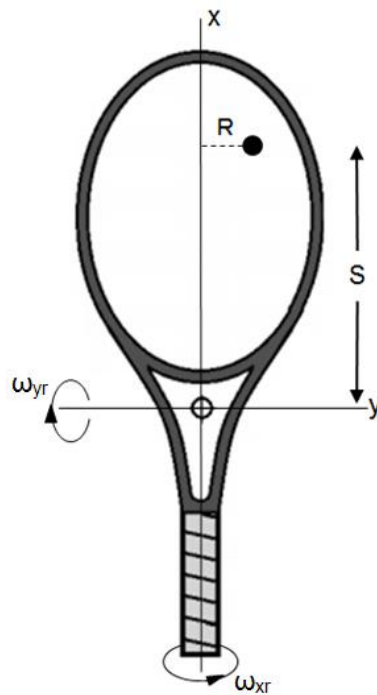
**Figure 27 - A Two Dimensional Diagram Aiding the Calculation of the *Vx, Vy,* and *Vz*
Component Velocities**

The resultant inbound ball velocity, however, is subject to change
relative to the desired impact position on the racket face. Consequently, for
each of the five previously selected impact positions, the inbound ball velocity
must be calculated respectively, for any given tennis racket. The results of
these calculations can be found in Appendix C.

The inbound ball spin rate and playing angle also play a vital role in
ensuring representative and realistic forehand simulations. Goodwill et al.
(2007) measured the spin rates of a tennis ball pre and post impact during a
Davis Cup match. The ball spin rates were measured for a range of tennis
shots, including serves and groundstrokes. Results found an average inbound
spin rate for a groundstroke of 3344 rpm, with a range between approximately
1000 and 5000 rpm. Kelley et al. (2009) used the same method as Goodwill et
al. (2007) to measure inbound spin rates during match play at the 2007
Wimbledon Qualifying Tournament. The mean spin rate off the ground was
found to be 3014 ±1208 rpm. Though reaching spin rates of approximately 3000
rpm would be ideal, the BOLA restricts the user through the selection of spin

levels (between 0 and 9). Preliminary testing identified level 7 and level 8 to produce approximately 2200 rpm and 4000 rpm respectively. It was therefore concluded, with reference to the previously stated real play data, selection of an inbound ball spin rate of 2200 rpm is not only representative of inbound conditions found within the field of play, but also achievable in a laboratory environment.

PCA results also identified representative playing angles for both respective forehand shots. Defined in Chapter 3, playing angle is the angle in which the ball impacts the racket face relative to the normal. Table 8 shows the average playing angles to be used, when testing, for a slice and topspin forehand shots.

Table 8 - Average Playing Angles for Slice and Topspin Forehand Shots as Identified by the PCA

	Playing Angle (˚)
Topspin	-26
Slice	21

4.4.3 **Resistive Torque**

A representative resistive torque value can be found through the quantification of the forces exerted onto the racket handle by a player. During impact, the forces exerted onto the racket handle are a resultant of the forces of a chain of components within the arm. As previously mentioned, although the racket is kept stationary throughout testing, the three-dimensional movement of the racket, as a result of the chain of components within the arm, are accounted for within the calculation of the resultant inbound ball velocity.

Savage (2006) further quantified the forces exerted by the hand onto the racket handle at the point of a ball racket impact. A strain gauge cantilever system consisting of four cantilevers with strain gauges in two full Wheatstone bridge configurations was developed to quantify the force of the tennis grip in

real-time. An elite male tennis player was used for this study, for which the player's arm was strapped to a table. This allowed for the racket to be both hand-held and stationary, with no influence of racket swing speed; as at the time of impact, the racket is assumed stationary. Grip forces exerted by the distal phalanges, proximal phalanges, metacarpal-phalangeal joint and metacarpals were found to be 50 N, 175 N, 90 N and 200 N respectively, shown in Figure 28 (a). Figure 28 (b) shows the respective forces acting on the racket handle.
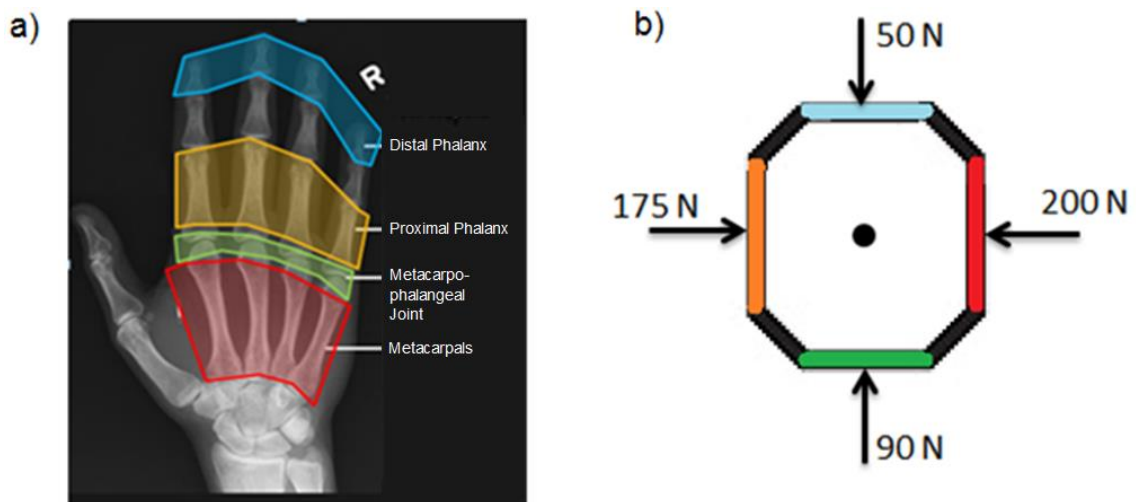
Figure 28 - a) Quantified Peak Forces of a Players Right Hand Acting on a, b) Tennis Racket Handle

Torque (τ) is defined as:

$$\tau = F \cdot d \qquad\qquad\qquad [10]$$

where F is the applied force, d is the perpendicular distance from the axis to the line of action of the force.

With respect to the equation, for ball-racket impacts, F refers to the forces exerted by the hand onto the racket handle. However, as previously stated for off axis impacts the racket is subjected to rotation about its longitudinal axis within the player's hand. Therefore, during rotation within the player's hand, the racket handle is also subjected to friction, illustrated by Figure 29.
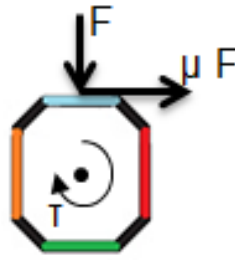
Figure 29 - Shear Force to Overcome Friction of a Dry Hand

The amount of torque (or moment force) applied to the racket handle to overcome a dry hand is given by:

$$\tau = \mu\, F \cdot d \tag{11}$$

where μ is the coefficient of friction between the hand and the racket handle and F is the quantified force exerted by the hand on the handle.

Common tennis grip materials consist of rubber, leather or synthetic polymer. The friction of coefficient between human skin and rubber has been found to be 0.9 (Seo & Armstrong, 2009). However, a friction coefficient of 1 can be used to assume an absolute maximum value of torque.

Assuming the racket handle to be circular, the diameter of an average handle is 33.7 mm. Therefore, the perpendicular distance from the axis of rotation to the applied force, d, is 16.87 mm (0.01687 m).

The calculated shear forces ($\mu\, F$), for a given μ of 1, equate to:

$$\mu\, F_1 = 200\ \text{N} \tag{12}$$

$$\mu\, F_2 = 50\ \text{N} \tag{13}$$

$$\mu\, F_3 = 175\ \text{N} \tag{14}$$

$$\mu\, F_4 = 90\ \text{N} \tag{15}$$

For each given shear force, a respective moment force is applied, shown by Figure 30.

71
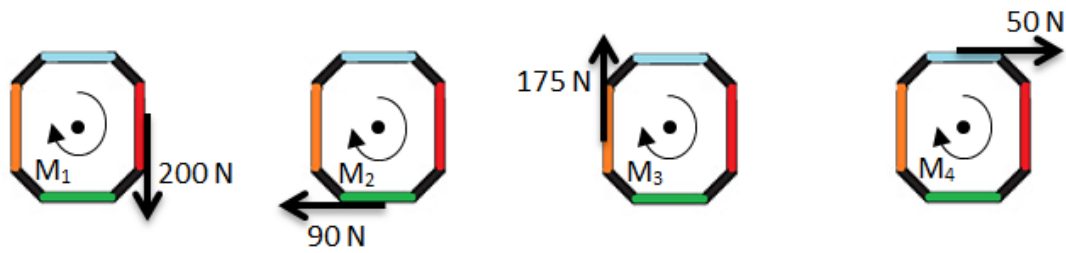
Figure 30 - Acting Shear Forces with their Respective Moment Forces

Therefore, the maximum torque applied to the racket handle is given as:

$$\tau < M1 + M2 + M3 + M4 \tag{16}$$

where,

$$M1 = \mu\, d\, F_1 \tag{17}$$

$$M2 = \mu\, d\, F_2 \tag{18}$$

$$M3 = \mu\, d\, F_3 \tag{19}$$

$$M4 = \mu\, d\, F_4 \tag{20}$$

Therefore,

$$\tau < \mu\, d\, F_1 + \mu\, d\, F_2 + \mu\, d\, F_3 + \mu\, d\, F_4 \tag{21}$$

$$\tau < \mu\, d\, (F_1 + F_2 + F_3 + F_4) \tag{22}$$

$$\tau < 1 \cdot 0.01687 \cdot (200 + 90 + 175 + 50) \tag{23}$$

$$\tau < 8.7 \text{ Nm}$$

4.5 *Appropriate Number of Test Repeats*

Preliminary testing by Spurr (2017) revealed inherent variability involved with oblique racket testing. For the discussed impact testing methodology, it is vital impacts are not affected by the identified inherent variability.

Monte Carlo simulation is a statistical technique used to model probabilistic systems and establish the odds for a variety of outcomes. A Monte Carlo simulation essentially uses random inputs, within realistic limits, to model

the system and produce probable outcomes (Mohsen G, Al-Fuqaha, Rayes, & Khan, 2010). With the use of preliminary input data, the Monte Carlo simulation will consider the range of possibilities to help reduce the uncertainty regarding an appropriate number of test repeats.

Preliminary impact testing, recording 42 impacts for the slice and topspin forehand, was conducted using the desired inbound parameters previously discussed. These parameters include: an inbound spin rate of approximately 2200 rpm topspin and 2200 rpm backspin, a playing angle of 21˚ and -26˚ and an average resultant inbound velocity of 29 m/s and 36 m/s for a slice and topspin forehand respectively. The Monte Carlo simulation was then run varying the number of test repeats from 3 to 20, for a total of 1000 iterations, using the digitised inbound ball spin, velocity and playing angle.

For each varying number of repeats, the mean and standard deviation of the mean was calculated using the results produced by the Monte Carlo simulation. The results of this calculation identified that as the number of test repeats increases, the variance for inbound ball spin, velocity and playing angle decreases for both topspin and slice forehand simulations. More specifically the results identified inbound spin to possess the largest variance, shown by Figure 31.
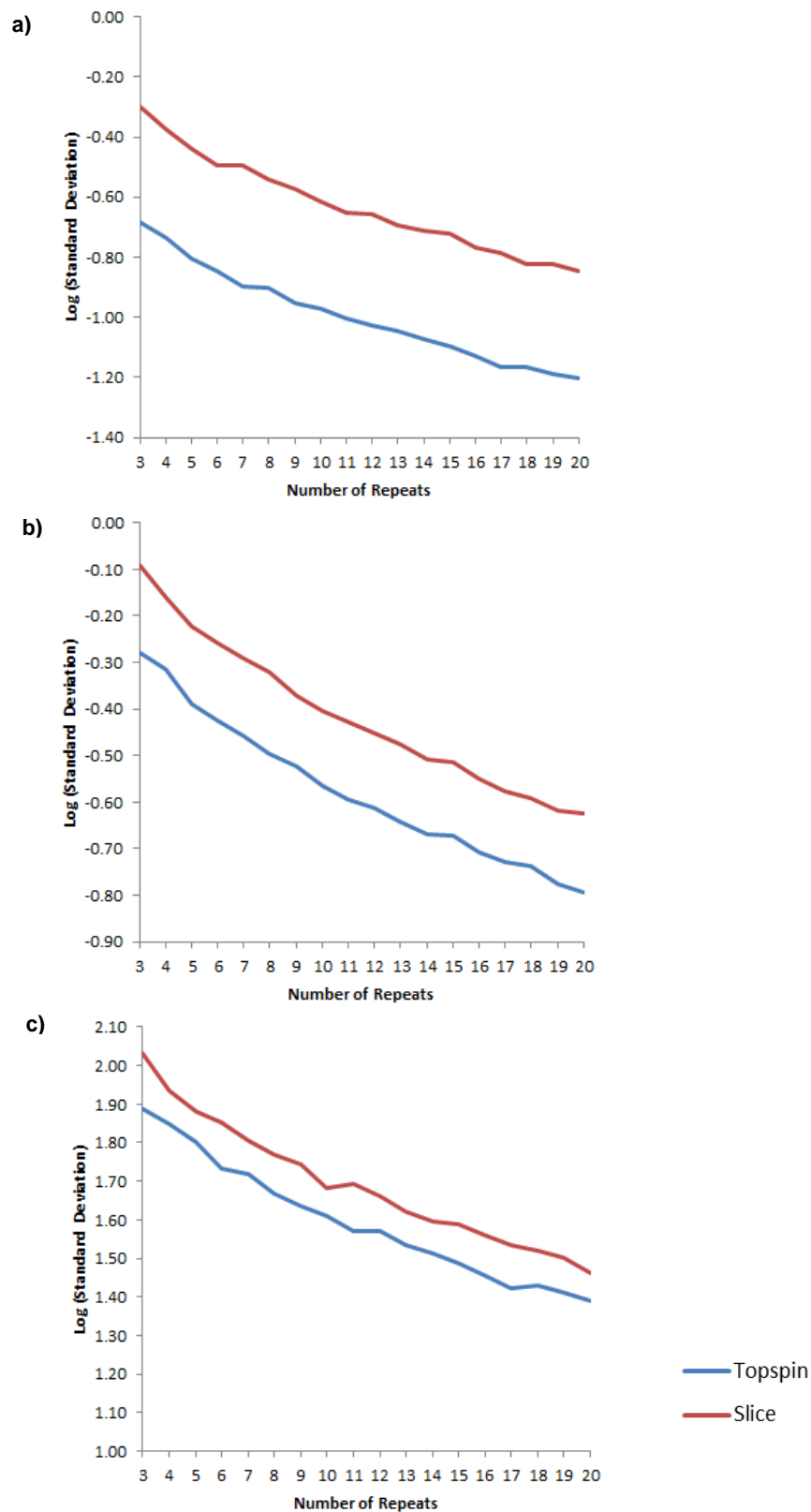
**Figure 31 - Log Results to Show the Change in Standard Deviation for a) Velocity,
b) Playing angle, c) Spin**

To ensure a repeatable data collection process, the logical solution is to increase the number of impact test repeats. However, increasing the number of test repeats also increases the total testing time. Further analysis of the inbound ball variability, for an average slice and topspin forehand, discovered that a total of 12 repeats decreased the inbound ball spin variance but also provides a balance between repeatability and practical feasibility.
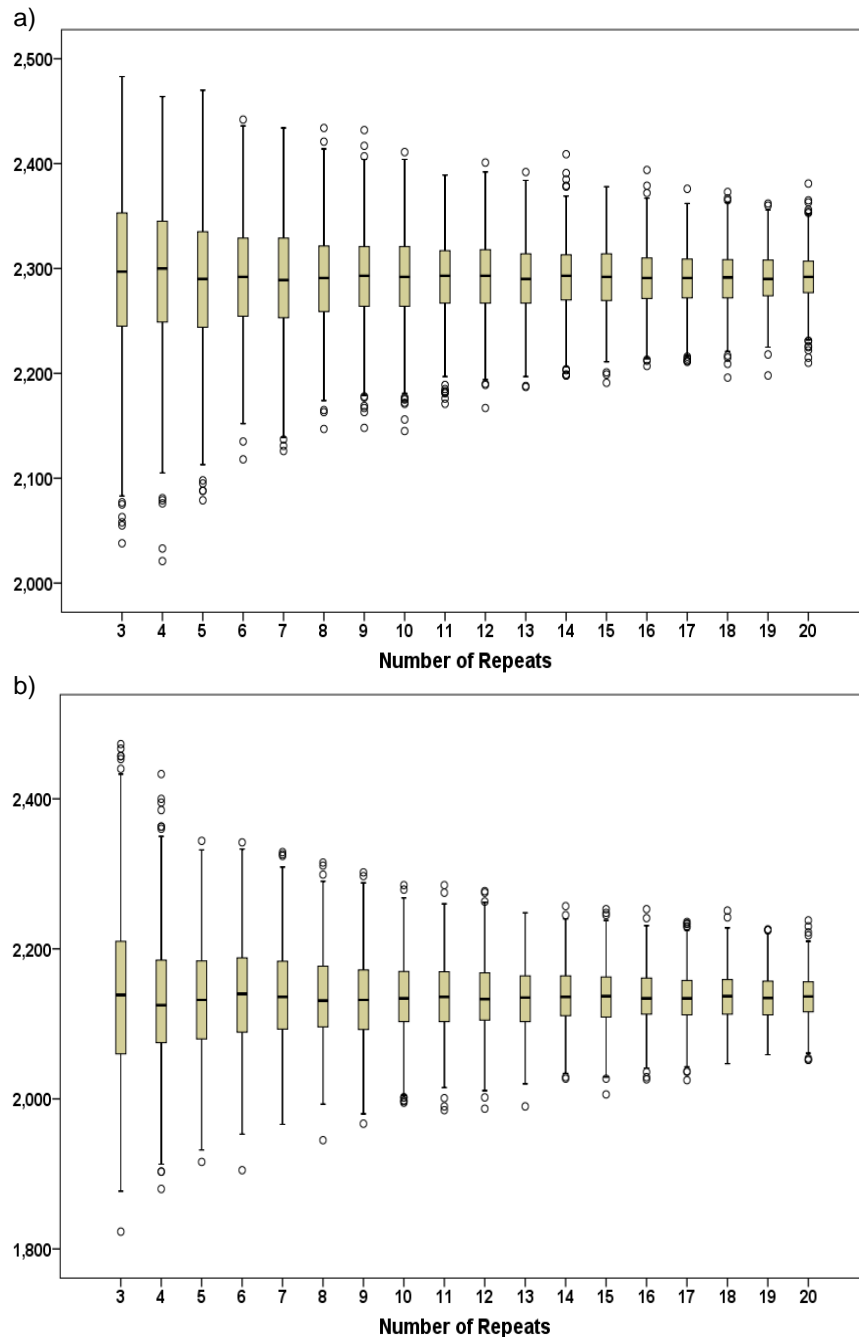
Figure 32 - Whisker Box Plots of Inbound Ball Spin for a) Topspin Forehand b) Slice Forehand

75

Summary of Experimental Input Parameters for Forehand Simulation

Table 9 summarises the discussed input parameters required to ensure realistic laboratory simulation of two distinct forehand shots; a topspin and slice forehand. As previously discussed, the resultant inbound ball velocity is subject to change relative to the desired impact position on each of the respective racket faces. For each forehand simulation, the results of the resultant inbound ball velocities, relative to each impact position for each selected racket, can be found in Appendix C.

Table 9 - Summary of Input Parameters for Forehand Simulations

	Inbound Playing Angle (˚)	Inbound Offset Angle (˚)	Inbound Ball Spin (rpm)	Racket Angular Velocity (rad/s)			Racket Linear Velocity (m/s)			Inbound Ball Velocity (m/s)			Resistive Torque (Nm)	Number of Repeats	Impact Position (mm)
				ω_{xr}	ω_{yr}	ω_{zr}	V_{xr}	V_{yr}	V_{zr}	V_{xb}	V_{yb}	V_{zb}			
Topspin Forehand	-26	0	2200	8.0	32.4	17.1	-3.8	7.2	18.6	-9.3	-0.6	1.1	8.7	12	NP (0,0) 1 (+60, 0) 2 (-60, 0) 3 (0, +60) 4 (0, -60)
Slice Forehand	21	0	2200	3.5	21.2	-11.9	0.8	-6.2	16.9	-9.3	-0.6	1.1			

4.6 *Conclusion*

This chapter describes the design of the impact test rig used to launch tennis balls onto a realistically supported tennis racket. The positioning of the tennis racket could be altered allowing impacts of multiple positions on the racket face. A BOLA machine, attached to the impact test rig, applies a desired level of spin to the ball when launching it at an oblique angle onto a horizontal and stationary tennis racket.

Data collection from the 2006 Wimbledon Qualifying Tournament found that players aim to hit the ball toward the racket's node point, with low success rates for every impact. The results informed the selection of the impact positions and are subject to change based on the position of the node point for any given racket. A range of rackets possessing different racket properties and property combinations were obtained for testing.

To simulate realistic forehand conditions the results of the PCA, discussed in Chapter 3, was used to identify the characteristics of a typical slice and topspin forehand. The results were then used to calculate the resultant inbound ball to racket velocity, relative to the impact position on the racket face. Representative playing angles were also identified within the results for an average topspin and slice forehand shot. Player testing data from the Davis Cup and Wimbledon qualifying tournament revealed realistic and attainable inbound ball spin rates.

To replicate a player's grip on the racket handle, a torque limiter was used to restrict racket rotation around the longitudinal axis. Quantified forces exerted onto the racket handle by a player during impact were used to calculate a representative resistive torque value of 8.7 Nm.

The inherent variability of the BOLA was assessed to determine the repeatability of the launch velocity, spin and playing angle. Inbound ball spin was identified to have the largest variance, but was found to decrease with an increase of repeats. From this evaluation, the number of inbound repeats was increased from 3 to 12.

5 Laboratory Testing - Testing and Results

5.1 *Introduction*

Chapter 4 discusses the development of a laboratory-based test protocol which measures input and output variables of a ball impact on a stationary racket. Through the use of previously collected player testing data, the test will accurately simulate specific forehand shot characteristics on a variety of stationary rackets possessing a range of properties and property combinations.

Although the methodology discussed in Chapter 4 aids with the development of an efficient and effective data collection process, the material properties of the equipment in use must also be considered. Ball and string degradation are known to have an effect on the rebounding tennis ball. To ensure negligible effects a structured and comprehensive test set up was implemented prior to laboratory impact testing. This included stringing the tennis racket, acclimatising the tennis balls and setting the laboratory climate conditions.

The ranges of the recorded rebound parameters are quantified and presented using histograms and tables for all five impact positions and the average of each parameter specific to the individual impact positions respectively.

5.2 *Aim*

Using the methodology and apparatus discussed in Chapter 4, the aim of this chapter is to design an efficient, effective and consistent data collection process, in a carefully controlled environment.

5.3 *Experimental Procedure*

The player testing data also informed the selection of the impact positions, which are subject to change based on the position of the node point for any given racket.

Quantified forces exerted onto the racket handle by a player during impact were used to calculate a representative resistive torque value and will remain constant throughout testing.

Ensuring the apparatus' inherent variability has negligible effects, preliminary studies revealed a decrease in launch variance with an increase in the number of impact repeats. Consequently, the number of inbound repeats was increased accordingly.

5.3.1 Impact Area

The 1 m^3 impact area was designed to minimise the amount of space required for the impact, whilst ensuring sufficient space to capture the ball prior and post impact. The area also considered enough space to accommodate a person and checkerboard in order to calibrate the volume for 3D analysis. The ball projection device was accommodated at the front of the impact area, with a net accommodating the rear, to catch the rebounding ball after impact. Two Phantom high-speed cameras were set up to one side of the impact area and recorded at 4000 fps. The two cameras were set to a resolution of 800-by-600 pixels, with an exposure time of 100 µs, and were connected via the *f-sync* output to synchronise the captured frames. A light gate attached to the front of the BOLA barrel, as previously mentioned, was connected to each of the cameras, ensuring coherent triggering for each impact. Two 500 W halogen lights were set up next to each camera, ensuring adequate lighting was provided for the recording of each impact. Figure 33 displays the discussed impact area, used throughout testing.

Figure 33 - Designed Impact Area

The designed impact area was situated in a room in which the laboratory climate conditions could be adjusted. Studies have identified that temperature and humidity can affect tennis ball properties; high humidity can increase the mass of the ball by increasing the moisture content and high temperatures can increase ball bounce height. Therefore, in keeping with ITF recommendation and standards, the laboratory operated at a temperature of 20 +/- 2° C and at 60 +/- 5 % relative humidity (ITF, 2017c). Temperature and humidity were monitored and recorded every 30 minutes to ensure a consistent climate for all impacts.

5.3.2 Tennis Balls

For all ball-racket impacts, approved 2017 ITF Technical-Specification tennis balls were used. It is known that the BOLA's launching mechanism degrades the tennis ball felt and softens the ball's rubber core for repeated launches. Previous research, as discussed in Chapter 2, quantified the effects of ball degradation due to the BOLA and suggested a limit of 50 impacts per

ball. The discussed test protocol calls for a total of 60 impacts for each simulated forehand shot. Therefore, for each forehand simulation two 2017 ITF Technical-Specification tennis balls, acclimatised for 24 hours, were used on rotation.

Three mutually perpendicular black lines were added to the ball to facilitate spin measurements; using a permanent marker pen to ensure durability throughout the repeated impacts. The marked lines provided a pattern for the algorithm to recognise, assisting spin measurement between high-speed camera frames.

Figure 34 - Black Lines Marked on a Tennis Ball to Facilitate Spin Measurements (Spurr, 2017)

5.3.3 Racket Strings

ITF polyester strings were used for all ball-racket impact testing and, in line with manufacturer's tension recommendations, were strung at approximately 60 lbs (267 N). Each racket was strung using a Prince 3000 Electronic Stringing Machine, shown in Figure 35. The amount of tension required and speed of the pull was set, to 60lbs and medium respectively, using the electronic tension head. The speed of the pull was altered based on the material of the string in use, for which a medium pulling speed was best suited for polyester strings.

Figure 35 - a) Prince 3000 Electronic Stringing Machine Used in the, b) Stringing Process

The string subjected to a tension force results in string elongation. Even if the tension force is held constant the string will keep stretching, at a slow rate for hours, effecting the stiffness (or tension) of the stringbed. This effect, also known as creep, is caused by the gradual breakage and slippage of bonds in the material that are subjected to the tension force. It has therefore been suggested to allow the stringbed to settle, once strung. Decreases in stringbed stiffness have been identified with ball-stringbed impacts over time (Brody et al., 2002; Goodwill, 2002), as previously discussed in Chapter 2.

Decreases in stringbed stiffness, due to creep or impact, are inevitable. The effects, however, can be assumed negligible if all aspects of stringing and impacting are kept consistent. To minimise the effects of decreased stringbed stiffness due to impact, the order in which the impact positions were targeted, for each simulated forehand, was kept consistent throughout testing. To

minimise the effects of decreased stringbed stiffness due to creep the racket was strung 24 hours prior to testing, thus providing a coherent timeframe whilst also allowing time for the stringbed to settle (Brody et al., 2002).

5.3.4 **Racket Position Accuracy and Repeatability**

The accuracy and repeatability of the racket positioning were identified as a source of impact position variability. Upon impact, the racket is subjected to translation in the y and z-axis and rotation about the x, y and z-axis. Racket rotation about the x and z-axis, illustrated in Figure 36, were found to be largely susceptible to variation. Ultimately, too much variation in racket positions would affect the effectiveness and efficiency of the previously discussed test protocol.
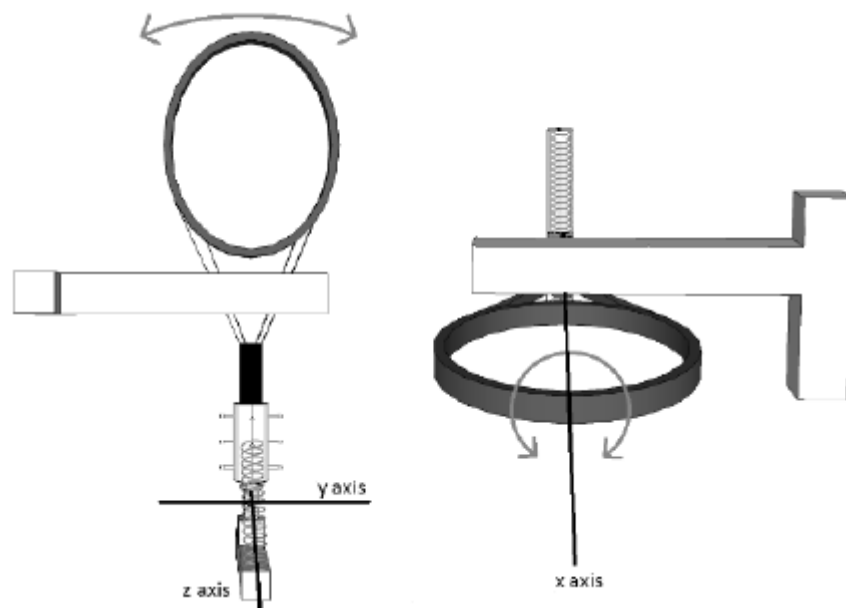
Figure 36 - Racket Rotation about the x-axis and z-axis

Racket alignment was a manual process and was inspected prior to each impact for each impact position, to minimise racket positioning variability. Prior research minimised the effects of the rotation about the z-axis and y-axis by aligning the racket with markers placed onto the restraining bar whilst also ensuring that both sides of the racket's throat touched the restraining bar (Spurr, 2017). Although effective for rackets of consistent sizing parameters, such

measures were not possible to achieve with rackets of varying lengths and head sizes.

To minimise the effects of the rotations about the x-axis, a calibrated electronic inclinometer was used to aid accurate racket alignment. The inclinometer was placed onto the stringbed surface and the racket was rotated until the inclinometer read $0.00°$. Figure 37 shows the inclinometer used in practice setting the racket stringbed parallel to the ground.

Figure 37 - The Electronic Inclinometer Used for Accurate Realignment

Racket alignment was ensured through the use of a BOLA insert laser pointer and stringbed markings of the desired impact positions relative to a given racket, prior to testing. Preceding every impact, the laser pointer was inserted into the front of the BOLA barrel and the racket beneath the BOLA was repositioned until the marking of the desired impact position was aligned with the trajectory of the laser pointer.

5.4 *Image Processing*

Digitisation of image coordinates (U, V) is a common measurement tool used to extract valuable point information. Combined with suitable calibrations, the extracted point information or U, V image coordinates can be reconstructed

into real-world X, Y, Z coordinates. This reconstruction then allows for the calculation of displacement, velocity and acceleration. Through appropriate calibration methods, two synchronised cameras provide the measures needed to reconstruct 2D images to 3D real-world coordinates, thus allowing for the calculation of displacement, velocity, playing and offset angles.

For a robust calibration model, a minimum of 40 images of an eight-by-eight checkerboard, with 30 mm-by-30 mm squares were taken throughout the test area volume. By having a minimum of 40 images, the camera sensor area was fully covered and the test area volume was adequately defined. Figure 38 (a) shows the visualisation of the calibration checkerboard as seen by the left and right camera respectively, whilst Figure 38 (b) shows all the checkerboard locations throughout the test area volume for the synchronised cameras. The largest calibration root mean squared (re-projection) error, for all recorded impacts, was recorded at ± 0.18 pixels.
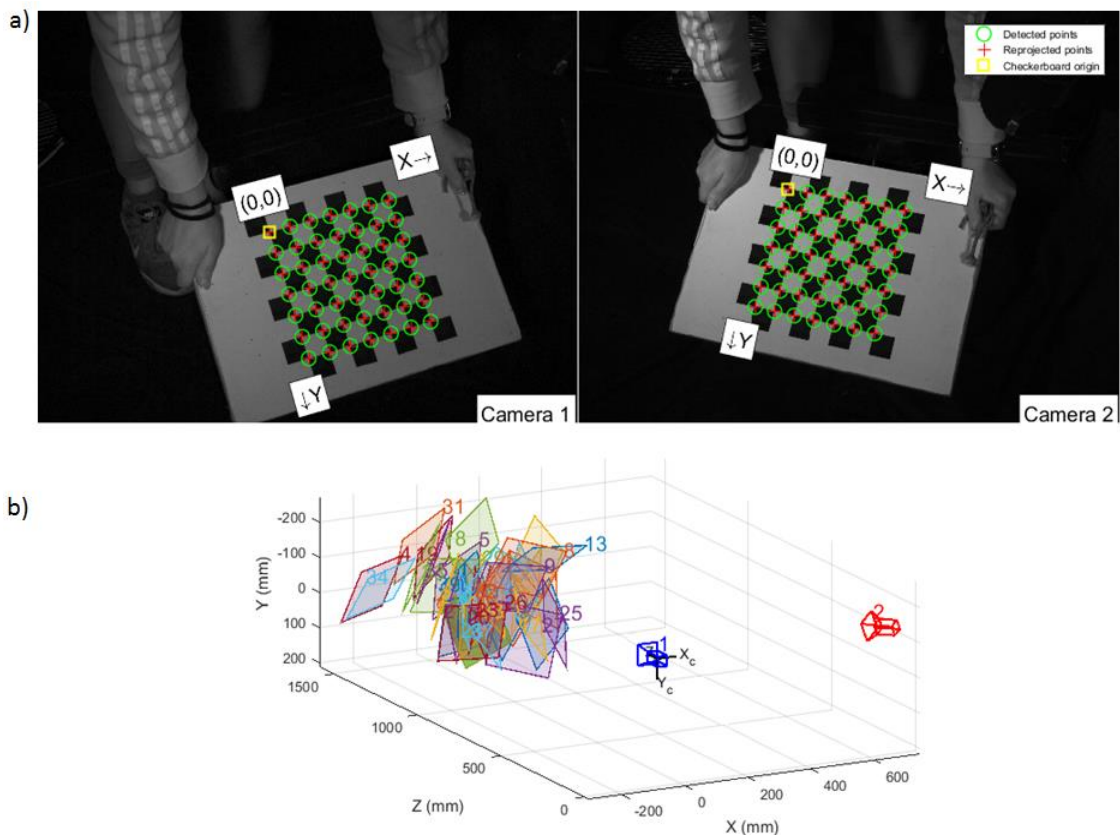
Figure 38 - Camera Calibration Checkerboard a) Seen by the Left and Right Camera Respectively and b) Located Throughout the Test Area Volume

The calibration process was completed within MATLAB and once the images had been processed, details of the intrinsic and extrinsic parameters of the camera were transferred into the MATLAB workspace. The ball centroids, within the images, were reconstructed into three-dimensional real-world coordinates using the camera calibration outputs and automated MATLAB algorithm, developed by Spurr (2017). The SpinTrack3D algorithm had also been modified and automated by Spurr (2017) for the measurement of ball spin. Ball spin was calculated using the cosine rule for given ball positions. The spin accuracy of the algorithm was measured through the simulation of zero-spin and high-spin within experimental setups. Mean absolute error for zero-spin and high-spin were found to be between 0.023 and 0.024 and -0.017 and -0.025 radians respectively.

The purpose of the algorithm was to automatically track the ball through a series of images, to facilitate data collection on a large scale. Figure 39 displays a visualisation of the MATLAB automated ball tracking algorithm for one ball racket impact.
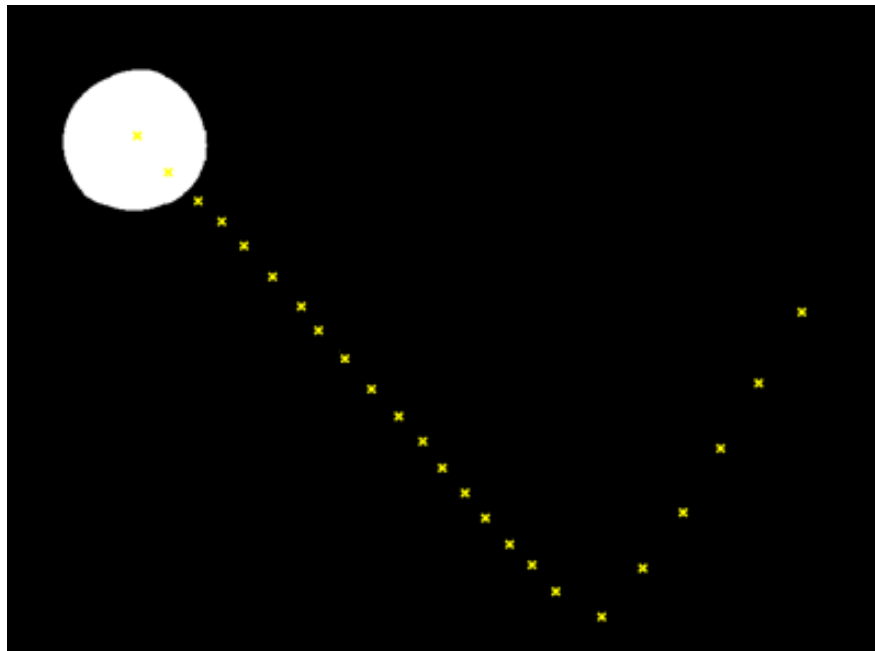
Figure 39 - Visualisation of the Automated Ball Tracking Algorithm

5.5 *Results*

This section investigates the range of values obtained through testing and image processing. The results are an average of the previously discussed 12 repeats and are presented for each simulated forehand separately. Although described previously, the rebound playing (α_2) and offset angles (β_2) are shown in Figure 40.
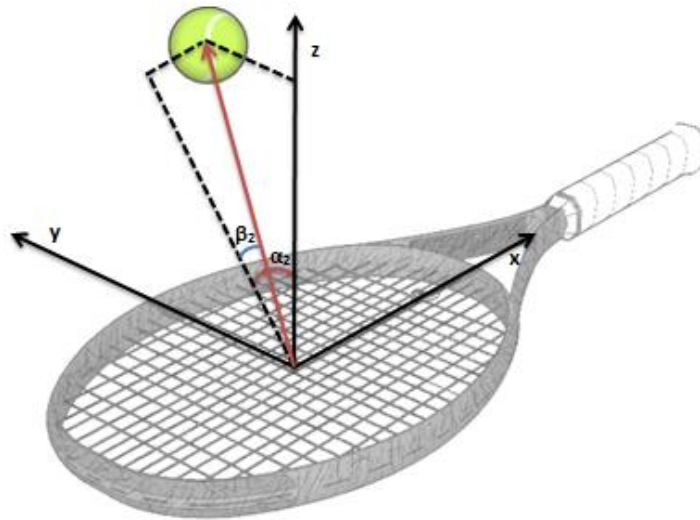
Figure 40 - Schematic of the Rebound Playing (α_2) and Offset Angle (β_2) Obtained after Impact

For this section, the impact positions will be referred to as Node Point, Impact 1, Impact 2, Impact 3 and Impact 4 and will represent the impact positions at the node point (0, 0 mm), (+60, 0 mm), (-60, 0 mm), (0, +60 mm), (0, -60 mm) respectively. Although previously discussed, the above impact positions are shown in Figure 41.
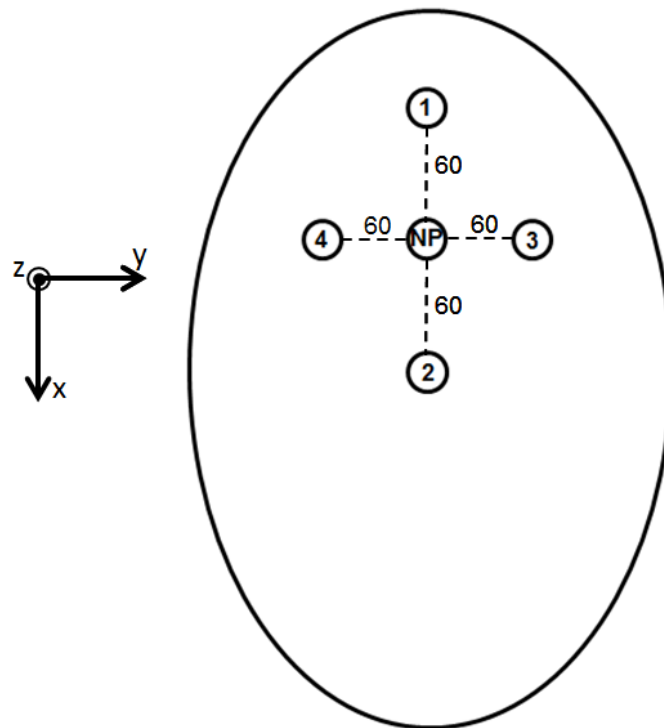
Figure 41 - A Depiction of the Selected Impact Positions

5.5.1 **Topspin Forehand**

The following results refer to the recorded impacts for all rackets, regarding the topspin forehand only.

Rebound Ball Spin

Figure 42 shows the spread of the rebound ball spin recorded for all five impact positions. The positive spin values denote topspin, associated with the completion of a topspin forehand. The mean spin values and standard deviations, for each impact position, are shown in Table 10.
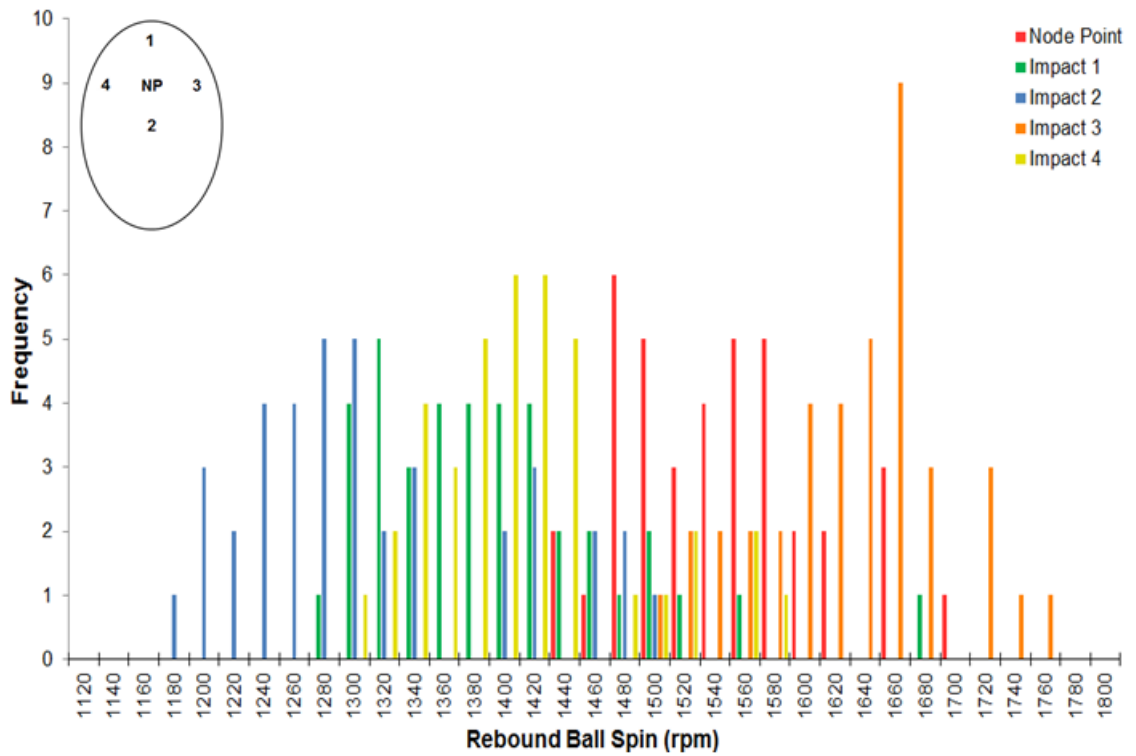
Figure 42 - A Frequency Histogram Showing the Rebound Ball Spin Values of All Five Impact Positions for the Topspin Forehand

Table 10 - Mean and Standard Deviation Rebound Spin Values of all Rackets for Each Impact for the Topspin Forehand

	Node Point	Impact 1	Impact 2	Impact 3	Impact 4
Mean (rpm)	1536	1385	1304	1620	1403
Standard Deviation (rpm)	63	82	89	61	68

Rebound Ball Velocity

The post impact ball velocity is the resultant of the x, y and z velocities of the rebound ball. The spread of these results are shown in Figure 43. Table 11 states each impact position's resultant rebound ball velocity averages and standard deviations.
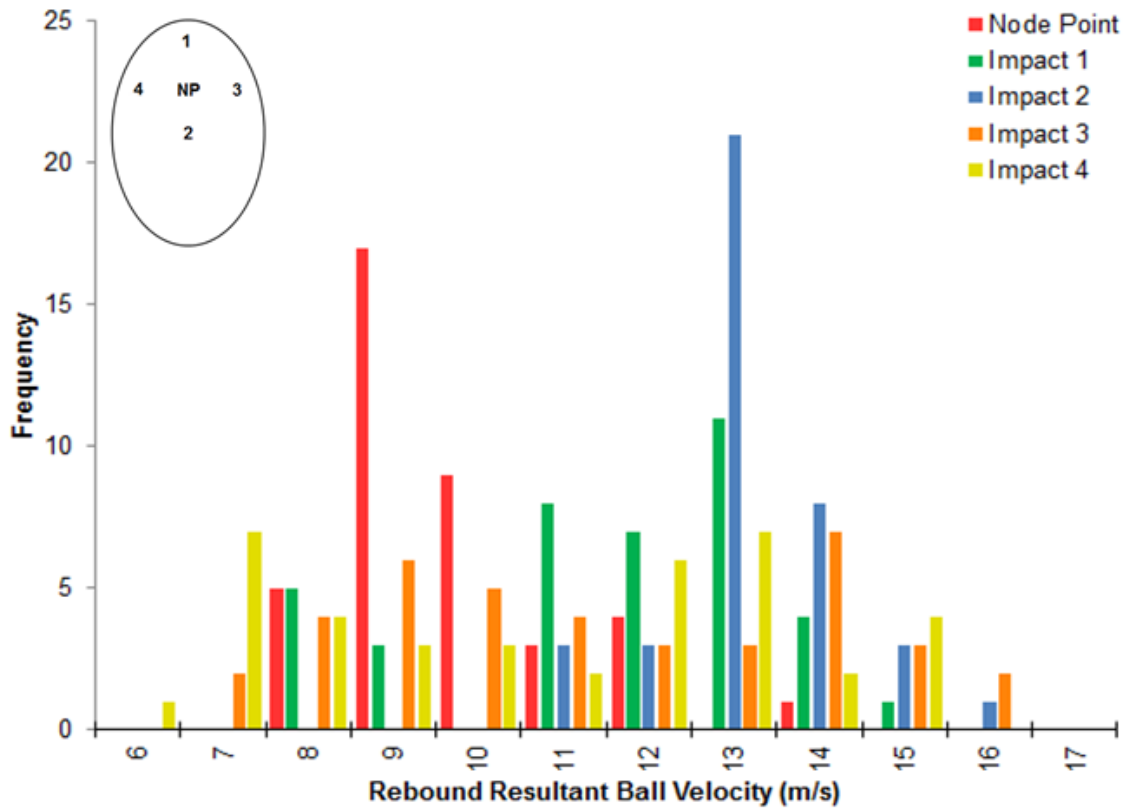
**Figure 43 - A Frequency Histogram Showing the Resultant Rebound Ball Velocity Values
of All Five Impact Positions for the Topspin Forehand**

**Table 11 - Mean and Standard Deviation Rebound Velocity Values of all Rackets for Each
Impact for the Topspin Forehand**

	Node Point	Impact 1	Impact 2	Impact 3	Impact 4
Mean (m/s)	9.2	11.0	12.7	10.8	10.1
Standard Deviation (m/s)	1.2	2.0	1.1	2.6	2.7

Rebound Playing Angle

Figure 44 shows the range of the rebound playing angle recorded at
each impact position for all 39 rackets. Presenting the means and standard
deviations for each impact position is Table 12.
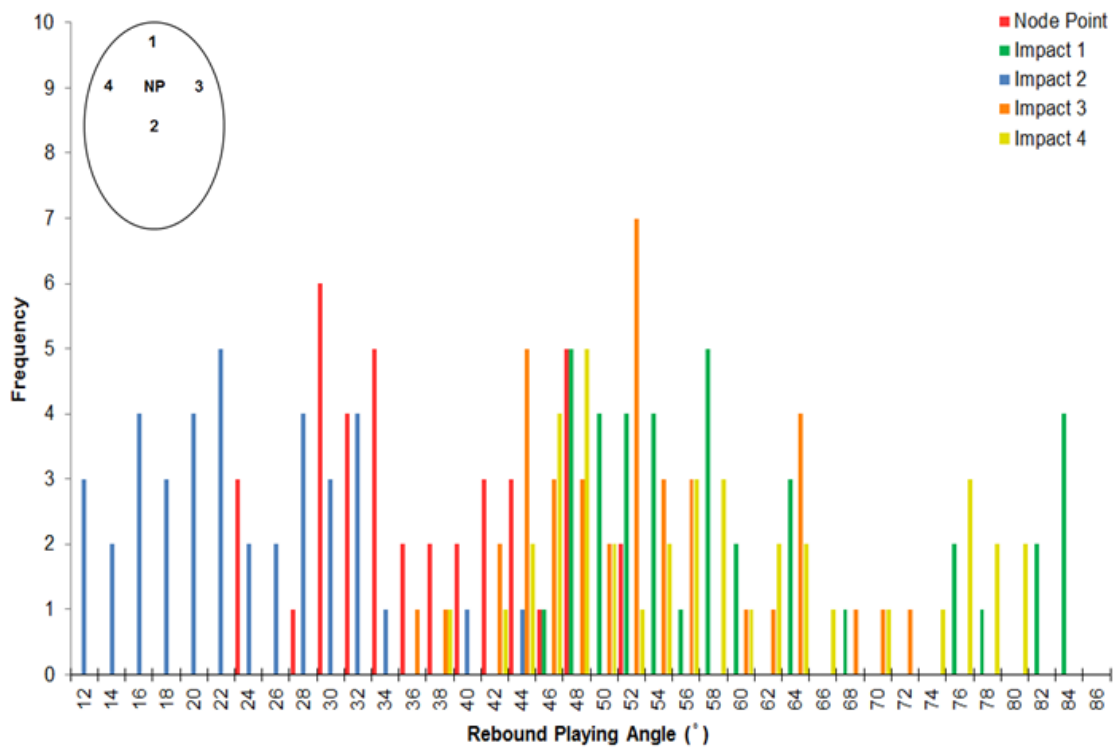
Figure 44 - A Frequency Histogram Showing the Rebound Playing Angle Values of All Five Impact Positions for the Topspin Forehand

Table 12 - Mean and Standard Deviation Rebound Playing Angle Values of all Rackets for Each Impact for the Topspin Forehand

	Node Point	Impact 1	Impact 2	Impact 3	Impact 4
Mean (˚)	36	60	22	51	57
Standard Deviation (˚)	8	12	8	9	12

Rebound Offset Angle

Figure 45 shows the spread of the rebound offset angle recorded for all five impact positions. The mean spin values and standard deviations, for each impact position, are shown in Table 13. The negative and positive rebound offset angles are a result of the direction of the rebounding tennis ball, relative to the perpendicular rebound playing angle.
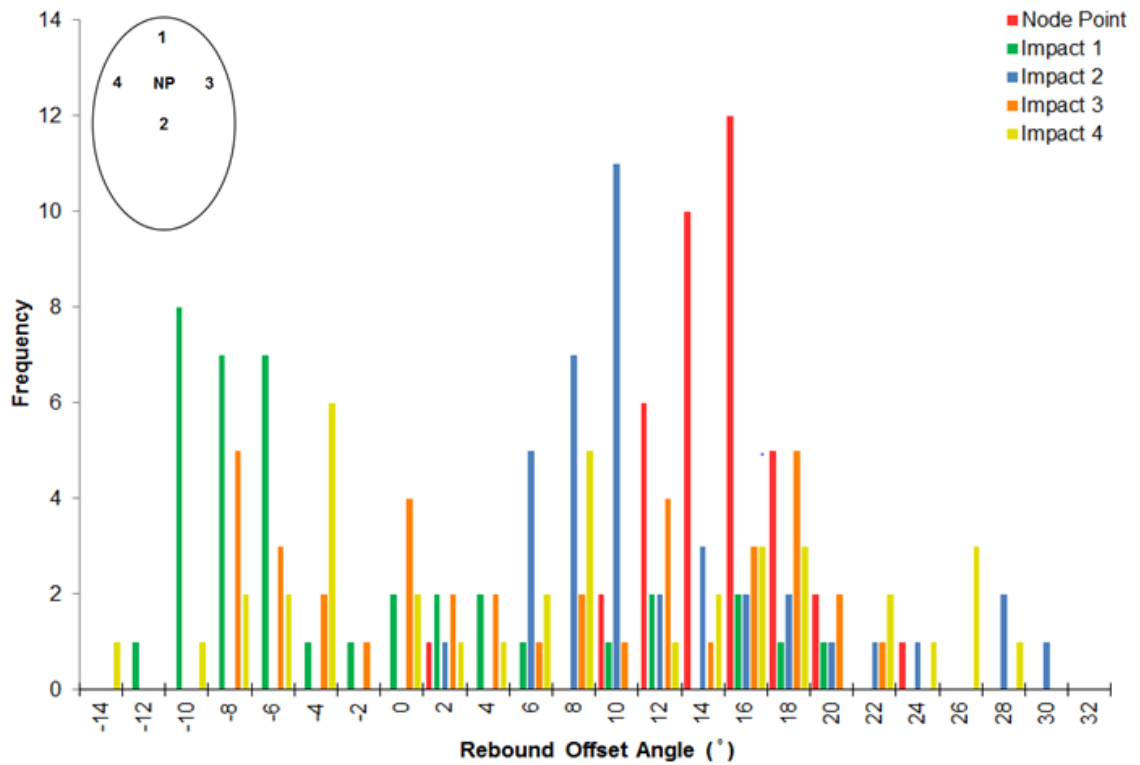
Figure 45 - A Frequency Histogram Showing the Rebound Offset Angle of All Five Impact Positions for the Topspin Forehand

Table 13 - Mean and Standard Deviation Rebound Offset Angle Values of all Rackets for Each Impact for the Topspin Forehand

	Node Point	Impact 1	Impact 2	Impact 3	Impact 4
Mean (˚)	14	-3	11	5	7
Standard Deviation (˚)	4	9	6	10	12

5.5.2 Slice Forehand

The following results refer to the recorded impacts for all rackets, regarding the slice forehand only.

Rebound Ball Spin

Figure 46 shows the spread of the rebound ball spin recorded for all five impact positions. The negative spin values denote backspin, associated with the

completion of a slice forehand. The mean spin values and standard deviation, for each impact position, are shown in Table 14.
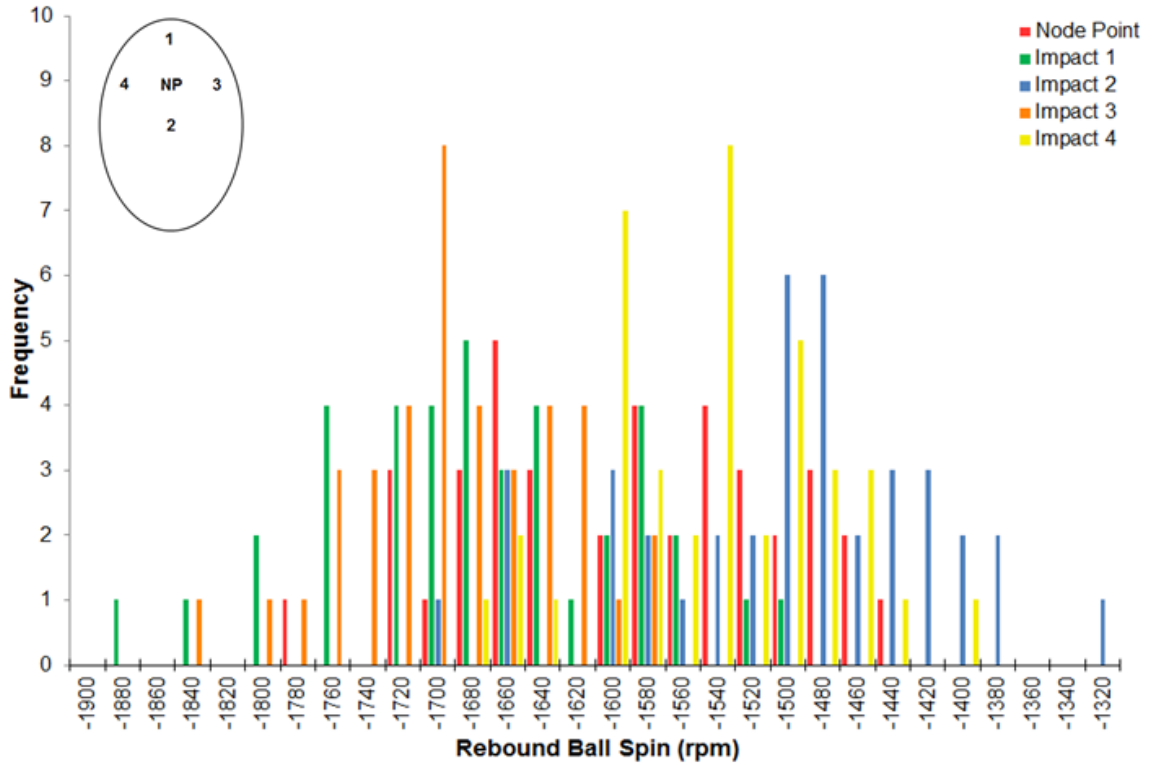
Figure 46 - A Frequency Histogram Showing the Rebound Ball Spin Values of All Five Impact Positions for the Slice Forehand

Table 14 - Mean and Standard Deviation Rebound Spin Values of all Rackets for Each Impact for the Topspin Forehand

	Node Point	Impact 1	Impact 2	Impact 3	Impact 4
Mean (rpm)	-1600	-1683	-1512	-1700	-1556
Standard Deviation (rpm)	84	75	80	59	62

Rebound Ball Velocity

As previously mentioned, the post impact ball velocity is the resultant of the x, y and z velocities of the rebound ball. Figure 47 shows the spread and the

range of rebound ball velocity. Table 15 presents each impact position's resultant rebound ball velocity averages and standard deviations.
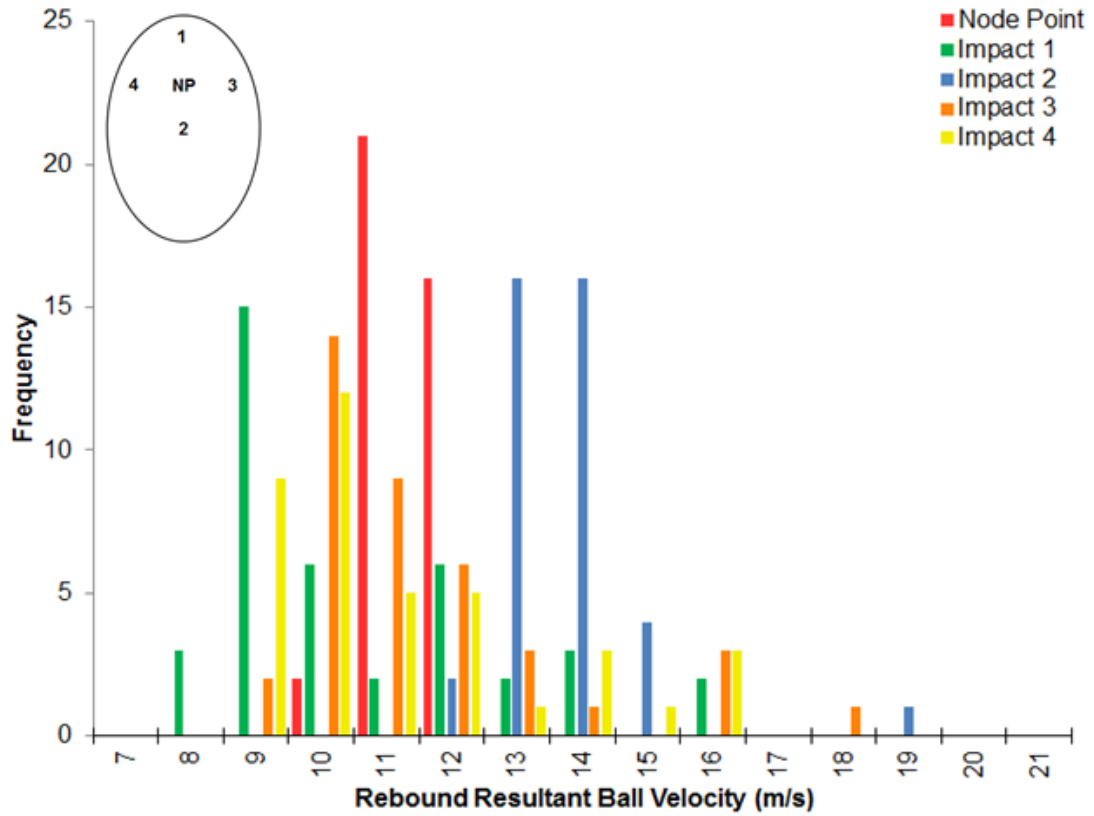
Figure 47 - A Frequency Histogram Showing the Resultant Rebound Ball Velocity Values of All Five Impact Positions for the Slice Forehand

Table 15 - Mean and Standard Deviation Rebound Velocity Values of all Rackets for Each Impact for the Topspin Forehand

	Node Point	Impact 1	Impact 2	Impact 3	Impact 4
Mean (m/s)	10.9	10.1	13.2	11.1	10.6
Standard Deviation (m/s)	0.5	2.1	1.1	2.0	2.1

Rebound Playing Angle

Figure 48 shows the range of the rebound playing angle recorded at each impact position for all 39 rackets. Presenting the means and standard deviations, at each impact position, is Table 16.
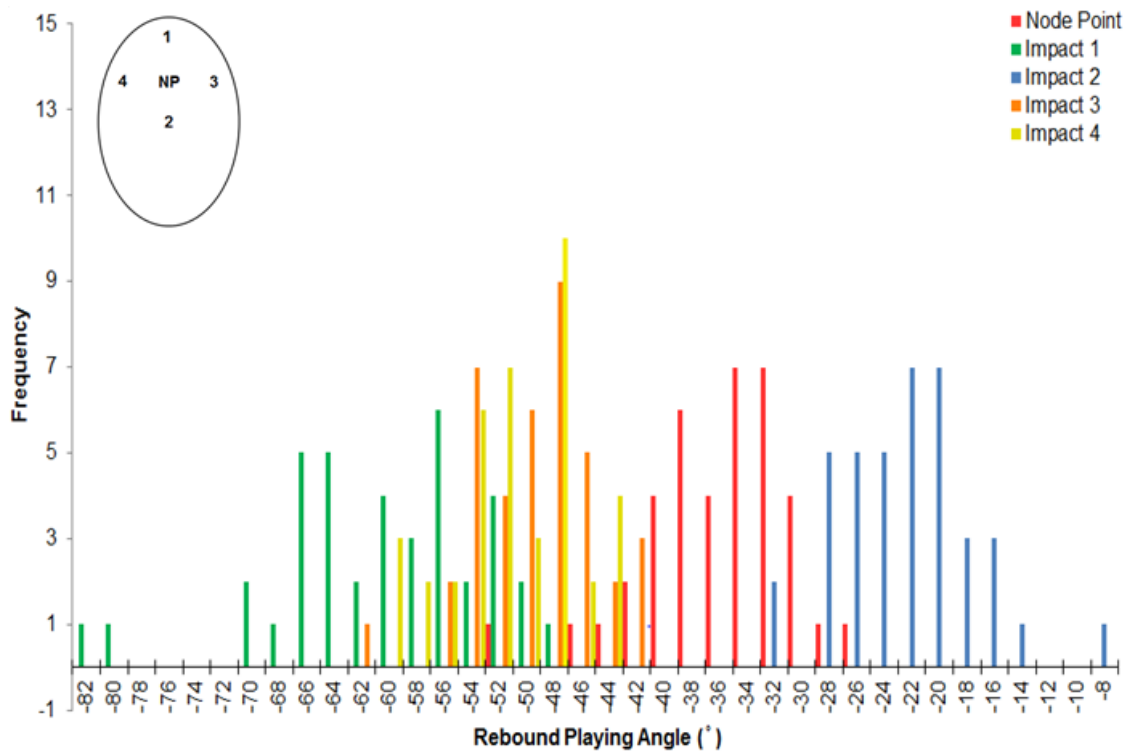
Figure 48 - A Frequency Histogram Showing the Rebound Playing Angle Values of All Five Impact Positions for the Slice Forehand

Table 16 - Mean and Standard Deviation Rebound Playing Angle Values of all Rackets for Each Impact for the Topspin Forehand

	Node Point	Impact 1	Impact 2	Impact 3	Impact 4
Mean (˚)	-36	-61	-24	-51	-52
Standard Deviation (˚)	3	6	4	4	4

Rebound Offset Angle

Figure 49 shows the spread of the rebound offset angle recorded for all five impact positions. The mean spin values and standard deviations, for each impact position, are shown in Table 17.
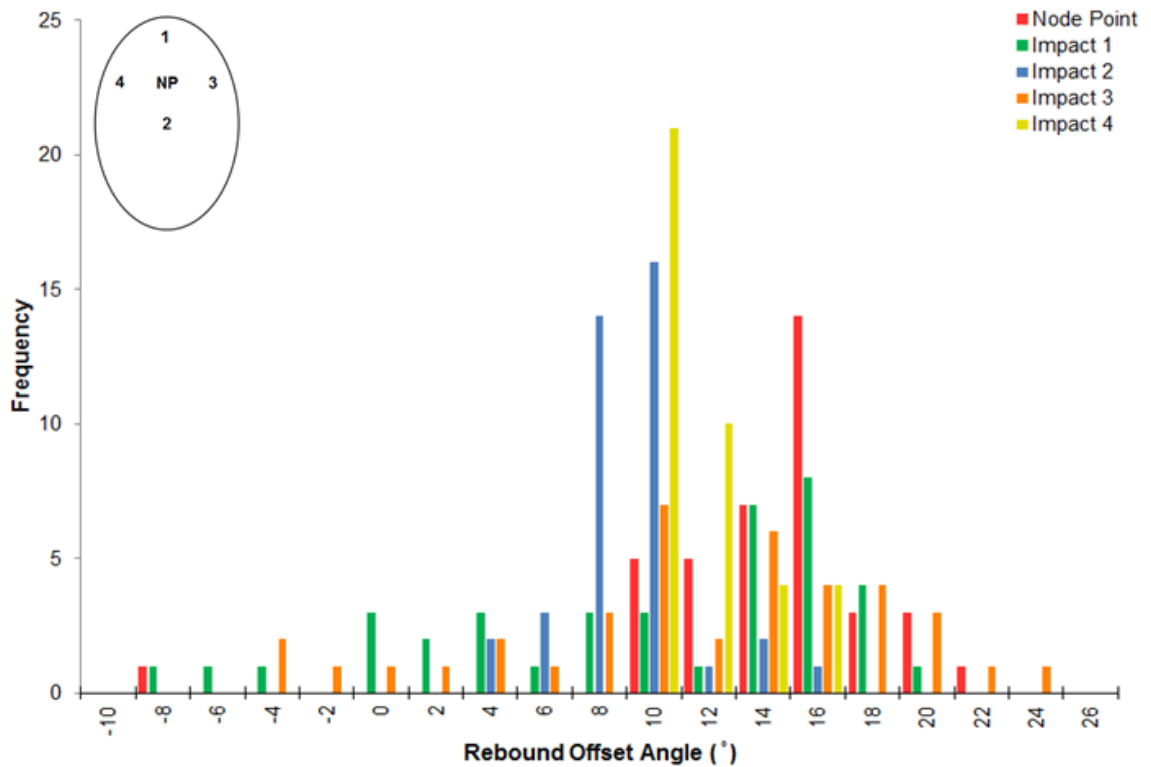
Figure 49 - A Frequency Histogram Showing the Rebound Offset Angle of All Five Impact Positions for the Slice Forehand

Table 17 - Mean and Standard Deviation Rebound Offset Angle Values of all Rackets for Each Impact for the Topspin Forehand

	Node Point	Impact 1	Impact 2	Impact 3	Impact 4
Mean (˚)	14	10	8	10	10
Standard Deviation (˚)	3	6	2	7	6

5.6 *Discussion*

This chapter describes a comprehensive procedure implemented prior and post impact testing. 24 hours prior to impact testing the racket was strung and the balls were acclimatised, within a pre-set laboratory climate system advised by the ITF. The implementation of this procedure prior to impact testing not only ensures consistency between all impacts but also ensures negligible effects of ball and/or string degradation post impact.

Post impact, the recorded impacts were subjected to a robustly calibrated automated image processing algorithm. When calibrated, the algorithm turns 2D coordinates into 3D real-world coordinates, allowing for the calculation of inbound and rebound ball displacement, velocity and relevant angles. For all calibrations, a minimum of 40 calibration images were used, ensuring a maximum re-projection error of ± 0.18 pixels. A re-projection error of ± 0.18 pixels equates to ± 0.225 mm and therefore, results in a maximum re-projection error no larger than 0.75 % of the measured 30 mm square size. Rebound ball spin was also obtained using a modified SpinTrack3D algorithm within MATLAB, for which the absolute error was found to be ± 0.25 radians (0.04 revolutions). Four rebound parameters were recorded: velocity, spin, rebound playing angle and rebound offset angle.

Topspin Forehand

The topspin forehand reported an overall range of approximately 600 rpm for rebound ball spin. The greatest averaged rebound ball spin was recorded at impact position 3, whereas the lowest rebound ball spin was recorded at impact position 2. Impact position 3 refers to an off-axis impact, for which frame rotation could be assumed as the causation of the increased rebound ball spin rates.

Resultant rebound ball velocity was found to be greatest at impact position 2 and lowest at the node point. Although the node point is identified as a sweet spot and has been found to be the aimed impact position throughout

previously recorded player testing, results identified this position to possess the lowest averaged resultant rebound ball velocity. However, the greatest averaged resultant rebound ball velocity was found to occur at impact position 2, which is in agreement with previous findings discussed within Chapter 2.

Impact position 1 and impact position 2 were found to possess the largest and smallest rebound playing angles respectively. For impacts occurring at the tip, the racket recoils quickly resulting in larger rebound angles from the normal. Large rebound playing angles can also be seen for impacts 3 and 4, both occurring off the longitudinal axis. In this case, the recorded rebound playing angles are due to the racket rotation during impact. These results are in agreement with previous findings, as discussed in Section 2.5. Though both impact positions are found along the rackets longitudinal axis the averaged difference between impact position 1 and 2 was 38˚.

The rebound offset angle reported a range of 40˚, between all impact positions. Such a range is to be expected as a result of the multiple impact locations (Allen, 2009). The greatest difference between impact positions, for averaged rebound offset angle, was calculated at 17˚ and was observed between the node point and impact position 1. Using a bespoke trajectory model, discussed in section 6.4, this difference was found to result in an on-court impact location difference of 13m parallel to the baseline. For both rebound angles, such ranges could be the difference between the ball landing within or beyond the bounds of the tennis court.

Slice Forehand

The slice forehand reported a range of approximately 500 rpm for the 39 tennis racket and all five impact positions. Rebound ball spin was found to be greatest at impact position 3 and lowest at impact position 2. Similarly to the topspin forehand, the increase in rebound ball spin could be assumed to be due to increased frame rotation upon impacts. Although there is a range of approximately 400 rpm for all recorded impacts, a maximum difference of

188 rpm was only observed between the averaged results for each impact position.

The resultant rebound ball velocity was found to be greatest at impact position 2 and lowest at impact position 1. Impact position 1 is located at the tip of the racket, also referred to as the dead spot. For impacts of a moving ball onto a stationary racket, impacts towards the tip of the racket can result in decreased resultant rebound ball velocity. Similarly, impact position 2 is located towards the GSC of the racket and results in larger rebound ball velocities. These results are in agreement with previous findings discussed in Chapter 2.

Although an overall range of 74° was observed for rebound playing angle, a maximum average difference of 37° was calculated between impact positions 1 and 2. Similar to the findings for the topspin forehand, impact position 1 possessed the largest averaged rebound playing angle and impact position 2 possessed the smallest averaged rebound playing angle. As previously mentioned, impact position 1 is located towards the tip of the racket, which upon impact the racket will recoil quickly resulting in larger angles from the normal. These results are in agreement with previous findings, as discussed in Section 2.5.

The rebound offset angle, recorded for all impact positions, reports a range of 32°. The resultant averages for each impact position were calculated to be positive, regardless of a rebound offset range of -6 to 24°. The largest and smallest rebound offset angles were found at the node point and impact position 2 respectively. This difference is calculated at 6°, which can result in an on-court impact location difference of 5 m. For both rebound angles, such ranges could be the difference between the ball landing within or beyond the bounds of the tennis court.

For both forehand shots, results show an increase in rebound ball spin when impacting the racket face at position 3 in comparison to impacts at position 4. When impacting the racket at impact position 3, the racket rotates

away from the leading edge of the ball, increasing the angle of impact and laterally deflecting strings into the ball creating more spin.

Due to the complexity and multi-dimensionality of the data, further analysis and examinations will need to be conducted through the use of machine learning techniques.

5.7 *Conclusion*

The methodology and apparatus, discussed in Chapter 4, along with the pre- and post-testing procedures discussed within this chapter, delivers an effective and consistent process for a large data collection.

The overall ranges observed for each rebound parameter are found to vary between the simulated forehands. However, general trends regarding impact positions generating greater and lower rebound results are found for both the slice and the topspin forehands.

With the results that have been obtained in this testing, a clustering method can be used to aid the analysis of the relationships between racket behaviour and racket properties, for specific forehand shots.

6 Cluster Analysis

6.1 *Introduction*

The methodology, apparatus and testing procedures, previously discussed, provided a large dataset to assess the behavioural performance of 39 different tennis racket (previously discussed in Section 4.3.2). The dataset includes four different rebound behavioural characteristics, recorded at five different impact positions upon the racket face, for two realistically simulated forehand shots.

Through the use of cluster analysis methods, it is possible to ascertain clusters of rackets resulting in similar behavioural characteristics. The cluster behavioural characteristics can then be examined, identifying significant behavioural differences.

For each forehand shot, hierarchical cluster analysis will be conducted, accompanied by a principal component analysis, to ensure an accurate selection of the number of clusters. Appropriately selecting the number of clusters, statistical behavioural differences between clusters will be investigated using a one-way ANOVA. Through the use of impact vector diagrams, the resulting differences between behavioural clusters will be shown, thus providing perception visual representation to the impact results.

6.2 *Aim*

This chapter aims to identify clusters of rackets possessing similar behavioural characteristics for the topspin and slice forehand individually.

6.3 *Hierarchical Cluster Analysis*

As discussed within Chapter 2, hierarchical cluster analysis is the most suitable clustering method for this analysis. Hierarchical Clustering provides a structure that is more informative than the unstructured set of flat cluster results provided by a Partitioning, Distribution or Density-based clustering model.

Ward's method is an agglomerative method of hierarchical clustering, in which the fusion between observations or clusters is based on the size of an error sum-of-squares. The aim at each stage is to ensure a minimal increase in the total within-in cluster variance. This increase is proportional to the squared Euclidean distance between the merged centroids; however, prior to the computation of the distances between cluster centroids, the cluster centroids are weighted.

A dendrogram is a commonly used two-dimensional visual representation of the hierarchical relationship between the observations and clusters, whilst also illustrating the fusions or divides at each stage of the analysis. The nodes of a dendrogram refer to the clusters, and the lengths of the stems refer to the distances at which the clusters were joined. There is no numerical information attached to the stems and are termed unweighted or ranked. The topology of the dendrogram is a result of the arrangement of the nodes and stems found within. The explained terminology is visually shown in Figure 50, using an example dendrogram (Landau, Stahl, Everitt, & Leese, 2011).
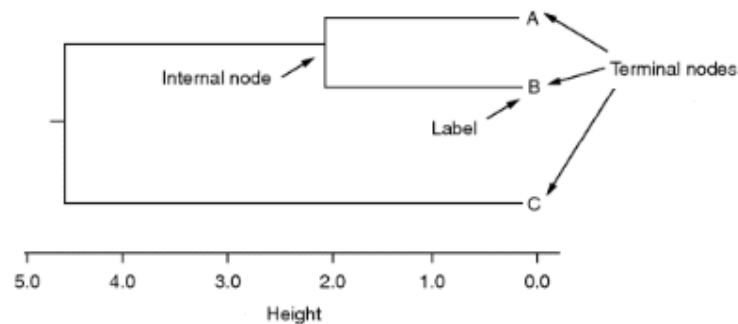
Figure 50 - Example Dendrogram Including Dendrogram Terminology

The number of clusters is not set prior to this method of analysis, and whilst the dendrogram visually informs the fusion of the nodes, it can only informally suggest the number of clusters. The height at which the dendrogram is 'cut', defines a partition such that the number of clusters is found below that height.

6.4 *Input Parameters*

To determine racket clusters of similar behaviour, rebound ball spin, resultant velocity, playing angle and offset angle recorded for all five impact positions was used to perform the hierarchical cluster analysis.

Prior to analysis, the data was normalised and then weighted according to the relative importance of each parameter with reference to their on-court impact location effects. Data normalisation is required when the ranges of the input parameters vastly differ, whilst also removing the effect of the parameters measurement units. An applied weighting assigns weaker or stronger parameter importance within the data set. A bespoke Matlab trajectory model was used to identify the effect of each parameter, relative to the parameter's on-court effect. The trajectory model uses the equations of aerodynamic forces for the calculation of the drag force (F_D) and the lift force (F_L) acting on the ball:

$$F_D = \tfrac{1}{2}\rho A C_D U_\infty^2 \qquad\qquad\qquad [24]$$

$$F_L = \tfrac{1}{2}\rho A C_L U_\infty^2 \qquad\qquad\qquad [25]$$

where ρ is the density of air, A is the cross-sectional area of the ball, U_∞ is the ball velocity and the coefficients of drag and lift are C_D and C_L respectively. The forces C_D and C_L are dependent on the spin rate of the ball, for which the spin ratio, α, of the ball is calculated using:

$$\alpha = \frac{\omega r}{U} \qquad\qquad\qquad [26]$$

where r and ω are the radius and spin of the ball respectively. The final aspect of the aerodynamic model, used within the bespoke trajectory model, is spin decay. The spin decay is given by,

$$SDR = \frac{r^2 \frac{d\omega}{dt}}{U_\infty^2} \qquad\qquad\qquad [27]$$

where $d\omega/dt$ is the change in spin rate over time.

103

The effect of the rebound spin, resultant velocity, playing angle and offset angle were individually modelled and analysed, using the maximum and minimum values of the ranges for all five impact positions. The difference in court impact location between the maximum and minimum values was the weight applied for each given parameter. Weighting accordingly ensures representative importance is given to the parameters of the greatest on-court effect.

6.5   *Topspin Forehand Results*

The defined clusters are differentiated through the use of various colours which will remain consistent for all methods of analysis within Section 6.5.

6.5.1 **PCA Results**

As previously mentioned, the hierarchical clustering dendrogram can only informally suggest the number of clusters best suited for the data. Although PCA is not a method of analysis used for clustering, a PCA was conducted prior to the hierarchical clustering, to extract key data features and information in which drive the racket's overall behaviour. These results were then used to make a more informed decision regarding the dendrogram cut height.

PC1 and PC2 were reported to account for 42% and 25% of the variance of the data respectively. Bivariate Pearson's correlation identified PC1 to have the best correlation with rebound playing angle at impact position 4 ($r = 0.817$, $p < 0.001$), followed by rebound playing angle at impact position 1 ($r = 0.725$, $p < 0.001$), then rebound playing angle at impact position 3 ($r = 0.594$, $p = 0.001$) and finally rebound offset angle at impact position 3 ($r = 0.468$, $p = 0.003$). Therefore, the largest variation captured by PC1 could be explained by differences in rebound playing angle, at impact positions 1, 3 and 4. Similarly, a bivariate Pearson's correlation was conducted on all rebound parameters with PC2. PC2 was identified to have the best correlation with rebound playing angle at impact position 2 ($r = 0.653$, $p < 0.001$), followed by rebound playing angel at the node point ($r = 0.508$, $p = 0.001$). Therefore the

largest variation, captured by PC2, could be explained by differences in rebound playing angle at the node point, impact position 2.

Figure 51 - Results of PC1 and PC2 with Indication of the 4 Identified Clusters for the Topspin Forehand

6.5.2 Hierarchical Cluster Analysis

The hierarchical cluster analysis results, for the topspin forehand, are visually shown using the dendrogram in Figure 52. The vertical axis represents the clusters, on which the racket labels are also presented, whilst the horizontal axis represents the distance (or dissimilarity) between clusters, or 'height'.

To make an informed decision regarding the dendrogram cut height, the PCA and hierarchical results must concurrently be taken into account. Though isolation of the plotted Components 1 and 2 could visually argue for three distinct clusters, the largest variation captured by PC2 could be explained by differences in the rebound playing angle at the node point and impact position 2. It can, therefore, be assumed that it is these variations which result in the initial separation and larger height fusion of clusters 2 and 3. This can be seen

105

in Figure 52, where initially clusters 2 and 3 are separate until the cluster fusion at a height of approximately 22. Therefore, a cut height of approximately 21 was selected, thus resulting in four distinct clusters.
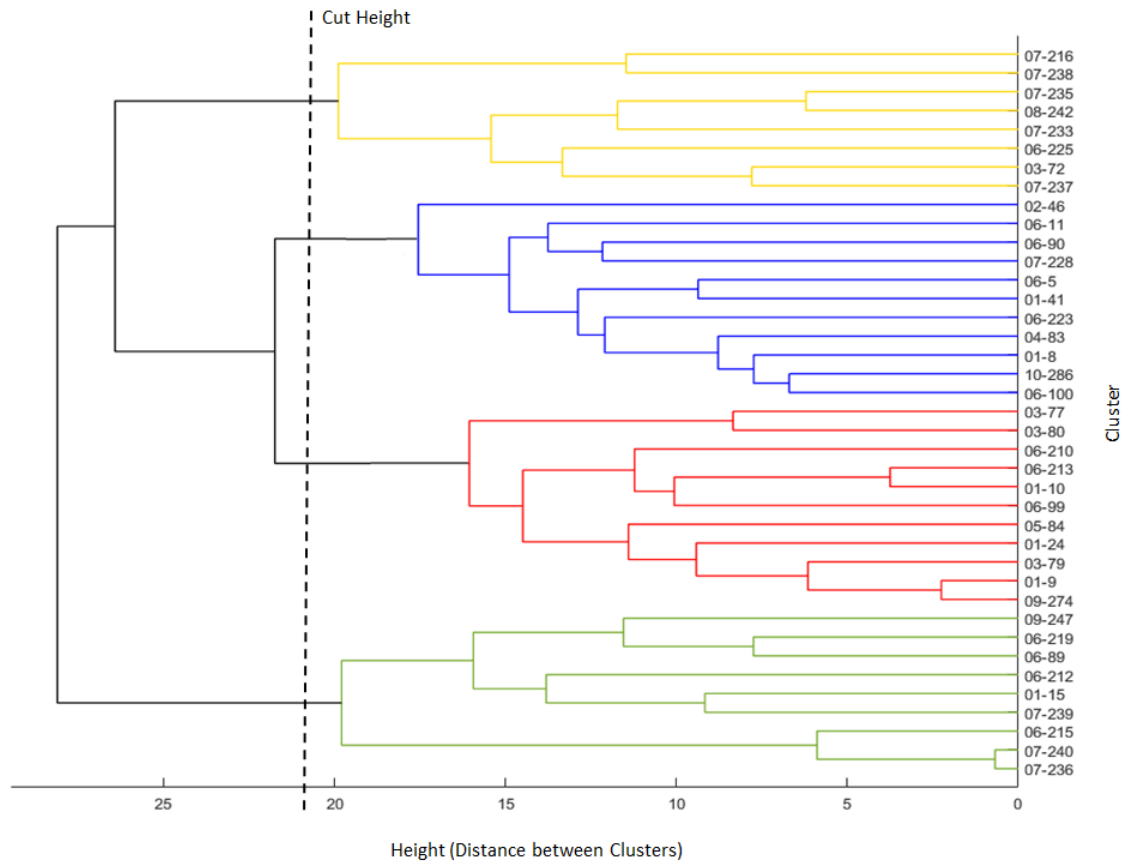
Figure 52 - Dendrogram Showing Topspin Forehand Hierarchical Cluster Analysis Results

6.5.3 Behavioural Cluster Results for Each Impact Position

A total of four clusters were previously identified, each possessing different behavioural characteristics. The behavioural characteristics consist of all recorded rebound parameters at all five impact positions. With the use of radar graphs, Figure 53 shows a comparison between the normalised and averaged behavioural cluster results for each impact position.

A one-way ANOVA was also used to determine any significant differences in racket parameters between the clusters, whilst a Tukey's post hoc analysis will be used to identify the affected clusters. The overall behavioural results of each cluster and for each racket can be found in Appendix D.
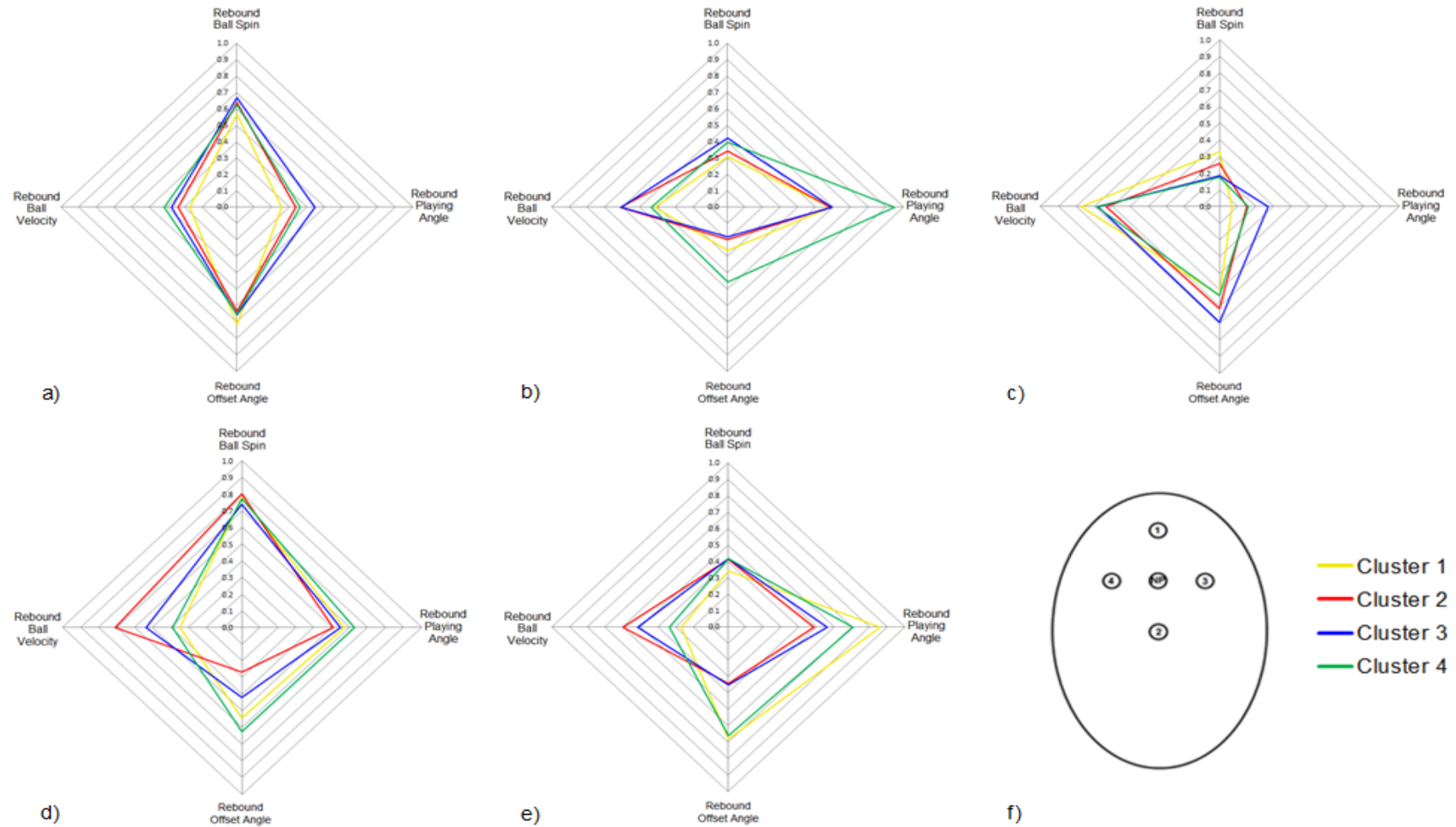
Figure 53 - Radar Graphs Comparing the Normalised Topspin Forehand Cluster Averages for the a) Node Point, b) Impact Position 1, c) Impact Position 2, d) Impact Position 3, e) Impact Position 4 and f) Impact Position Located on an Average Tennis Racket

Node Point

The means and standard deviations of each cluster, for the node point, are shown within Table 18. As previously mentioned, these results were normalised and plotted using a radar graph to visually aid the understanding of behavioural cluster differences; shown in Figure 53 (a).

Table 18 - Averages and Standard Deviations of the Behavioural Clusters Identified for the Node Point

Cluster	Rebound Spin (rpm)	Rebound Playing Angle (˚)	Rebound Offset Angle (˚)	Resultant Rebound Velocity (m/s)
Cluster 1	1499 ± 47	30 ± 3 ⌐*	17 ± 2	8 ± 0
Cluster 2	1542 ± 57	35 ± 8 ⌐**	13 ± 2	9 ± 1
Cluster 3	1560 ± 72	43 ± 4 ⌐	14 ± 5	9 ± 1
Cluster 4	1534 ± 57	36 ± 8 ⌐	15 ± 4	10 ± 2

A one-way ANOVA was conducted, identifying significant differences for rebound playing angle ($F_{(3, 35)}$ = 7.948, $p < 0.001$) at the racket's node point. The Tukey's post hoc test further revealed the effected clusters, with a significant difference, between cluster 1 and cluster 3 ($p < 0.001$) and between cluster 2 and cluster 3 ($p = 0.025$).

Impact Position 1

The behavioural means and standard deviations for each cluster, for impact position 1, are shown in Table 19. Figure 53 (b) illustrates the normalised and averaged results of each parameter, within each cluster, on a radar graph to help visualise the behavioural differences between clusters for impact position 1.

Table 19 - Averages and Standard Deviations of the Behavioural Clusters Identified for Impact Position 1

Cluster	Rebound Spin (rpm)	Rebound Playing Angle (˚)	Rebound Offset Angle (˚)	Resultant Rebound Velocity (m/s)
Cluster 1	1349 ± 67	53 ± 7	- 3 ± 8	10 ± 2
Cluster 2	1369 ± 49	53 ± 6	- 6 ± 6	12 ± 2
Cluster 3	1415 ± 82	54 ± 4	- 7 ± 7	12 ± 2
Cluster 4	1399 ± 77	80 ± 3	5 ± 10	10 ± 2

One-way ANOVA found significant differences for rebound playing angle ($F_{(3, 35)}$ = 56.372, $p < 0.001$), rebound offset angle ($F_{(3, 35)}$ = 4.255, $p = 0.012$) and resultant rebound ball velocity ($F_{(3, 35)}$ = 3.017, $p = 0.043$). The Tukey's post hoc test revealed significant differences between many clusters for the previously stated behavioural parameters.

For rebound playing angle the significant differences were found between cluster 1 and cluster 4 ($p < 0.001$), cluster 2 and cluster 4 ($p < 0.001$) and cluster 3 and cluster 4 ($p < 0.001$).

For rebound offset angle the significant differences were found between cluster 2 and cluster 4 ($p = 0.024$) and cluster 3 and cluster 4 ($p = 0.013$).

Impact Position 2

The means and standard deviations of each cluster, for the node point, are shown within Table 20. The normalised and averaged results can be visually compared using the radar graph shown in Figure 53 (c).

Table 20 - Averages and Standard Deviations of the Behavioural Clusters Identified for Impact Position 2

Cluster	Rebound Spin (rpm)	Rebound Playing Angle (˚)	Rebound Offset Angle (˚)	Resultant Rebound Velocity (m/s)
Cluster 1	1359 ± 81	15 ± 3	8 ± 1	14 ± 1
Cluster 2	1320 ± 97	21 ± 4	12 ± 5	12 ± 1
Cluster 3	1275 ± 66	30 ± 7	15 ± 9	13 ± 0
Cluster 4	1271 ± 41	22 ± 7	9 ± 3	13 ± 1

Significant differences, using the one-way ANOVA, were found for rebound playing angle ($F_{(3, 35)}$ = 10.156, p < 0.001) and resultant rebound ball velocity ($F_{(3, 35)}$ = 3.739, p = 0.020).

For rebound playing angle, Tukey's post hoc test revealed significant differences between cluster 1 and cluster 3 (p < 0.001), cluster 2 and cluster 3 (p = 0.008) and cluster 3 and cluster 4 (p = 0.023).

For resultant rebound ball velocity, significant differences were revealed between cluster 1 and cluster 2 (p = 0.011).

Impact Position 3

The behavioural means and standard deviations for each cluster, for impact position 3, are shown in Table 21. Similarly, with the use of a radar graph the normalised and averaged results of each parameter, within each cluster, are plotted to help visualise the behavioural differences between clusters for impact position 3, shown in Figure 53 (d).

Table 21 - Averages and Standard Deviations of the Behavioural Clusters Identified for Impact Position 3

Cluster	Rebound Spin (rpm)	Rebound Playing Angle (˚)	Rebound Offset Angle (˚)	Resultant Rebound Velocity (m/s)
Cluster 1	1625 ± 25	53 ± 11	9 ± 9	9 ± 3
Cluster 2	1637 ± 59	48 ± 5	-3 ± 9	12 ± 2
Cluster 3	1601 ± 73	51 ± 5	4 ± 9	13 ± 2
Cluster 4	1618 ± 62	56 ± 9	12 ± 4	10 ± 1

One-way ANOVA identified significant differences for rebound offset angle ($F_{(3, 35)} = 6.263$, $p = 0.002$) and resultant rebound ball velocity ($F_{(3, 35)} = 5.287$, $p = 0.004$). Similarly, Tukey's post hoc test revealed significant differences between many clusters for the previously stated behavioural parameters.

For rebound offset angle the significant differences were found between cluster 1 and cluster 2 ($p = 0.025$) and cluster 2 and cluster 4 ($p = 0.001$).

For resultant rebound ball velocity the significant differences were found between cluster 1 and cluster 2 ($p = 0.007$) and cluster 2 and cluster 4 ($p = 0.014$).

Impact Position 4

The means and standard deviations of each cluster, for impact position 4, are shown in Table 22. Figure 53 (e) illustrates the normalised and averaged results of each parameter, within each cluster, on a radar graph to help visualise the behavioural differences between clusters for impact position 4.

Table 22 - Averages and Standard Deviations of the Behavioural Clusters Identified for Impact Position 4

Cluster	Rebound Spin (rpm)	Rebound Playing Angle (˚)	Rebound Offset Angle (˚)	Resultant Rebound Velocity (m/s)
Cluster 1	1369 ± 30	74 ± 6	14 ± 10	8 ± 2
Cluster 2	1410 ± 61	46 ± 4	-2 ± 9	11 ± 2
Cluster 3	1413 ± 88	51 ± 6	1 ± 11	13 ± 1
Cluster 4	1413 ± 62	62 ± 7	14 ± 7	9 ± 2

The one-way ANOVA identified significant differences for rebound playing angle ($F_{(3, 35)} = 37.862$, $p < 0.001$), rebound offset angle ($F_{(3, 35)} = 4.988$, $p = 0.006$) and resultant rebound ball velocity ($F_{(3, 35)} = 4.383$, $p = 0.010$). Tukey's post hoc test revealed significant differences between many clusters for the previously stated behavioural parameters.

For rebound playing angle, the significant differences were found between cluster 1 and cluster 2 ($p < 0.001$), cluster 1 and cluster 3 ($p < 0.001$), cluster 1 and cluster 4 ($p = 0.002$), cluster 2 and cluster 4 ($p < 0.001$) and cluster 3 and cluster 4 ($p = 0.002$).

For rebound offset angle the significant differences were found between cluster 2 and cluster 4 ($p = 0.034$) and cluster 3 and cluster 4 ($p = 0.042$).

For resultant rebound ball velocity, the significant differences were only found between cluster 1 and cluster 2 ($p = 0.016$).

6.5.4 **Impact Vector Diagrams**

Although the radar graphs provide a visual aid for the comparison between the normalised and averaged behavioural cluster results, there is no visual representation as to the cluster effects upon impact on a tennis racket. The previously conducted analysis, regarding cluster formation, identified the largest cluster variations to occur at impact position 1, impact position 3 and

impact position 4. Figure 54 provides impact visualisation, through the use of vector diagrams, to visualise and compare effects between clusters for impact positions 1, 3 and 4 respectively.
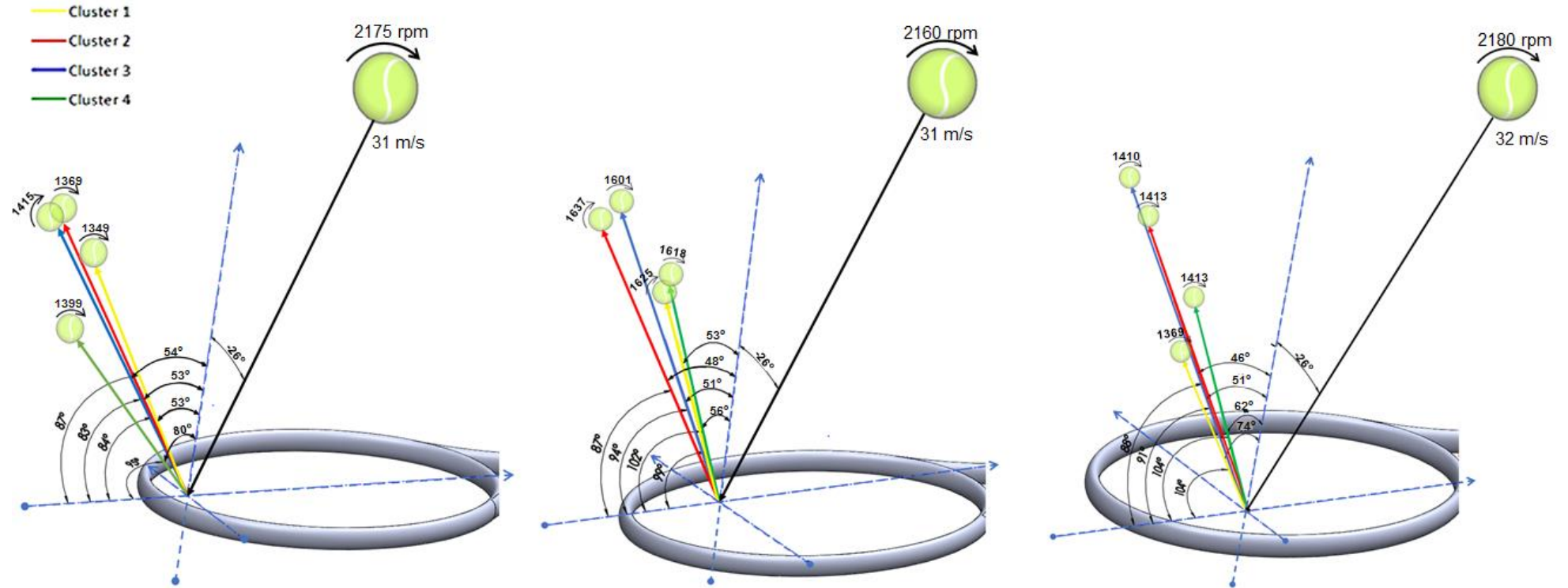
Figure 54 - Impact Vector Diagrams Comparing Topspin Forehand Cluster Averages for the a) Impact Position 1, b) Impact Position 3, c) Impact Position 4

6.6 *Slice Forehand Results*

The defined clusters are differentiated through the use of various colours which will remain consistent for all methods of analysis within Section 6.6.

6.6.1 PCA Results

Similar to the approach discussed within Section 6.5.1, for the topspin forehand, a PCA was conducted prior to the hierarchical clustering analysis for the extraction of key data features and information which drive the overall behaviour of the racket. The results of the PCA will then aid the decision regarding the dendrogram cut height.

PC1 and PC2 account for 47 % and 25 % of the variance of the data respectively. Bivariate Pearson's correlation identified PC1 to have the best correlation with rebound playing angle at impact position 1 ($r = 0.950$, $p < 0.001$), followed by resultant rebound ball velocity at impact position 1 ($r = 0.777$, $p < 0.001$), then resultant rebound ball velocity at impact position 4 ($r = 0.751$, $p < 0.001$) and finally rebound offset angle at impact position 3 ($r = 0.745$, $p = 0.001$). Therefore the largest variation, captured by PC1, could be explained by differences in rebound playing angle at impact position 1, the resultant rebound ball velocity at impact positions 1 and 4, and the rebound offset angle at impact position 3. Similarly, a bivariate Pearson's correlation was conducted on all rebound parameters with PC2. PC2 was identified to have the best correlation with rebound playing angle at impact position 3 ($r = 0.803$, $p < 0.001$), followed by rebound playing angel at the node point ($r = 0.797$, $p < 0.001$) and rebound playing angle at impact position 4 ($r = 0.631$, $p < 0.001$). Therefore, the largest variation captured by PC2 could be explained by differences in rebound playing angle, at the node point and impact positions 3 and 4.
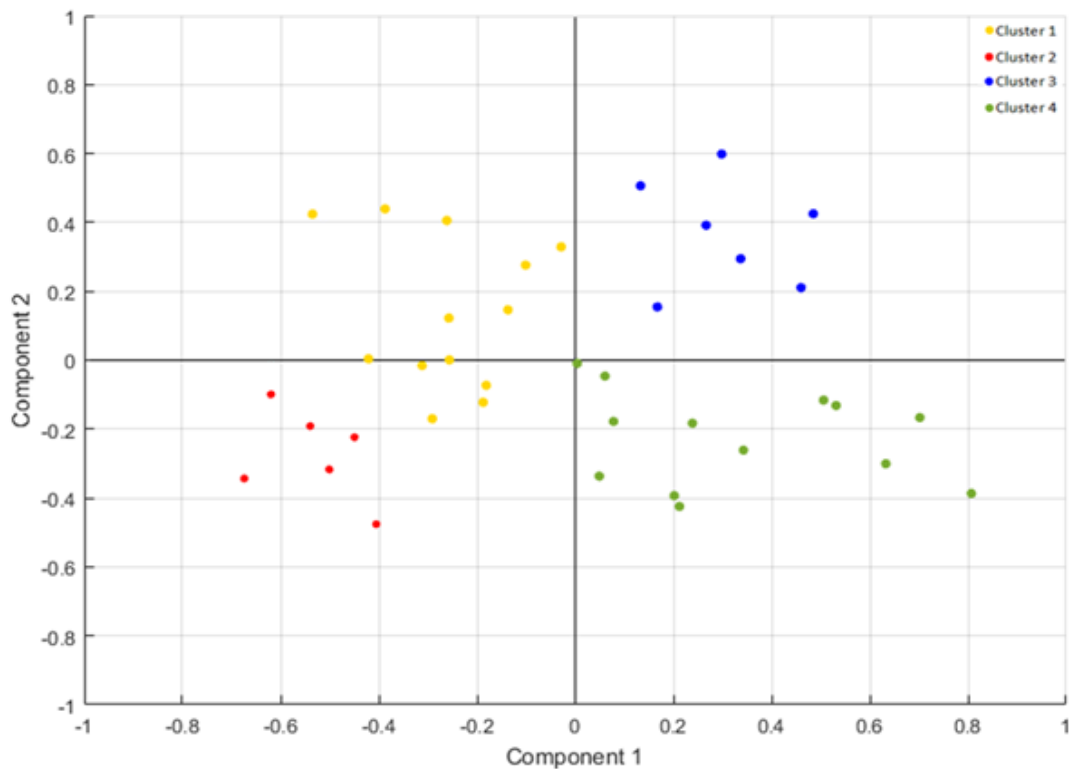
Figure 55 - Results of PC1 and PC2 with Indication of the 4 **Identified Clusters for the Slice Forehand**

6.6.2 **Hierarchical Cluster Analysis**

The hierarchical cluster analysis results, for the slice forehand, are visually shown using the dendrogram in Figure 56. The vertical axis represents the clusters, on which the racket labels are also presented, whilst the horizontal axis representing the height is the distance (or dissimilarity) between clusters.

To make an informed decision regarding the dendrogram cut height, the PCA and hierarchical results must be taken into account simultaneously. Though Figure 55 could visually argue for the distinction of two or three clusters, the PCA results combined with the hierarchical clustering analysis indicate otherwise. The largest variations captured by PC2 could be assumed to result in the initial separation and larger height fusion of clusters 1 with 2 and 3 with 4. This can be seen in Figure 56, where the clusters are initially separated until they are fused at a height above 13. Therefore, a cut height of approximately 13 was selected, thus resulting in four distinct clusters.
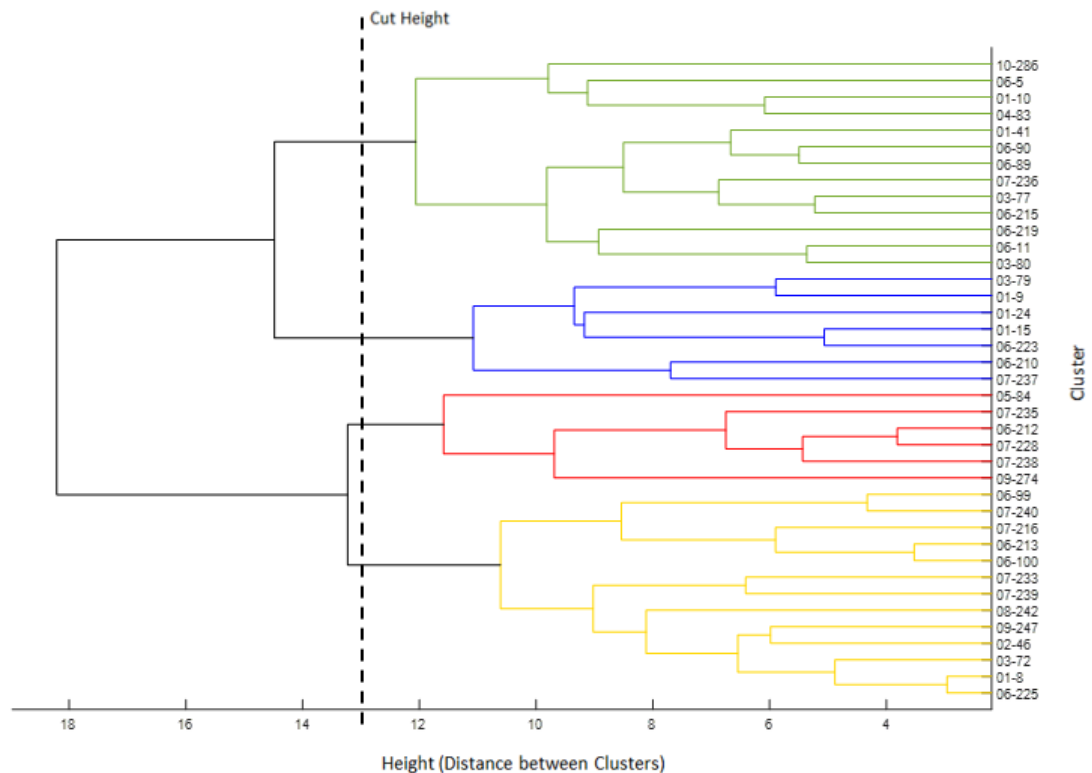
Figure 56 - Dendrogram Showing Slice Forehand Hierarchical Cluster Analysis Results

6.6.3 Behavioural Cluster Results

A total of four clusters were distinguished, each possessing different behavioural characteristics. As previously stated, the behavioural clusters are formed on the basis of all recorded rebound parameters, for all five impact positions. Figure 57 shows a comparison between the normalised and averaged behavioural cluster results for each impact position through the use of radar graphs.

Similarly, a one-way ANOVA will be used to determine any significant differences between the parameters defining racket behaviour, whilst a Tukey's post hoc analysis will be used to identify the affected clusters. The overall behavioural results of each cluster and for each racket can be found in Appendix E.
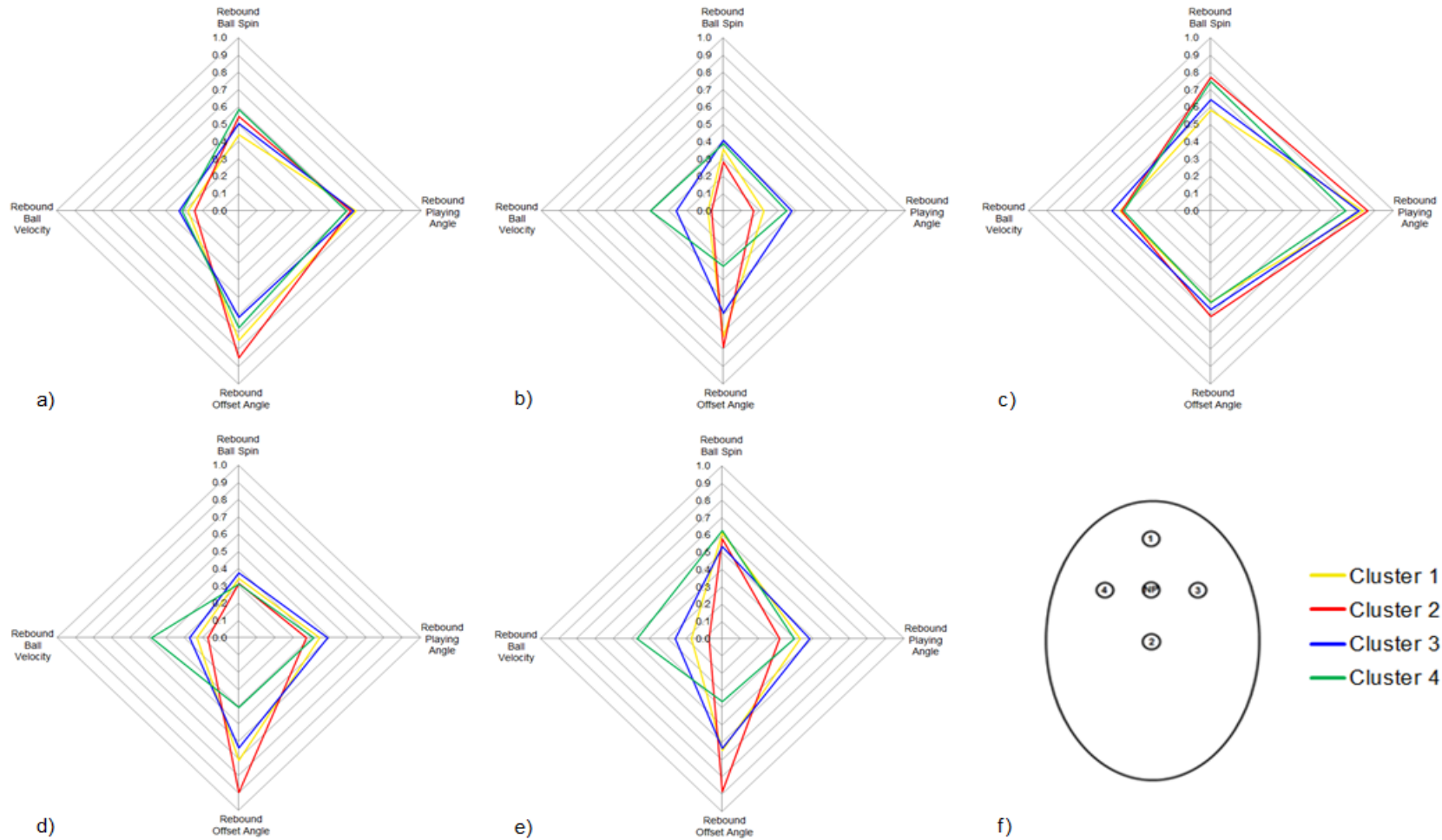
Figure 57 - Radar Graphs Comparing the Normalised Slice Forehand Cluster Averages for the a) Node Point, b) Impact Position 1, c) Impact Position 2, d) Impact Position 3, e) Impact Position 4 and f) Impact Position Located on an Average Tennis Racket

Node Point

The means and standard deviations of each cluster, for the node point, are shown within Table 23. As previously mentioned, these results were normalised and plotted using a radar graph to visually aid the understanding of behavioural cluster differences; shown in Figure 57 (a).

Table 23 - Averages and Standard Deviations of the Behavioural Clusters Identified for the Node Point

Cluster	Rebound Spin (rpm)	Rebound Playing Angle (˚)	Rebound Offset Angle (˚)	Resultant Rebound Velocity (m/s)
Cluster 1	-1640 ± 79	-35 ± 4	14 ± 2	11 ± 0
Cluster 2	-1590 ± 83	-37 ± 4	18 ± 2 ⎤*	10 ± 1 ⎤*
Cluster 3	-1610 ± 84	-36 ± 8	10 ± 4 ⎦	11 ± 0 ⎦
Cluster 4	-1560 ± 82	-39 ± 4	12 ± 6	11 ± 0

The one-way ANOVA found significant differences for rebound offset angle $(F_{(3, 35)} = 3.572, p = 0.024)$ and resultant rebound ball velocity $(F_{(3, 35)} = 3.199, p = 0.035)$ at the racket's node point. The Tukey's post hoc test revealed the effected clusters, with a significant difference, to be cluster 2 and cluster 3 for both rebound offset angle ($p = 0.025$) and resultant rebound ball velocity ($p = 0.025$).

Impact Position 1

The behavioural means and standard deviations for each cluster, for impact position 1, are shown in Table 24. Figure 57 (b) illustrates the normalised and averaged results of each parameter, within each cluster, on a radar graph to help visualise the behavioural differences between clusters for impact position 1.

Table 24 - Averages and Standard Deviations of the Behavioural Clusters Identified for Impact Position 1

Cluster	Rebound Spin (rpm)	Rebound Playing Angle (˚)	Rebound Offset Angle (˚)	Resultant Rebound Velocity (m/s)
Cluster 1	-1688 ± 69	-66 ± 6	14 ± 2	9 ± 0
Cluster 2	-1726 ± 74	-70 ± 5	16 ± 2	8 ± 1
Cluster 3	-1659 ± 88	-55 ± 3	9 ± 4	11 ± 1
Cluster 4	-1670 ± 90	-57 ± 3	1 ± 6	12 ± 2

One-way ANOVA found significant differences for rebound playing angle ($F_{(3, 35)} = 19.334$, $p < 0.001$), rebound offset angle ($F_{(3, 35)} = 25.644$, $p < 0.001$) and resultant rebound ball velocity ($F_{(3, 35)} = 17.038$, $p < 0.001$). The Tukey's post hoc test revealed significant differences between many clusters for the previously stated behavioural parameters.

For rebound playing angle the significant differences were found between cluster 1 and cluster 3 ($p < 0.001$), cluster 1 and cluster 4 ($p < 0.001$), cluster 2 and cluster 3 ($p < 0.001$) and cluster 2 and cluster 4 ($p < 0.001$).

For rebound offset angle the significant differences were found between cluster 1 and cluster 4 ($p < 0.001$), cluster 2 and cluster 3 ($p = 0.049$), cluster 2 and cluster 4 ($p < 0.001$) and cluster 3 and cluster 4 ($p = 0.001$).

For resultant rebound ball velocity the significant differences were found between cluster 1 and cluster 4 ($p < 0.001$), cluster 2 and cluster 3 ($p = 0.040$) and cluster 2 and cluster 4 ($p < 0.001$).

Impact Position 2

The means and standard deviations of each cluster, for the node point, are shown within Table 25. The normalised and averaged results can be visually compared using the radar graph shown in Figure 57 (c).

Table 25 - Averages and Standard Deviations of the Behavioural Clusters Identified for Impact Position 2

Cluster	Rebound Spin (rpm)	Rebound Playing Angle (˚)	Rebound Offset Angle (˚)	Resultant Rebound Velocity (m/s)
Cluster 1	-1564 ± 81	-21 ± 3	7 ± 2	13 ± 1
Cluster 2	-1461 ± 37	-19 ± 5	10 ± 3	13 ± 1
Cluster 3	-1531 ± 72	-23 ± 3	9 ± 2	14 ± 2
Cluster 4	-1475 ± 58	-28 ± 3	7 ± 2	13 ± 1

Significant differences, using the one-way ANOVA, were found only for rebound playing angle ($F_{(3, 35)}$ = 12.569, $p < 0.001$). The Tukey's post hoc test further revealed the significant differences to be between cluster 1 and cluster 4 ($p < 0.001$), cluster 2 and cluster 4 ($p < 0.001$) and cluster 3 and cluster 4 ($p = 0.018$).

Impact Position 3

The behavioural means and standard deviations for each cluster, for impact position 3, are shown in Table 26. Similarly, with the use of a radar graph the normalised and averaged results of each parameter, within each cluster, are plotted to help visualise the behavioural differences between clusters for impact position 3; shown in Figure 57 (d).

Table 26 - Averages and Standard Deviations of the Behavioural Clusters Identified for Impact Position 3

Cluster	Rebound Spin (rpm)	Rebound Playing Angle (˚)	Rebound Offset Angle (˚)	Resultant Rebound Velocity (m/s)
Cluster 1	-1695 ± 59	-50 ± 3	13 ± 3	10 ± 1
Cluster 2	-1711 ± 47	-55 ± 5	19 ± 2	10 ± 1
Cluster 3	-1677 ± 56	-46 ± 2	11 ± 3	11 ± 1
Cluster 4	-1712 ± 62	-52 ± 3	3 ± 6	13 ± 2

One-way ANOVA identified significant differences for rebound playing angle ($F_{(3, 35)}$ = 8.164, $p < 0.001$), rebound offset angle ($F_{(3, 35)}$ = 21.541, $p < 0.001$) and resultant rebound ball velocity ($F_{(3, 35)}$ = 10.036, $p < 0.001$). Similarly to the results for impact position 1, Tukey's post hoc test revealed significant differences between many clusters for the previously stated behavioural parameters.

For rebound playing angle the significant differences were found between cluster 1 and cluster 2 ($p = 0.015$), cluster 2 and cluster 3 ($p < 0.001$), and cluster 3 and cluster 4 ($p = 0.005$).

For rebound offset angle the significant differences were found between cluster 1 and cluster 2 ($p = 0.037$), cluster 1 and cluster 4 ($p < 0.001$), cluster 2 and cluster 3 ($p = 0.007$), cluster 2 and cluster 4 ($p < 0.001$), and cluster 3 and cluster 4 ($p = 0.004$).

For resultant rebound ball velocity the significant differences were found between cluster 1 and cluster 4 ($p < 0.001$), cluster 2 and cluster 4 ($p < 0.001$), and cluster 3 and cluster 4 ($p = 0.024$).

Impact Position 4

The means and standard deviations of each cluster, for impact position 4, are shown in Table 27. Figure 57 (e) illustrates the normalised and averaged results of each parameter, within each cluster, on a radar graph to help visualise the behavioural differences between clusters for impact position 4.

Table 27 - Averages and Standard Deviations of the Behavioural Clusters Identified for Impact Position 4

Cluster	Rebound Spin (rpm)	Rebound Playing Angle (˚)	Rebound Offset Angle (˚)	Resultant Rebound Velocity (m/s)
Cluster 1	-1547 ± 48	-51 ± 3	11 ± 5	10 ± 1
Cluster 2	-1567 ± 67	-59 ± 2	19 ± 2	8 ± 0
Cluster 3	-1592 ± 55	-47 ± 2	11 ± 2	11 ± 1
Cluster 4	-1540 ± 67	-53 ± 3	2 ± 7	13 ± 2

One-way ANOVA identified significant differences for rebound playing angle ($F_{(3, 35)}$ = 21.758, $p < 0.001$), rebound offset angle ($F_{(3, 35)}$ =13.642, $p < 0.001$) and resultant rebound ball velocity ($F_{(3, 35)}$ = 18.508, $p < 0.001$). Once more, Tukey's post hoc test revealed significant differences between many clusters for the previously stated behavioural parameters.

For rebound playing angle the significant differences were found between cluster 1 and cluster 2 ($p < 0.001$), cluster 1 and cluster 3 ($p = 0.033$), cluster 2 and cluster 3 ($p < 0.001$), cluster 2 and cluster 4 ($p = 0.001$), and cluster 3 and cluster 4 ($p < 0.001$).

For rebound offset angle the significant differences were found between cluster 1 and cluster 2 ($p = 0.045$), cluster 1 and cluster 4 ($p = 0.001$), cluster 2 and cluster 4 ($p < 0.001$), and cluster 3 and cluster 4 ($p = 0.012$).

For resultant rebound ball velocity the significant differences were found between cluster 1 and cluster 4 ($p < 0.001$), cluster 2 and cluster 3 ($p = 0.035$), cluster 2 and cluster 4 ($p < 0.001$), and cluster 3 and cluster 4 ($p = 0.008$).

6.6.4 Impact Vector Diagrams

The radar graphs provide a visual aid for the comparison between the normalised and averaged behavioural cluster results, however, there is no visual representation as to the cluster effects upon impact on a tennis racket. Similar to the results obtained for the topspin forehand, the previously conducted analysis, regarding cluster formation, identified the largest cluster variations to occur at impact position 1, impact position 3 and impact position 4. Figure 58 provides impact visualisation, through the use of vector diagrams, to visualise and compare effects between clusters for impact positions 1, 3 and 4 respectively.
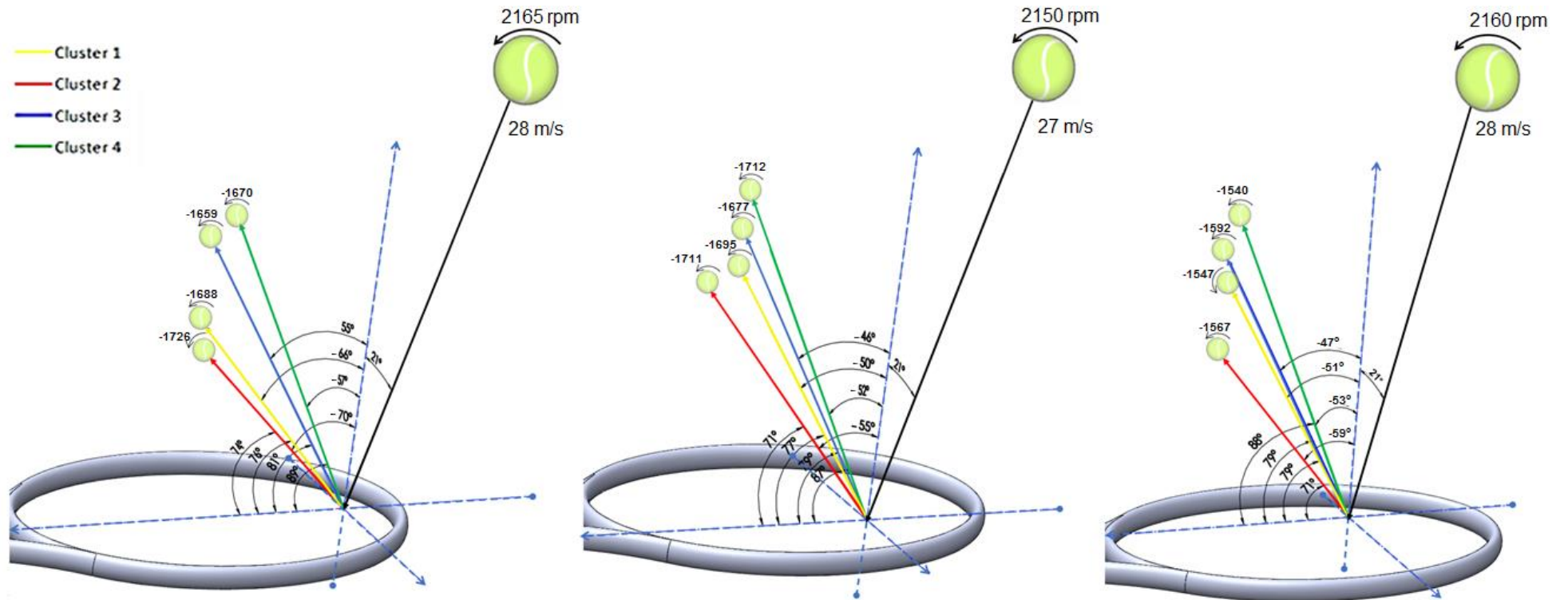
Figure 58 - Impact Vector Diagrams Comparing Slice Forehand Cluster Averages for the a) Impact Position 1, b) Impact Position 3, c) Impact Position 4

6.7 *Discussion*

Prior to the analysis, the data was normalised and weighted according to relative on-court importance. Normalisation of the data, prior to analysis, alters the different numeric values in the dataset to a common scale, without distorting differences in the ranges of values. Since hierarchical cluster analysis, like most clustering algorithms, requires some definition of distance, normalisation and weighting of the data accordingly, provides representative importance to the parameters of the greatest on-court effect. The formation of clusters could then be assumed to possess rackets of similar on-court effects, whilst also possessing on-court dissimilarities to rackets of a different cluster.

Individually, neither the PCA nor the hierarchical cluster analysis provides a definitive answer as to the number of suitable clusters. However, combining the results and findings of both the PCA and hierarchical cluster analysis, it is possible to make an informed decision as to the number of appropriate behavioural clusters.

Initially, individual analysation of the hierarchical dendrogram or PC plot, for the topspin forehand, a total of three clusters look to be the appropriate selection; merging of cluster 2 with cluster 3. However, the largest variation of PC2 could be explained by differences in rebound playing angle at the node point and impact position 2 and thus, results in the initial separation and larger height fusion of clusters 2 and 3. The behavioural differences between all clusters can be seen within Figure 53, but more specifically Figure 53 also shows the statistically significant differences for rebound playing angle between clusters 2 and 3 at the node point and impact position 2, reiterating the separation and larger height fusion of clusters 2 and 3. The use of a trajectory model, simulating the results upon a tennis court, revealed the statistical difference to result in height flight of the ball. Though the ball may land in a similar location on the court the difference in height flight could potentially provide the opposition with more time to react to the ball.

Though significant differences are observed between clusters 2 and 3 at the node point and impact position 2, Figure 53 shows the greatest discrepancies between behavioural clusters to occur at impact positions 1, 3 and 4. As previously depicted and discussed impact position 1 occurs towards the tip of the racket, whereas impact positions 3 and 4 occur above and below the longitudinal axis. At impact position 1 similarities between clusters 1, 2 and 3 can be observed, however statistical differences regarding rebound playing and offset angle were identified between clusters 1, 2 and 3 with cluster 4. Such results and discrepancies between clusters can be attributed to the transfer of all momentum from the ball into the racket, causing the racket to recoil quickly and thus, resulting in a larger rebound playing angle. At impact position 3 and 4 similarities can be observed between cluster 1 with 4 and clusters 2 with 3, for which statistical differences were also identified defining the behavioural differences between cluster 1 and 4 with clusters 2 and 3. Behavioural differences can be seen between clusters 1 and 4 with clusters 2 and 3 regarding rebound playing angle, rebound offset angle and rebound ball velocity. Such results can be attributed to larger racket rotations about the longitudinal axis, and the 'wasted' energy in doing so.

For the slice forehand, initial analysis of the hierarchical dendrogram and PC plot individually, also indicate a total of two or three appropriate clusters; merging of cluster 1 with cluster 2 and/or cluster 3 with cluster 4. However, the variations explained by PC2 could result in the initial separation and larger height fusion of clusters 1 with 2 and 3 with 4.

Figure 57 and Figure 58 show the differences between behavioural clusters for each impacted position for the slice forehand. Similar to the results of the topspin forehand, similar behavioural characteristics and trends can be observed between clusters when impacting the racket's node point and impact position 2, and the greatest between cluster discrepancies occur at impact positions 1, 3 and 4. For impacts occurring at impact position 1 (tip), similarities between behaviour clusters 1 with 2 and clusters 3 with 4, for which significant differences were identified between the two behavioural 'trends' regarding rebound playing angle and rebound ball velocity. Such results could be

attributed to a larger transfer of momentum between the ball and rackets within clusters 1 and 2, resulting in the racket to recoil quickly, and thus increasing rebound ball angle and decreasing rebound ball velocity.

For impacts occurring off the longitudinal axis, impact positions 3 and 4, the radar graphs (Figure 57) and Figure 58 show the behavioural differences between all clusters. When the ball is struck at impact position 3 and impact position 4, significant differences were identified between all clusters regarding rebound playing angle, rebound offset angle and rebound ball velocity. An increase in rebound playing angle and decrease in rebound ball velocity can be a result of increased racket rotations about the longitudinal axis. A trajectory model simulating the results upon a tennis court revealed sizeable ball flight and court impact location differences between all clusters at impact position 3. The largest on-court differences, however, were found between clusters 3 and 4, to which a ball struck by an average racket from cluster 4 will result in a deeper court impact location whilst possessing a higher ball flight, approximately 1.6m and 3m respectively. At impact position 4, trajectory simulations indicated that when the ball is struck by an average racket from cluster 1 and 3, the ball result in a deeper court impact location and higher ball flight in comparison to a ball struck by an average tennis racket from cluster 2 and 4 respectively.

For both simulated forehand shots, the greatest differences between clusters are observed at impact positions 1, 3 and 4 (tip and both off-axis impacts respectively). Though behavioural results, when impacted at the tip of the racket, may not influence cluster formation as strongly as the behavioural results at impact position 3 or 4, many statistical differences were found between clusters. Trajectory simulations have revealed that these differences can result in deeper impact location and ball flight height for both forehand shot types. This could be the difference of whether the ball lands within or beyond the bounds of the court and whether the flight height provides the opposition enough time to react to the impacted ball.

6.8 *Conclusion*

To make an appropriate decision regarding the dendrogram cut height, the PCA and hierarchical results must be taken into account simultaneously. The PCA identified the key features in which drive tennis rackets behaviour, aiding the understanding of the hierarchical dendrogram initial cluster separations and height fusions. Ultimately a total of four clusters were identified, for both the topspin and slice forehand, each possessing similar within-cluster behavioural characteristics and dissimilar behavioural characteristics between clusters.

The largest behavioural variations between clusters were observed at impact position 1, impact position 3 and impact position 4. Trajectory models indicate these variations to be the result in the depth of court impact location and height of ball flight throughout the trajectory.

7 Effecting Racket Properties

7.1 *Introduction*

A hierarchical cluster analysis was conducted clustering rackets possessing similar behavioural characteristics, as discussed in Chapter 6. The behavioural clusters were formed on the foundation of all recorded rebound parameters for all five impact positions. With the aid of a PCA, a total of four clusters of distinct behavioural characteristics were identified.

Consequently, within each distinct cluster are ranges of rackets, owning a variety of specific properties. Between-cluster property differences and within-cluster property variances will be investigated through the calculation of the means and standard deviations.

Relationships between the subsequent racket properties and behavioural clusters will be investigated through the use of multinomial logistic regression. This method of analysis will also see the development of a model for the use of prediction, for which model development and accuracy will be further analysed.

7.2 *Aim*

This chapter aims to identify fundamental relationships between the racket properties and distinct behavioural clusters, for the development of an accurate predictive model.

7.3 *Racket Properties Subsequent to Behavioural Clusters*

Analysis conducted in Chapter 6 identified a set of four behavioural clusters for both laboratory simulated forehand shots. The formation of the clusters ensured the grouping of varying racket properties, resulting in similar behaviour. The subsequent racket properties of these behavioural clusters are investigated within this section.

7.3.1 **Topspin Forehand**

The racket property means and standard deviations, of each cluster, are shown in Table 28. The property combinations of each racket, within each cluster, can be found in Appendix F.

Table 28 - Averages and Standard Deviations of the Racket Properties for Each Cluster

Cluster	Racket Mass (g)	Balance Point (mm)	Head Length (mm)	Head Width (mm)	Strung Area (in²)	Racket Length (mm)	Swingweight (RDC)	Twistweight (RDC)	Frame Stiffness (RDC)
Cluster 1	292 ± 33	330 ± 15	335 ± 14	254 ± 15	99 ± 6	688 ± 4	280 ± 18	12 ± 2	68 ± 3
Cluster 2	292 ± 33	334 ± 21	343 ± 21	250 ± 11	103 ± 8	695 ± 10	296 ± 17	8 ± 3	66 ± 5
Cluster 3	299 ± 43	332 ± 24	341 ± 22	250 ± 17	103 ± 13	698 ± 11	300 ± 24	11 ± 4	65 ± 6
Cluster 4	302 ± 26	325 ± 13	337 ± 16	254 ± 13	101± 9	688 ± 3	286 ± 16	10 ± 4	66 ± 3

To aid the between cluster comparisons, the resulting racket properties were normalised, averaged and plotted using a radar. The results of this can be seen in Figure 59 (a). The upper and lower standard deviations for each property, of each cluster, were also normalised and plotted using the radar graphs shown in Figure 59 (b) and (c). To visually aid the interpretation of the within-cluster variance Figure 59 (d), (e), (f) and (g) show the normalised means and standard deviations for cluster 1, 2, 3 and 4 respectively.

Table 28 informs the between cluster differences, whilst Figure 59 visually aids the comparison of cluster differences. Together, Table 28 and Figure 59 reveal although no two clusters possess the same combinations of mean racket properties, there are large within-cluster racket property variations.

Differences in cluster property averages are observed for balance point, head length, swingweight and twistweight. However, a one-way ANOVA analysis identified a significant difference for racket length only ($F_{(3, 35)} = 3.639$, $p = 0.022$). The Tukey's post hoc analysis revealed the significant difference to be between cluster 3 and cluster 4 ($p = 0.044$). Assuming to be the effect of the

amount variance within cluster 1, no significant differences were observed between clusters 1 and 3 for racket length.

Clusters 1 and 4 may initially appear to follow a similar trend for most cluster property averages, however, the segregating differences can be seen in both twistweight and frame stiffness, shown in Figure 59 (a). Furthermore, though cluster 1 possesses the largest cluster average for frame stiffness and twistweight, it does not possess the largest upper bound for both these properties, shown in Figure 59 (f). It does, however, possess a larger lower bound thus resulting in a less within-cluster variance for both twistweight and frame stiffness, as shown in Figure 59 (b) and (g).

Clusters 2 and 3 also may initially appear to follow a similar trend in cluster property averages, but deviate for racket length, swingweight, twistweight and frame stiffness; Figure 59 (a). Additionally, both cluster 2 and 3 possess the largest amount of within-cluster variance regarding most, if not all, racket properties. This can be seen in both Figure 59 and Table 28.
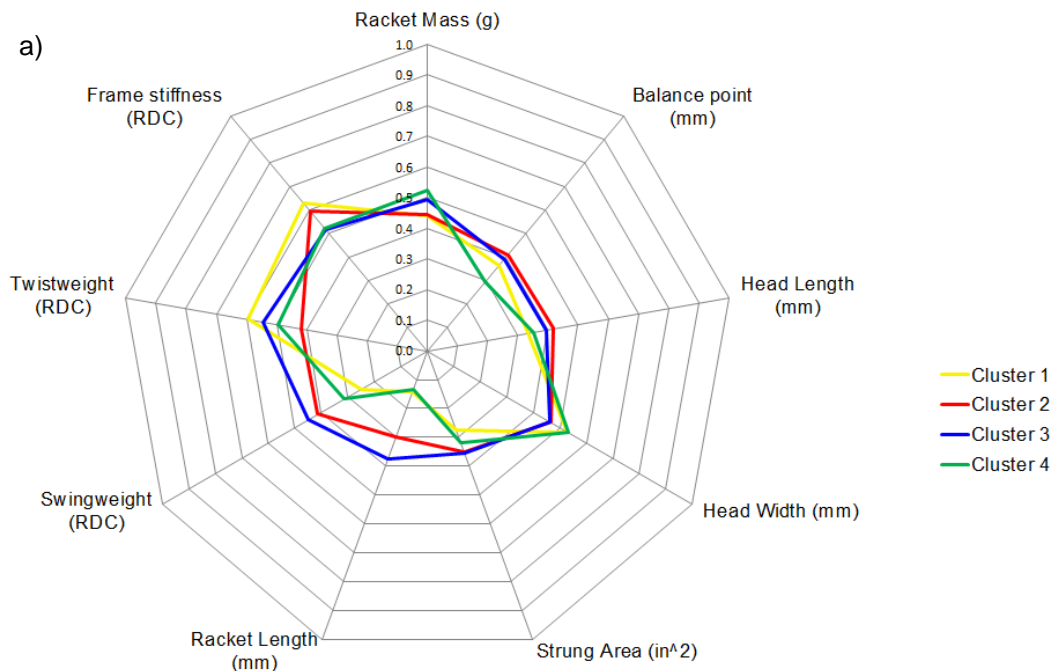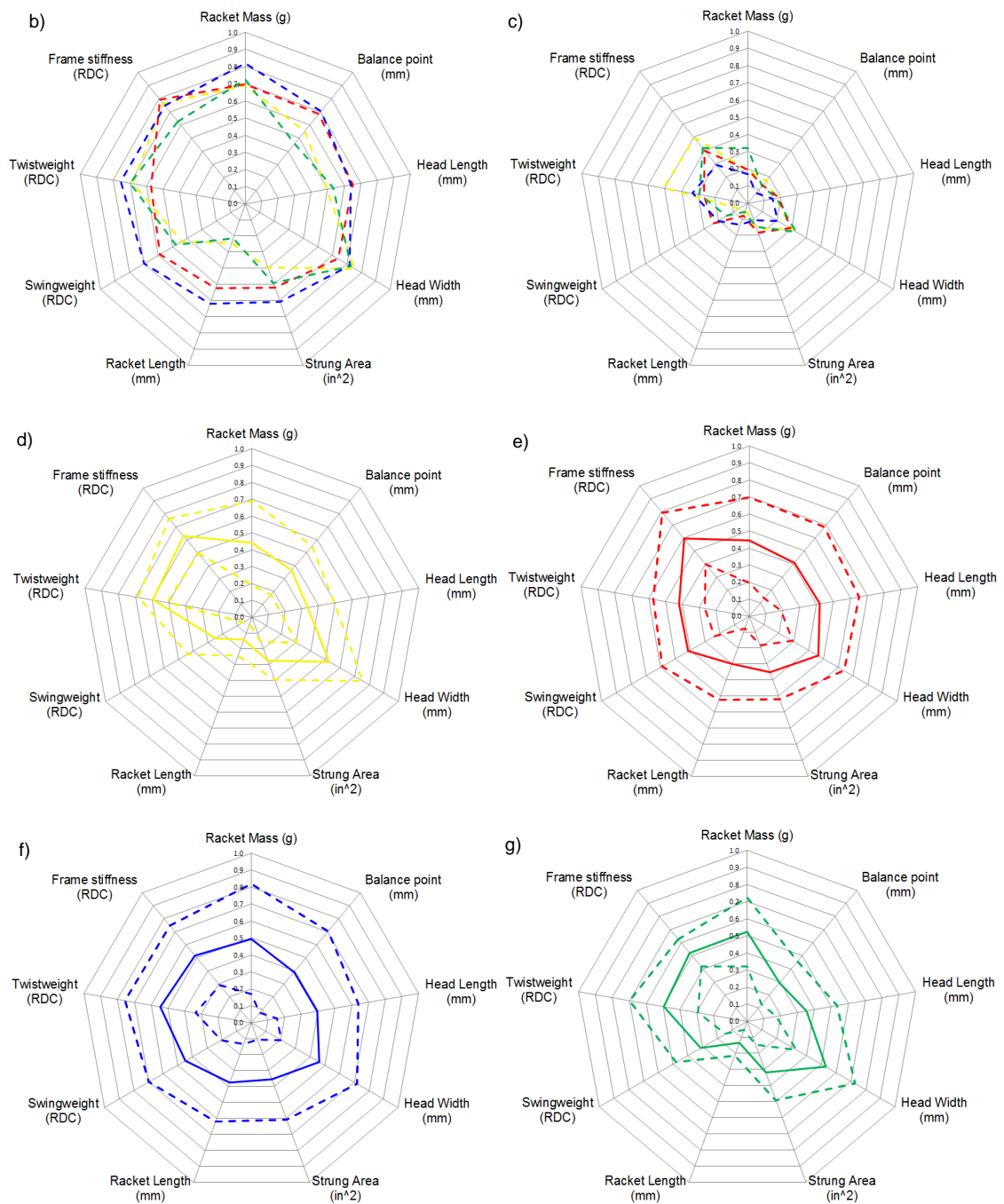
Figure 59 - Topspin Forehand Radar Graphs showing the a) Normalised Means of Racket Property Combinations for all Four Clusters, b) Normalised +1 Standard Deviations of the Four Clusters, and c) the Normalised -1 Standard Deviations of the Four Clusters and the Normalised Means and Standard Deviations of d) Cluster 1, e) Cluster 2, f) Cluster 3 and g) Cluster 4

Table 28 and Figure 59 allows for the comparison of clusters and thus the following deductions. An average racket from cluster 1 will possess the

following properties: light mass, head-light, a short and wide head, a large strung area, short racket length, low swingweight, high twistweight and are stiff.

An average racket from cluster 2 will possess the following properties: light mass, head-heavy, a long and narrow head, a large strung area, long racket length, high swingweight, low twistweight and are average in stiffness.

An average racket from cluster 3 will possess the following properties: heavy mass, head-heavy, a long and narrow head, a large strung area, long racket length, high swingweight, high twistweight and are least stiff.

An average racket from cluster 4 will possess the following properties: heavy mass, head-light, a short and wide head, an average strung area, short racket length, low swingweight, average twistweight and are average in stiffness.

The racket properties relevant to each cluster are a direct result of the behavioural cluster formation. Discussed within Section 6.7 and illustrated in Section 6.5.4, the formation of the behavioural clusters were driven by the between-cluster differences observed at impact positions 1, 3 and 4 (tip, left and right of the longitudinal axis).

Significant differences were identified between the behavioural clusters 2 and 4 regarding rebound playing angle, rebound offset angle and rebound ball velocity when impacting the racket at positions 1, 3 and 4; discussed within Section 6.5.3. As mentioned previously an average racket from cluster 2 will possess light mass, a heavy head, a large strung area, and high swingweight properties. Whereas an average racket from cluster 4 will possess heavy mass, a light head, a large strung area (but slightly less than that of cluster 2) and low swingweight in comparison. Previous research, discussed within Section2.4, has shown that an increase in strung area increases the sweet spot upon the racket face, increasing the rebounding ball's velocity and reducing 'negative' effects (increased deviation from the normal). Similarly, increasing swingweight increases the racket's resistance to rotation along the longitudinal axis. As a result, a ball impacting a racket towards the tip will rebound with greater velocity

and will deviate less from the normal. Ultimately, although a racket from cluster 4 may possess greater total mass to that of a racket from cluster 2, a head heavy racket (a racket whose weight is distributed towards the tip and thus presents with a higher balance point) will rotate less about its COM, increasing rebound ball velocity and decreasing the amount the ball will deviate from the normal. Therefore, the observed decrease in rebound playing and offset angle and increase in rebound ball velocity, for behavioural cluster 2 in comparison to behavioural cluster 4, could be a result of the increased racket's balance point, strung area and swingweight. As a result, cluster 2, in comparison to cluster 4, may be perceived as possessing rackets with more 'control' and 'power' when completing a topspin forehand.

7.3.2 Slice Forehand

The racket property means and standard deviations for each cluster are shown in Table 29. The overall property combinations for each racket, within each cluster, can be found in Appendix G.

Table 29 - Averages and Standard Deviations of the Racket Properties for Each Cluster

Cluster	Racket Mass (g)	Balance Point (mm)	Head Length (mm)	Head Width (mm)	Strung Area (in^2)	Racket Length (mm)	Swingweight (RDC)	Twistweight (RDC)	Frame Stiffness (RDC)
Cluster 1	318 ± 31	320 ± 13	331 ± 13	249 ± 14	95 ± 6	688 ± 5	298 ± 23	10 ± 4	64 ± 5
Cluster 2	299 ± 29	325 ± 14	330 ± 10	248 ± 13	99 ± 3	685 ± 1	279 ± 15	11 ± 1	66 ± 5
Cluster 3	283 ± 29	342 ± 19	348 ± 17	258 ± 14	104 ± 8	697 ± 7	299 ± 12	9 ± 4	68 ± 3
Cluster 4	281 ± 32	338 ± 21	349 ± 22	256 ± 14	106 ± 11	699 ± 10	287 ± 20	11 ± 4	68 ± 5

To aid the between cluster comparisons, the resulting racket properties were normalised, averaged and plotted using a radar. The results of this can be seen in Figure 60 (a). The upper and lower standard deviations for each property, of each cluster, were also normalised and plotted using the radar graphs shown in Figure 60 (b) and (c). To visually aid the interpretation of the within-cluster variance Figure 60 (d), (e), (f) and (g) show the normalised means and standard deviations for cluster 1, 2, 3 and 4 respectively.

Table 29 and Figure 60 reveal no two clusters possess the same combinations of mean racket properties, though in some cases clusters may share a similar or equal mean value for one or two racket properties. Furthermore, large within-cluster racket property variations were also revealed; shown in Figure 60 (d), (e), (f), and (g).

Unlike results for the topspin forehand, differences in cluster property averages are observed for all properties except twistweight and frame stiffness. A one-way ANOVA analysis identified a significant difference for racket mass ($F_{(3, 35)}$ = 3.201, p = 0.035), balance point ($F_{(3, 35)}$ = 3.221, p = 0.034), head length ($F_{(3, 35)}$ = 3.336, p = 0.030), strung area ($F_{(3, 35)}$ = 4.487, p = 0.009) and racket length ($F_{(3, 35)}$ = 7.934, $p < 0.001$). Tukey's post hoc analysis, however, only revealed a significant difference between cluster 1 and cluster 4 for both racket mass (p = 0.034) and strung area (p = 0.007), whereas for racket length, significant differences were found between cluster 1 and cluster 4 (p = 0.004), cluster 2 and cluster 3 (p = 0.019) and cluster 2 and cluster 4 (p = 0.002).

Table 29 and the visual aid of Figure 60 reveal distinct cluster average differences between clusters 1 and 2 with clusters 3 and 4 for mass, balance point, head length, head width, strung area and racket mass. The one-way ANOVA found between cluster significance for all stated properties, with the exception of head width. This is assumed to be the result of the amount variance within all clusters for head width. Clusters 1 and 2 not only possess smaller upper boundary conditions but also possess smaller within-cluster variance for balance point, head length, strung area and racket length, thus resulting in smaller property cluster averages.

Clusters 3 and 4 possess similar trends for most cluster property averages but disconnect due to differences in swingweight and twistweight; Figure 60 (a). The observed similarities and differences are assumed to be a result of the within-cluster variances observed for both clusters 3 and 4; Figure **60** (f) and (g) respectively. Table 29 and Figure 60 (d) - (g) identify both clusters 3 and 4 to possess large within-cluster variances for mass, balance point, head

length, head width, strung area and racket length. However, cluster 3 confines to the lowest within-cluster variance for swingweight and frame stiffness.
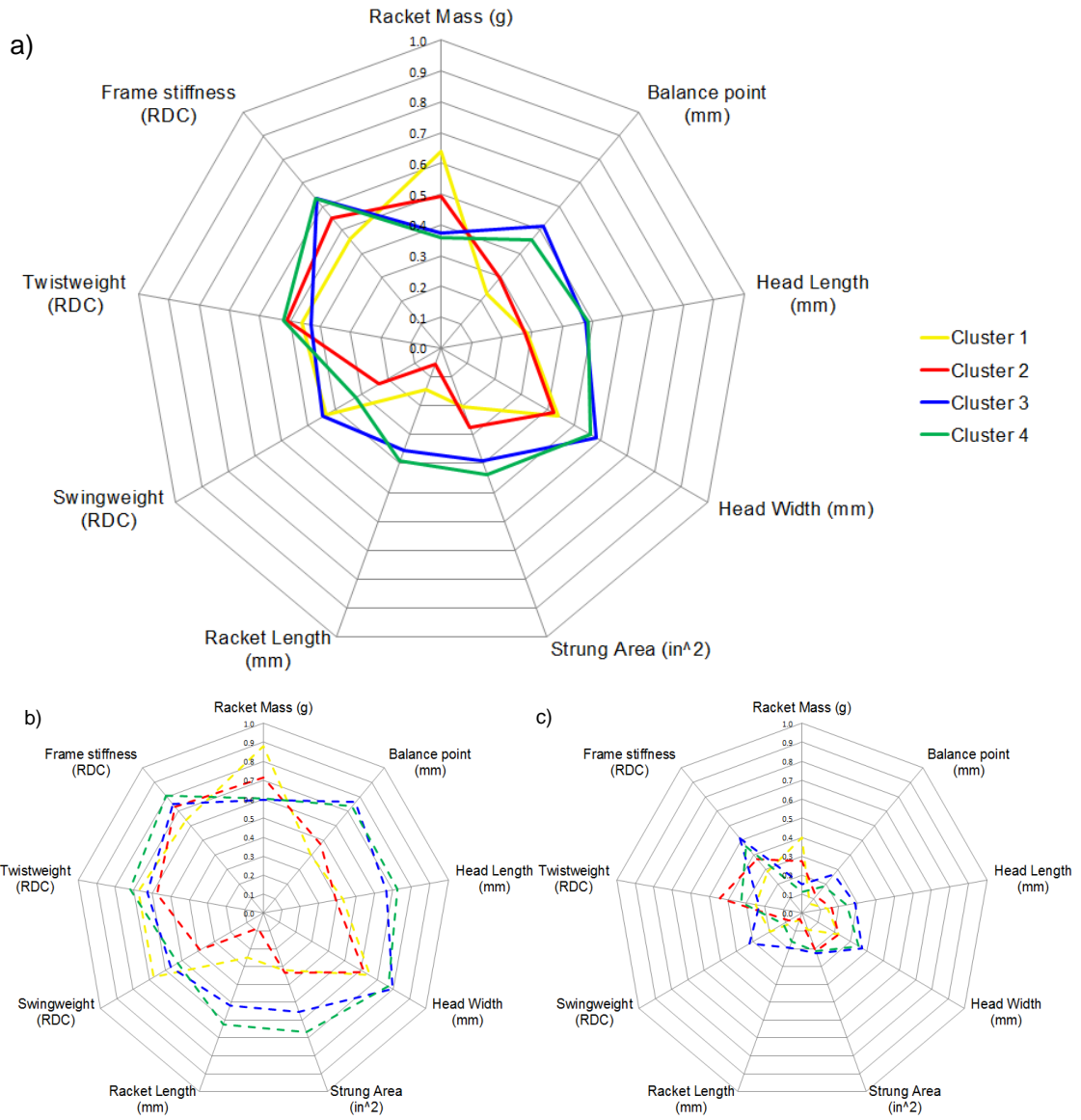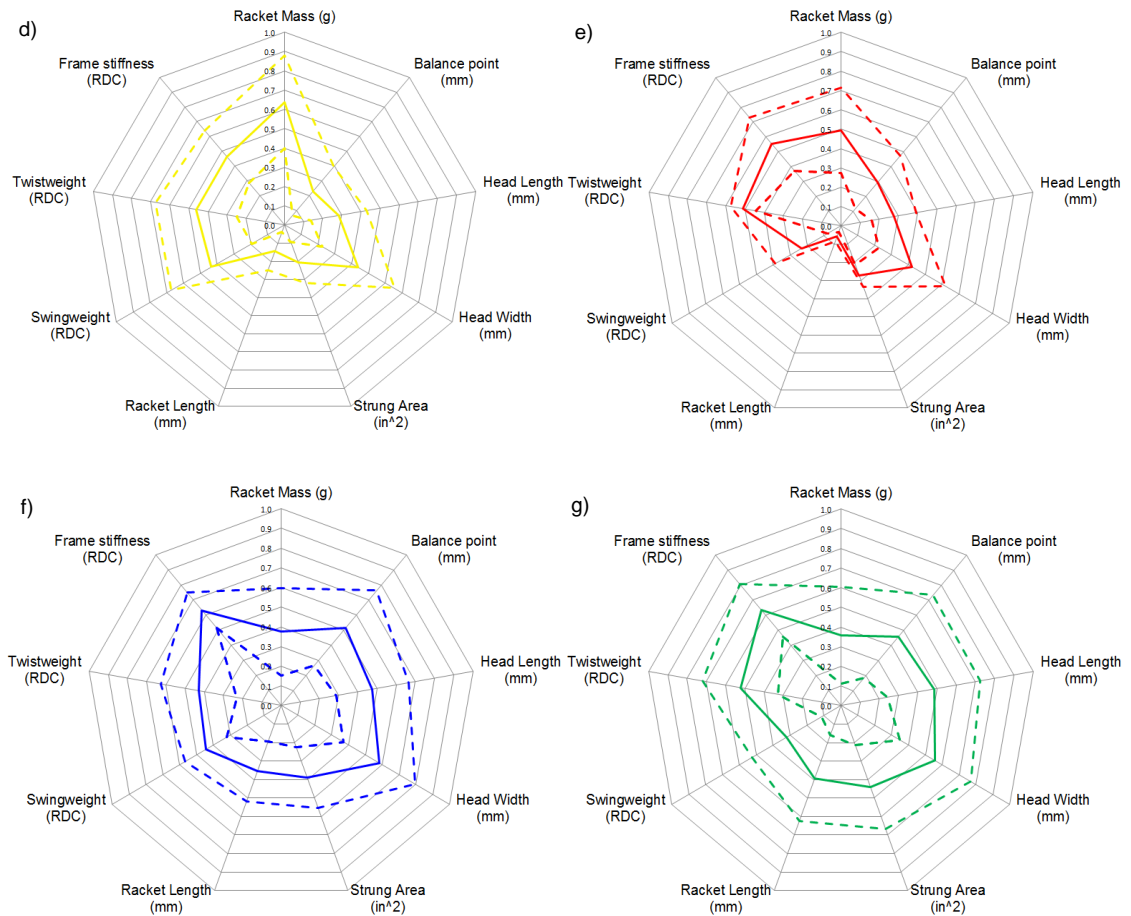
Figure 60 - Slice Forehand Radar Graphs showing the a) Normalised Means of Racket Property Combinations for all Four Clusters, b) Normalised +1 Standard Deviations of the Four Clusters, and c) the Normalised -1 Standard Deviations of the Four Clusters and the Normalised Means and Standard Deviations of d) Cluster 1, e) Cluster 2, f) Cluster 3 and g) Cluster 4

Table 29 and Figure 60 allows for the comparison of clusters and thus the following deductions. An average racket from cluster 1 will possess the following properties: heavy mass, head-light, a short and narrow head, a small strung area, short racket length, high swingweight, average twistweight and are least stiff.

An average racket from cluster 2 will possess the following properties: average mass, head-light, a short and narrow head, an average strung area, short racket length, low swingweight, high twistweight and possess average stiffness.

An average racket from cluster 3 will possess the following properties: light mass, head-heavy, a long and wide head, a large strung area, long racket length, high swingweight, low twistweight and are stiff.

An average racket from cluster 4 will possess the following properties: light mass, head-heavy, a long and wide head, a large strung area, long racket length, average swingweight, high twistweight and are stiff.

As previously mentioned, the racket properties relevant to each cluster are a direct result of the behavioural cluster formation. Similarly to the results of the topspin forehand, the formation of the behavioural clusters were driven by the between-cluster differences observed at impact positions 1, 3 and 4; discussed within section 6.7 and illustrated in section 6.6.4.

Significant differences were identified between the behavioural clusters 2 and 4 regarding rebound playing angle, rebound offset angle and rebound ball velocity when impacting the racket at positions 1, 3 and 4; discussed within section 6.6.3. As previously mentioned an average racket from cluster 2 will possess the following properties; head-light, a short and narrow head, an average strung area, low swingweight and average frame stiffness. Whereas an average racket from cluster 3 will possess the following properties in comparison: head-heavy, a long and wide head, a larger strung area, higher swingweight and higher frame stiffness. As previously mentioned increasing a rackets strung area, swingweight and balance point reduces ball deviation from the racket normal and increases post impact ball velocity. Following the impact of a ball upon the racket face, the racket will recoil and vibrate with associated energy losses. Previous research, discussed within section 2.4, has also found that energy losses associated with frame vibrations are dependent on impact position upon the racket face and the stiffness of the racket frame. For oblique spinning impacts, it was found that the ball will rebound with greater velocity with an increase in frame stiffness. Therefore, for impacts occurring at positions 1, 3 and 4, the observed decreases in rebound playing and offset angle and increase in rebound ball velocity, for behavioural cluster 3 in comparison to behavioural cluster 2, could be a result of the increased racket's balance point,

strung area, swingweight and frame stiffness. As a result, cluster 3, in comparison to cluster 2, may be perceived as possessing rackets with more 'control' and 'power' when completing a slice forehand.

Though previous research provides a general insight into an average racket's behaviour with respect to the properties it possesses (for a given cluster), due to the diverse property combinations for within each cluster there is no clear indication as to the driving properties which result to the formation of the behavioural clusters.

7.4 *Relationships between Behavioural Clusters and Racket Properties*

Statistical analysis is required to identify behavioural cluster-racket property relationships, due to the within-cluster variance of each racket property.

Multinomial logistic regression (MNLR) is a statistical method for analysis of a dataset in which one or more independent variables determine a set of three or more categorical dependent variables. The independent variables can be of any type: nominal, ordinal and/or interval. MNLR, not only, reveals fundamental relationships between a set of independent variables (predictors) and the categorical characteristic of interest (dependent variables) (Fields, 2009), but also develops a model (further discussed in Section 7.4.3) which can be used for prediction (Sperandei, 2014). Further explanation of MNLR will be conducted concerning the identified behavioural clusters (dependent variables) and the rackets of given properties (independent variables).

The fundamentals of MNLR are similar to those of multiple regression analysis, however, unlike traditional multiple regression which uses least square estimation methods, multinomial logistic regression uses maximum likelihood estimation to evaluate the probability of cases (Fields, 2009). Therefore, the value that is being predicted is a value of probability. More specifically, for each behavioural cluster, MNLR develops a model which predicts the probability of

whether a racket of given properties corresponds to one behavioural cluster or another (Mertler & Reinhart, 2016).

Discriminant function analysis (DFA) possesses similarities to multinomial logistic regression and is considered an appropriate alternative to MNLR. However, discriminant function analysis requires adherence to the assumptions of normality, linearity and homoscedasticity of the independent variables. Multinomial logistic regression does not require such assumptions, thus resulting in a more flexible method of analysis (Tate, 1992). In addition, the production of negative predictive probabilities, which can occur through the application of multiple regression analysis involving dichotomous outcomes, cannot be achieved through the means of MNLR. Finally, multinomial logistic regression can also produce nonlinear models, adding to its overall flexibility.

7.4.1 **Main Effects**

A main effect is the effect of an independent variable on a dependent variable, whilst ignoring the effects of any other independent variable. Using MNLR methods in SPSS, the effect of the racket properties on the behavioural clusters were investigated. For each investigation, the analysis model was included for review.

Topspin Forehand

MNLR analysis for the topspin forehand identified statistical significance of three main effects:

1. Head width ($p = 0.026$)
2. Strung area ($p = 0.005$)
3. Twistweight ($p = 0.017$)

Mass, balance point, head length, racket length and swingweight were not found to have a statistical effect on the relationship between racket property and behavioural cluster.

Slice Forehand

MNLR analysis for the slice forehand revealed statistical significance of three main effects:

1. Head Length ($p = 0.028$)
2. Strung Area ($p < 0.001$)
3. Swingweight ($p = 0.004$)

Mass, balance point, head width, racket length and twistweight were not found to have a statistical effect on the relationship between racket property and behavioural cluster.

7.4.2 Interaction Effects

An interaction effect is when the effect when one independent variable is co-dependent on the value of another independent variable. The interacting effect of the racket properties on the behavioural clusters was investigated using Multinomial Logistic Regression methods in SPSS.

Topspin Forehand

MNLR analysis for the topspin forehand identified statistical significance of between the following properties:

1. Strung area with swingweight ($p = 0.007$)
2. Twistweight with frame stiffness ($p = 0.017$).

MNLR revealed the relationships between two sets of interacting racket properties for the prediction of the categorical behavioural characteristics previously defied (discussed within section 6.5.3). Though statistical interaction effects were identified, the effects of these co-dependent properties have not previously been investigated for which a Bivariate Pearson's correlation was used to explore the potential correlations between properties.Strung area was found to possess very weak positive correlation with swingweight ($r = 0.125$, $p = 0.447$). Similarly, it was found that twistweight with frame stiffness also possess a very weak positive correlation ($r = 0.086$, $p = 0.601$).
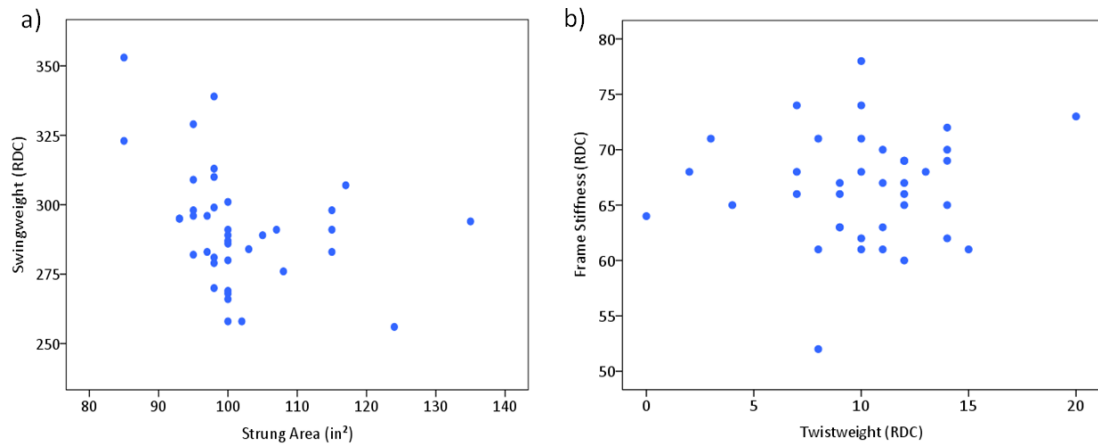
Figure 61 - Results of a) Swingweight vs Strung Area and b) Frame Stiffness vs Twistweight

Slice Forehand

MNLR analysis for the slice forehand identified statistical significance of between the following properties:

1. Strung Area with Racket Length ($p < 0.001$)
2. Head Length with Swingweight ($p = 0.012$)

MNLR revealed the relationships between two sets of interacting racket properties for the prediction of the categorical behavioural characteristics previously defied (discussed within section 6.5.3). Though statistical interaction effects were identified, the effects of these co-dependent properties have not previously been investigated for which a Bivariate Pearson's correlation was used to explore the potential correlations between properties. Strung area was found to possess a strong positive correlation with racket length (r = 0.734, $p < 0.001$), whereas a weak negative correlation was found between head length and swingweight (r = -0.355, $p = 0.027$).
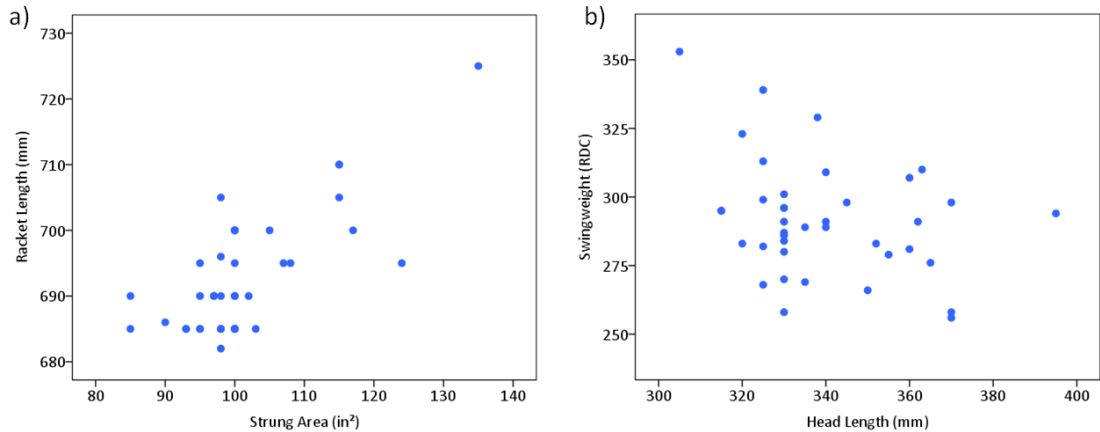
Figure 62 - Results of a) Racket Length vs Strung Area, and b) Swingweight vs Head Length

7.4.3 Model Summary

MNLR analysis also produces a model that best predicts different possible outcomes of categorically distributed dependent variables, given a set of independent variables.

Similar to other forms of regression, MNLR develops a model which can be used for prediction, but rather than predicting a value of the dependent variable, it can be used to calculate the probability of an independent variable corresponding to a dependent variable.

$$P\,(Y) = \frac{1}{1+e^{-\,(b_0\,+\,b_1X_{1i}\,+\,b_2X_{2i}\,+\,...\,+\,b_nX_{ni})}} \qquad [28]$$

where *P(Y)* is the probability of *Y* occurring, *e* is the base of natural logarithms, b_0 is a constant, X_n is a predictor variable with b_n as their respective coefficient (or weight).

As well as assessing the significance of the independent variables, the full model is also tested using the log-likelihood statistic, which is equivalent to the residual sum of squares, representing the unexplained variance after the model has been fitted. Therefore, large log-likelihood values indicate poorly fitting statistical models, as the larger the value the more the unexplained variance. Two models are generally compared when performing MNLR; the intercept only model and the final model, also referred to as the null and full

model. The null model simply fits an intercept for the prediction of the dependent variable, as it does not control for any predictor variables, whereas the full model includes the specified predictor variables and is developed through an iterative process. The Likelihood Ratio tests show whether significant improvements have been made on the null model and is achieved through the calculation of the difference between the -2 log-likelihoods for the null and full models. This calculation is also referred to as the chi-square likelihood ratio statistic.

The likelihood ratio chi-squared statistic also tests the models goodness-of-fit. Both Pearson and Deviance are chi-squared based statistical tests, analysing the significant difference of the predicted values from the model from the given observed values. If the results of these tests are not significant ($p > 0.05$) then the model is a good fit as the predicted values do not differ significantly from that observed.

The accuracy of the model is further assessed through the means of a classification table. A perfect model, a model possessing 100 % accuracy, would only show values on the diagonal of the table, thus correctly classifying all cases.

Topspin Forehand

Table 30 shows the model fitting information assessing the null model (intercept only) and the full model (final model) for the topspin forehand. Results indicate that the full model possesses a higher degree of accuracy for prediction, than that of the null model, χ^2 (15) = 36.178, p = 0.002.

Table 30 - Model Fitting Information of the Topspin Forehand

Model	Model Fitting Criteria	Likelihood Ratio Tests		
	-2 Log Likelihood	Chi-Square	df	Sig.
Intercept Only	107.429			
Final	71.251	36.178	15	.002

Table 31 provides further evidence for the final model's goodness-of-fit. Both Pearson and Deviance show values of non-significance, indicating a good fit of the full model.

Table 31 - Goodness-of-Fit for Topspin Forehand

	Chi-Square	df	Sig.
Pearson	102.703	99	.705
Deviance	71.251	99	.972

Table 32 reports the accuracy of the full model for the topspin forehand. Though the model presents a high degree of accuracy for the prediction of rackets possessing behavioural characteristics found within cluster 1, the level of accuracy is found to decrease for clusters 2, 3 and 4, consequently, resulting in a model with an overall accuracy level of 56.4 %.

For the prediction of rackets possessing behavioural characteristics found within cluster 4, less than half were correctly predicted with an observed spread of predictions across all behavioural clusters. Similarly, rackets of behavioural cluster 2 show accuracy rates of just over half, with approximately 36 % of rackets incorrectly predicted to behavioural cluster 3 and, in doing so, the subsequent behavioural characteristics of these rackets are wrongly predicted.

Table 32 - Classification Table Results for Topspin Forehand

Observed	Cluster 1	Cluster 2	Cluster 3	Cluster 4	Percent Correct
Cluster 1	6	0	1	1	75.0%
Cluster 2	0	6	4	1	54.5%
Cluster 3	1	3	6	1	54.5%
Cluster 4	2	2	1	4	44.4%
Number of Rackets	$\frac{9}{39}$	$\frac{11}{39}$	$\frac{12}{39}$	$\frac{7}{39}$	
Overall Percentage	23.1%	28.2%	30.8%	17.9%	**56.4%**

Slice Forehand

Table 33 shows the model fitting information assessing the null model (intercept only) and the full model (final model) for the slice forehand. Results indicate that the full model possesses a higher degree of accuracy for prediction, χ^2 (15) = 47.859, p = 0.00, than that of the null model.

Table 33 - Model Fitting Information of the Slice Forehand

Model	Model Fitting Criteria	Likelihood Ratio Tests		
	-2 Log Likelihood	Chi-Square	df	Sig.
Intercept Only	103.637			
Final	55.778	47.859	15	.000

Analysis of the model's goodness-of-fit, through means of Pearson and Deviance statistics, further indicated a good fit of the full model. This can be seen in the non-significant Pearson and Deviance values, found within Table 34.

Table 34 - Goodness-of-Fit for Topspin Forehand

	Chi-Square	df	Sig.
Pearson	68.714	99	.991
Deviance	55.778	99	1.000

Table 35 reports the accuracy of the full model, for the slice forehand. Classification results show the model to possess perfect accuracy for the prediction of rackets possessing behavioural characteristics of cluster 2. High accuracy rates were also observed for the prediction of rackets possessing behavioural characteristics found within clusters 1 and 4 with minimal spread of incorrect predictions.

However, the accuracy of the model can be seen to vastly decrease for the prediction of overall racket properties, ensuing behavioural characteristics, belonging to cluster 3. Table 35 shows, approximately, an equal spread across clusters 1, 3 and 4, thus resulting in low accuracy rates. This lower level of accuracy consequently results in an overall full model accuracy rate of 66.7 %.

Table 35 - Classification Table Results for Slice Forehand

Observed	Cluster 1	Cluster 2	Cluster 3	Cluster 4	Percent Correct
Cluster 1	9	2	0	2	69.2%
Cluster 2	0	6	0	0	100.0%
Cluster 3	2	0	2	3	28.6%
Cluster 4	4	0	0	9	69.2%
Number of Rackets	$\dfrac{15}{39}$	$\dfrac{8}{39}$	$\dfrac{2}{39}$	$\dfrac{14}{39}$	
Overall Percentage	38.5%	20.5%	5.1%	35.9%	**66.7%**

7.5 *Discussion*

The hierarchical cluster analysis conducted within Chapter 6, identified four distinct behavioural clusters for both the topspin and the slice forehand. Each cluster contained a range of rackets possessing similar behavioural characteristics and dissimilar behavioural characteristics to those of a different cluster. Statistical analysis of the cluster's subsequent racket properties revealed overall significant differences between clusters for racket length for the simulated a topspin forehand. Whilst for the simulated slice forehand, overall significant differences between clusters were identified for racket mass, balance point, head length, strung area and racket length. Johnson & McHugh (2006) revealed the topspin forehand to be a type of shot most commonly used within tennis practice, accounting for a total of 72 % of all executed forehand groundstrokes, whilst the slice forehand was found to be the least executed, standing at 4 %. The topspin forehand is the first 'technical' shot type taught to both beginners and juniors, whereas the slice forehand is considered technically challenging to execute successfully. McMorris (2014) stated how changes in equipment can lead to the adaptation of skill and technique. Therefore, assuming no technique amendment from the player due to biofeedback, the statistical properties differing between the slices' behavioural clusters reveal the implications of the rackets' mechanical properties to the success of the slice forehand.

Although statistical differences of racket properties were identified between clusters, large within-cluster variances were also identified for all racket properties. Such variances were observed within all identified clusters, for both simulated forehands. Multinomial logistic regression (MNLR) was conducted to reveal the underlying relationships between the subsequent racket properties and the behavioural clusters. Initially, relationships between the individual racket properties and behavioural groups were investigated. MNLR revealed head length, strung area and twistweight to have a significant main effect on the behavioural clusters for the topspin forehand. For the slice forehand, head width, strung area and swingweight were found to have a

significant effect on the behavioural clusters. Previous research and findings have associated strung area with both head length and head width and though strung area was the only property to have a significant main effect for both the topspin and slice forehand, the result of this association can be seen in the previously stated significant main effects. Upon these results, and previous findings, MNLR was then used to identify relationships between multiple racket properties and the behavioural clusters for both the topspin and slice forehand shot.

The MNLR analysis of the topspin forehand revealed relationships between two distinct interaction effects and the behavioural clusters formed. A significant interaction effect was found between strung area with swingweight. Bivariate Pearson's revealed a very weak correlation between strung area and swingweight, $r = 0.125$. However, MNLR identified strung area to be a significant main effect of the behavioural clusters, whilst also having significant dependency on the interaction with swingweight and vice versa. A racket possessing a larger strung area signifies an increase in racket head (increase in head length and/or head width), thus resulting in a larger sweet spot. Previous findings indicate that a larger sweet spot increases the rebounding ball's resultant velocity but also reduces the effects of impacts occurring off the longitudinal axis. Similarly, an increase in swingweight has also been found to increase resultant rebound ball velocity. Large mean property differences, for both strung area and swingweight, can be seen between clusters 1 with 2 and clusters 1 with 3; as seen in Table 28 and Figure 59 (a). Though the largest mean property difference for strung area and swingweight can be seen between clusters 1 and 3, cluster 3 also possesses the largest amount of variance, shown by Table 28 and Figure 59 (f). This variance could produce larger property cluster means without necessarily producing significant cluster behavioural differences. Cluster 2, however, comprises of equal and/or similar property means as cluster 3 but with a reduced amount of variance. Behavioural cluster results, discussed in Section 6.5.3, reveal a significant increase in resultant rebound ball velocity for cluster 2 at impact positions 3 and 4, both of which are impact locations off the longitudinal axis. Similarly, a significant

decrease in rebound offset angle was also observed for cluster 2, thus reducing the effects of off-axis impacts. Although the one-way ANOVA identified a significant property difference between clusters for only racket length, MNLR not only revealed strung area to have a significant effect on the behavioural clusters but it also revealed an interacting effect with swingweight on said behavioural clusters. Investigations regarding the exposed property effects, both main and interacting, indicate that with an increase in strung area and swingweight, the effects of impact occurring off the longitudinal axis will decrease whilst resultant rebound ball velocity will increase.

The second interaction effect, of the topspin forehand analysis, was observed between twistweight with frame stiffness. The MNLR identified twistweight to have a significant main effect of the behavioural cluster, whilst also revealing a significant interacting dependence on frame stiffness, regardless of virtually no property correlation between these two properties, $r < 0.01$. As discussed within Chapter 2, twistweight is the resistance to angular acceleration of the frame about the longitudinal axis. Brody (1985) proved that racket mass multiplied by its head width squared gives a very good approximation of the racket's twistweight, to which head width was also identified as an individual significant predictor of behavioural cluster (main effect). Previous findings have concluded that an increase in twistweight reduces the negative effects of off-axis impacts, whilst frame stiffness has been found to have virtually no effect for impacts at or close to the node point. However, the effects of frame stiffness are found to be greater for impacts typically struck towards the racket tip. As previously illustrated throughout this thesis, such as Figure 57 (f), impact position 1 occurs away from the node and towards the tip of the racket. Large mean property differences, though not significant, for both twistweight and frame stiffness can be seen between clusters 1 with 2; shown within Table 28. In contradiction with previous findings, behavioural cluster results for impact positions 3 and 4, discussed in Section 6.5.3, indicate a significant increase in both rebound offset angle and playing angle with an increase in twistweight. Similarly, in contradiction with previous findings, resultant rebound ball velocity was found to decrease with an

increase in frame stiffness; shown in Table 19. Though cluster 2 may possess the smallest cluster property averages for frame stiffness and twistweight, it does, however, possess large cluster property averages for both strung area and swingweight; seen within Table 28. As discussed above, with an increase swingweight and/or strung area, resultant rebound ball velocity will also increase whilst also reducing the negative effects of impacts occurring off the longitudinal axis. A significant increase in resultant rebound ball velocity, from cluster 1 to cluster 2, at impact positions 3 and 4 was revealed by the one-way ANOVA in Section 6.5.3. Similarly, a significant decrease in rebound offset angle was also observed for cluster 2, thus reducing the effects of off-axis impacts. Although the MNLR revealed a second interacting relationship between frame stiffness and twistweight, upon this investigation, it can therefore be assumed that the interacting effect of swingweight with strung area is a significantly stronger predictor of behavioural cluster formation and can potentially negate the effects of frame stiffness with twistweight. Additionally, within section 4.3.2, the spread, range, normality and fidelity of twistweight was identified and discussed. In comparison to all properties twistweight can be seen to possess the smallest variance and therefore the differences observed between clusters could have been identified as significant, reducing the fidelity of twistweight as a main and/or interacting predictor of behavioural clusters.

The MNLR analysis of the slice forehand also revealed relationships between two distinct interaction effects and the identified behavioural clusters. A significant interaction effect was found between racket length with strung area. Further investigation using bivariate Pearson's analysis revealed a strong correlation between said properties, $r = 0.734$. The MNLR analysis identified strung area to have a significant main effect on the behavioural cluster, whilst also possessing an interacting effect with racket length on behavioural clusters. As previously discussed a racket possessing a larger strung area implies a larger racket head and, thus, consequently implying a larger sweet spot. Previous findings indicate that a larger sweet spot increases the rebounding ball's resultant velocity and decreases the negative effects of impact occurring off the longitudinal axis. The one-way ANOVA identified a significant difference

for strung area between cluster 1 and cluster 4. Behavioural cluster results, discussed in Section 6.6.3, revealed that with a significant increase in strung area, resultant rebound ball velocity also significantly increased at impact positions 1, 3 and 4. Similarly, significant decreases regarding rebound offset angle were observed at impact positions 3 and 4, thus reducing the negative effects of off-axis impacts. It can therefore be assumed that this interaction effect is strongly influenced by the identified significant main effect of strung area ($p < 0.001$) than that of racket length ($p = 0.429$).

The second interaction effect for the slice forehand was found between head length with swingweight. Though only a weak negative correlation was observed, $r = -0.355$, the MNLR analysis not only revealed head length and swingweight to have significant main effects, but to also have significant dependency on each other as an interacting effect of behaviour. Large mean property differences, for both head length and swingweight, can be seen between clusters 2 with 3; as seen in Table 29 and Figure 60 (a). The swingweight of a racket is dependent on the racket's mass and the distribution of this mass throughout the racket; otherwise known as balance point. This occurrence can be observed in Table 29, in that though cluster 3 possesses a smaller cluster average of mass, it does, however, possess a larger cluster average of balance point. Such results indicate the mass distribution to occur more around the racket's head, and thus corresponding to the dependency of swingweight on both mass and balance point. Previous findings have shown that with an increase in swingweight, resultant rebound ball velocity also increases. Although the results between behavioural clusters 2 and 3, discussed in Section 6.6.3, show an increase in resultant rebound ball velocity at all impact positions, between clusters significant differences were only observed at the node point and impact positions 1 and 4. These results are in agreement with previous findings.

This method of analysis exposed interaction effects between properties which have not previously been reviewed, potentially due to the lack of correlation. However, investigations were limited to relationships between two racket properties only, due to the statistical lack of data (small sample size).

Previous research has shown swingweight to be dependent on a racket's mass and balance point, twistweight to be dependent on a racket's mass and head width, and finally, strung area to be dependent on the racket's head width and head length. Within each identified interaction effect is a racket property whose value is dependent on one and/or more other properties. It can, therefore, be assumed that although interaction effects have currently been identified between two leading properties, there is the potential for interacting effects between three and/or more racket properties.

The identified and thoroughly discussed significant effects, both main and interaction, were then used to develop a model for uses of prediction. Comparison of the full model (final) was conducted against that of the null model (intercept only) for the assessment of performance. The null model simply fits an intercept for the prediction of the dependent variables, as it does not control for any predictor variables; such as the identified main and interaction effects. The full model includes the specified predictor variables and is developed through an iterative process which maximises the log-likelihood to predict the outcome of the dependent variable.

Table 30 presents the model fitting summary for the topspin forehand. As previously mentioned the -2 log-likelihood represents the unexplained variance of the data. For the full model, results show a decrease in this value, thus indicating more variance to have been explained. The chi-square test revealed the difference in explained variance to be significant, thus denoting the final model to predict significantly ($p = 0.002$) better than that of the null model as it explains a significant amount of the original variance. Further assessing the goodness-of-fit, Pearson and Deviance chi-squared statistics were produced. The Pearson statistic can be susceptible to sample size, thus producing the observed differences of results between the Pearson and Deviance tests. Though differences were observed, both Pearson and Deviance tests revealed insignificant findings, thus indicating a good fit of the final model.

The model fitting summary of the slice forehand is presented within Table 33. Similar to results observed for the topspin forehand,-2 log-likelihood results

were found to have decreased for the full model. The chi-squared tests presented a significant ($p < 0.001$) improvement of the full model in comparison to the null model; thus significantly increasing the explained variance. The model's goodness-of-fit was further assessed through the means of Pearson and Deviance chi-squared statistics, for which large insignificant values were presented thus indicating a good fit. Through the inclusion of both the main and interaction effects and maximising the log-likelihood of outcomes observed within the data, the full model showed a significant improvement, resulting in a model possessing a higher degree of prediction accuracy in comparison to the null model.

The accuracy of said models were then further investigated through the use of a classification table. An overall model prediction accuracy rate of 56.4% was observed for the topspin forehand; shown in Table 32. The model was found to predict overall racket properties ensuing behavioural characteristics of cluster 1 to a high degree of accuracy. This level of accuracy, however, was found to decrease for the prediction of racket ensuing behavioural characteristics for cluster 2, cluster 3 and cluster 4. Similarly, an overall model prediction accuracy rate of 66.7% was observed for the slice forehand; shown in Table 35. A perfect accuracy rate was observed for the prediction of overall racket properties ensuing behavioural characteristics of cluster 2, with high degrees of accuracy also observed for rackets ensuing behavioural characteristics of cluster 1 and cluster 4. However, the prediction rate for racket properties ensuing behavioural characteristics of cluster 3 vastly decreased, causing a decrease in the overall model prediction accuracy rate. Such inaccuracies are assumed to be the result of the large within-cluster variance of each racket property, found for both simulated forehand shots.

7.6 *Conclusion*

This chapter investigated the subsequent racket properties, of the distinct behavioural clusters discussed in Chapter 6, and exposed large within-cluster variations despite between-cluster property average differences. However, statistical between-cluster average differences were only observed for racket

length when simulating a topspin forehand, whereas when simulating slice forehand overall significant differences between clusters were observed for racket mass, balance point, head length, strung area and racket length. From this evaluation, 'technicality' of the slice forehand can be assumed to be influenced by the mechanical properties a racket retains. Although statistical differences of racket properties were identified between clusters, large within-cluster variances were also identified for all racket properties indicating the need for machine learning techniques to identify relationships between racket properties and behaviour.

Multinomial logistic regression is a strong and effective method of analysis to understanding functional relationships between clusters of behavioural characteristics and multiple varying and interacting racket properties. Both individual and interacting properties were identified as predictors of clusters possessing distinct behavioural characteristics, regardless of property correlation. These findings indicate that the behaviour of a tennis racket, for typical forehand shots, are not dependent on one racket property or property combinations but rather a complex dynamic between all properties. Using the identified complex relationships between racket properties and behavioural characteristics for the development of a predictive model would aid the ITF to regulate the sport and intervene before 'game changing' rackets are able to have implications on the nature of the game.

However, this method of analysis for the development of a predictive model currently lacks accuracy. An increase in sample size could not only decrease the within-cluster variance of each racket property and uncover relationships between an increased number of interacting properties, but it could also develop more successful specific forehand models, for the prediction of typical behavioural characteristics.

8 Conclusion

8.1 *Introduction*

This chapter will discuss and conclude the results of this programme of research. First, a summary of the findings for each objective will be presented; categorised in accordance to the objectives outlined in Chapter 2. This will be followed by a conclusion and then possible further investigations.

8.2 *Summary of Research*

The aim of this thesis was to ascertain the relationships between racket properties and behavioural characteristics, for specific forehand shots found within the field of play. To address this aim, five objectives were formed. In this section, a summary of the findings for each objective is given.

Objective 1: Critically analyse existing literature in the field of ball to racket impacts relevant to this project.

Previous researchers have investigated the effects of racket properties for ball-racket impacts, showing how racket properties influence the rebound characteristics of the ball post-impact. However, due to the large number of potential testing parameters, ball to racket impacts have been limited to either perpendicular impacts along the longitudinal axis of a tennis racket, oblique impacts not representative of realistic playing conditions or oblique impacts limited to one tennis racket. Therefore, to advance knowledge regarding the effects of racket properties, it is vital to ensure testing is conducted on a wide range of racket properties and property combinations, whilst also ensuring accurate representation and laboratory simulation of typical forehand shots found within the field of play.

When undertaking laboratory experiments, conditions must be representative of those found within the field of play. Player testing is considered to be an appropriate method of determining ball and racket kinematics to ensure realistic simulation within a laboratory environment. More specifically, the player

Conclusion

testing data, collected at the 2006 and 2007 Wimbledon Qualifying Tournament provides great insight into the range of, both, racket and ball kinematics found within the field play. However, the data does not provide any indications as to the kinematics regarding different specific forehand shot types. Categorisation of the raw forehand player testing data, into groups of similar shot conditions, will not only further provide for realistic simulation of different forehand shot types, but will also reduce inconsistencies between studies regarding inbound testing parameters for an average forehand shot. Player testing results have also indicated impact locations to occur off the rackets longitudinal axis, for which a tight grip has been found to be favourable for such impacts. However, the value defining that of a tight grip has been found to be inconsistent between studies. Therefore, grip values must also be further investigated to ensure a correct representation of the interface between the racket and the player.

Undertaking large-scale laboratory-based testing ultimately produces a large, and possible, complex data sets. Cluster analysis is a method of unsupervised learning that aids the identification of patterns of an input data set, without pre-existing labels. Therefore, the goal of clustering is descriptive and can be used to identify distinct clusters within such a data set. Within sport, the most commonly used method of cluster analysis has been found to be a hierarchical cluster analysis. Hierarchical cluster analysis provides versatility regarding the method of approach, thus providing optimal cluster formations for the specified dataset. Such a method can be applied to identify distinct groups of similar racket behaviour, to uncover potential connections to racket properties or property combinations.

Objective 2: Determine the racket kinematics associated with specific forehand shots, using data collected from the practice courts at the 2006 Wimbledon Qualifying Tournament.

A large-scale laboratory-based data collection can quickly exceed practical expectations, due to the number of potential testing parameters. Therefore, careful consideration regarding the testing parameters is essential for the development of an effective and efficient test protocol for large-scale

Conclusion

data collection. Through the identification of typical racket kinematics for forehand shots found within the field of play can constrain and reduce the number of potential inbound testing parameters for a large-scale method, whilst also allowing for the simulation of specific shot types within a laboratory environment. To achieve this, a PCA and cluster analysis, on the male player testing data collected from the 2006 Wimbledon Qualifying Tournament, was conducted. Execution of this analysis identified the characteristics regarding two typical topspin forehand shots and a typical slice forehand shot. Though the two identified topspin forehand shots display similar racket kinematics, inbound offset angle is the defining characteristic distinguishing between two specific topspin forehands. Similarly, inbound playing angle, angular velocity in the z-axis and linear velocity in the y-axis, were the defining racket kinematic characteristics distinguishing a slice forehand from that of a topspin forehand.

Identification of such characteristics possesses a large amount of potential for the simulation of any specific shot type within a laboratory environment.

Objective 3: Develop a controlled test protocol, accurately and realistically simulating specific forehand shots in a laboratory-based environment.

Simulation of typical specific forehand shots restricts the number of inbound parameters allowing for large-scale racket impact testing. Detailed knowledge of the ball and racket kinematics for specific forehand shots found within the field of play enabled for the development of a representative and realistic laboratory-based impact testing. Due to the racket handle clamping limitation, this further reduces the number of inbound parameters, through the acknowledgement that the resultant inbound velocity along the x-axis cannot be assumed negligible for the calculation of racket orientation upon impact for forehand shots. The identified shot specific parameters, relative to a total of 39 rackets, combined with five impact positions, a representative torque value of 8.7 Nm, a total of 12 repeats to reduce the effects of the BOLA's inherent variability, ensured the implementation of a realistic and effective large-scale laboratory test method.

Conclusion

Irrespective of simulated shot type, the following analysis revealed 1) although players aim to strike the node point of the racket, the greatest resultant rebound ball velocity is generated for impacts towards the throat of the racket, 2) rebound playing angle increases as the impact moves towards the tip of the racket, 3) off-axis impacts occurring above the longitudinal axis possesses greater rebound ball spin and resultant velocity than off-axis impacts occurring below the rackets' longitudinal axis, 4) whether impacting above or below the longitudinal axis of the racket, similar rebound playing angles will be produced and finally, 5) when simulating forehand conditions in a laboratory environment, rebound offset angles are inevitable irrespective of impact position.

Objective 4: Distinguish clusters of rackets possessing similar behavioural characteristics for each given forehand simulation.

Analysis of the multi-dimensional data collected required the use of machine learning techniques such as cluster analysis. To reduce the scale and complexity of the recorded dataset, hierarchical cluster analysis was conducted to establish clusters of rackets possessing similar behavioural characteristics and dissimilar to those of another cluster. Through the use of a dendrogram, it is possible to visually review the relationships between the dataset and the clusters, however, it cannot formally define the number of clusters but rather informally suggest. Therefore, to provide the means for a formal decision regarding the appropriate number of behavioural clusters, the results of the dendrogram and PCA were evaluated simultaneously.

Results of this analysis revealed a total of four behavioural clusters for the topspin and slice forehand; each possessing similar within-cluster behavioural characteristics and dissimilar behavioural characteristics between clusters. Further review, of said clusters, identified the importance of varying racket properties when undertaking such analysis, as the results revealed that rackets of diverse property combinations can produce similar behavioural characteristics. Similarly, it also identified the importance of shot specific analysis when investigating the effects of racket properties by identifying that

Conclusion

racket's possessing similar behavioural characteristics for the topspin forehand may not possess similar behavioural characteristics for the slice forehand.

Objective 5: Identify the fundamental relationships between racket properties and behavioural characteristics for each given forehand simulation.

To establish the fundamental relationships between the racket properties and distinct behavioural clusters, for the development of a predictive model, a multinomial logistic regression was conducted. Results identified relationships between three racket properties and behavioural clusters, for both the topspin and slice forehand; where one or more was also found to be dependent on another property despite potentially possessing weak correlation. For a typical topspin forehand, head width, strung area and twistweight individually influence behavioural characteristics. The effects of strung area and twistweight, however, were found to possess a dependency on swingweight and frame stiffness respectively. For a typical slice forehand, head length, strung area and swingweight individually influence the behavioural characteristics. The effects of strung area and swingweight, however, also possessed dependency on head length and frame stiffness respectively. Such findings indicate that the behaviour of a tennis racket, for typical forehand shots, are not dependent on one racket property or property combinations but rather a complex dynamic between all properties. However, investigations were limited to relationships between two racket properties only, due to the statistical lack of data. Increasing the number of rackets selected for impact testing, thus the sample size, it is possible to investigation interacting effects and relationships between three and/or more racket properties.

The identified effects, both main and interaction, were then used to develop a predictive model, as a tool to be used by the ITF. Though the models presented for both the topspin and the slice forehand indicated good fit throughout the model development, the accuracies of said models possessed low levels for the prediction of a rackets' typical behavioural cluster characteristics. Though low levels of accuracy were observed for the model's overall performance, an increase in increase in sample size could also develop

161

more successful specific forehand models, for the prediction of typical behavioural characteristics.

8.3 *Conclusions*

The aim of this thesis was to ascertain the relationships between racket properties and behavioural characteristics, for specific forehand shots found within the field of play. Machine learning techniques, such as clustering and statistical methods, were used to analyse the data collected from a large-scale test protocol to gain further insight into the influences and effects that racket properties possess on the behavioural characteristics for different typical forehand shot types.

The main conclusions of the study are listed below;

- Off-axis impacts occurring at impact position 3 (transversely above the longitudinal axis) possess greater rebound ball spin than off-axis impacts occurring impact position 4 (transversely below the longitudinal axis). This is due to the direction of rotation of the racket head upon impact with respect to the off-axis impact location. For the generation of maximum rebound ball spin, players should aim to strike the ball below the rackets centre line.

- The behaviour between rackets becomes statistically differentiable for impacts occurring away from the central location upon the racket face; such as the tip and off the longitudinal axis. It was concluded that this was due to either the racket recoil or rotation upon impact. Though player testing has revealed that players aim to strike the racket's node point, they do so with little repetitive success. Therefore, impact locations such as these are inevitable and should be considered when impact testing to ensure a complete assessment and understanding of a racket's behaviour.

- Rackets of diverse property combinations can produce similar behavioural characteristics, for which statistical behavioural similarities will be observed for impacts occurring at the tip and off the longitudinal

axis. Such results show the necessity of varying all properties and property combinations when impact testing, for investigations regarding the effects of racket properties on racket behaviour or performance.

- Racket behaviour, or performance, is dependent on its physical properties as both individual and interacting entities. The specific properties determining racket behaviour, however, vary according to shot type. Therefore, to assess and/or predict racket behaviour, with respect to racket properties, impact testing must consider the combined effects of rackets properties and their relationship to specific shot types.

- The developed models currently show overall low levels of prediction accuracy, although possessing high accuracy predictions levels of prediction of racket properties ensuing behavioural characteristics for specific clusters. It was concluded that such inaccuracies are to be the result of the large within-cluster variance of each racket property. Impact testing of all shot types found within the field of play, with an increase in racket sample size, would ensure for the development of an accurate and versatile predictive model to be used as a tool by the ITF when investigating how shot type and racket properties can affect rebound ball trajectory, velocity and spin.

8.4 *Further Research*

This comprehensive investigation has highlighted the potential for further research, which are discussed below.

8.4.1 Specific Forehand Characteristics for all Shot Types

A main tenet of the principal component analysis combined with the cluster analysis was to reduce the number of inbound parameters for laboratory-based testing, whilst achieving realistic and representative simulation of different forehand shots. The racket kinematics of 'typical' forehand shots for a topspin forehand and a slice forehand were identified, drastically reducing the number of inbound parameters for consideration. However, a forehand shot can be executed as flat, topspin or slice. Whilst each specific forehand possesses

typical racket kinematics, they can also be considered umbrella terms for the more technical aspects of their execution. For instance, a topspin and a slice forehand can be executed as a baseline shot, lob shot or defensive shot, whilst a slice forehand can also be executed as a drop-shot. The racket kinematics for all typical and technical forehand shots, found within the field of play, are still unknown.

A complete analysis of racket kinematics for all shot types would further provide for realistic simulation of different forehand strokes, both typical and technical, within a laboratory environment.

8.4.2 Development of the Effective and Efficient Test Protocol

The impact experiments were limited in that inbound offset angle could not be varied. This was due to the limitation of the racket handle clamp restricting linear movement along the x and y-axis. Development of a racket handle clamp incorporating the ability for the movement of the racket's natural response to offset impacts would allow for the analysis of all identified specific forehand shots found within the field of play.

Quantified forces allowed for the calculation and application of realistic resistive torque values for laboratory testing. However, this value was calculated for as an absolute maximum, assuming a friction coefficient of 1. Depending on the grip material used, this value may exceed values found within the field of play. The calculated resistive torque was also kept consistent for both simulated forehand shots. Forces exerted by the player's hand onto the racket handle during impact may vary between shot types, thus resulting in the need for shot specific resistive torque values. Although this involves the consideration of another testing parameter, quantifying the forces exerted by players during impacts of specific forehand shots would increase the accuracy of laboratory-based simulations.

8.4.3 **Development of Effecting Racket Properties and the Predictive Model**

Currently, investigations regarding property interaction effects were only feasible between two properties, due to the need for more data. Increasing the racket sample size would allow for further investigations of property interaction effects between 3 and/or more properties. It could also warrant for more succinct behavioural cluster formations, and thus reduce the within-cluster property variance. Multinomial logistic regression proved beneficial for the investigation regarding behaviour-property relationships. However, it proved ineffective for the development of an accurate predictive model. Similarly, further increasing the racket sample size, expanding the system's domain, would increase the accuracy and functionality of the predictive model.

Evaluation of match play statistics for the US Open, French Open and Wimbledon tournaments found that serves accounted for 34%, forehands accounted for 32%, backhands accounted for 28% of the shots hit within a game (Johnson & McHugh, 2006). For the development of a comprehensive predictive model, a complete understanding of the behaviour-property relationships for all shot types must first be appraised. Furthering such knowledge and achieving said model would allow the ITF to intervene before 'game changing' rackets are able to have implications on the nature of the game.

References

Allen, T. (2009). *Finite Element Model of a Tennis Ball Impact with a Racket*. Sheffield Hallam University.

Allen, T., Choppin, S., & Knudson, D. (2016). A Review of Tennis Racket Performance Parameters. *Sports Engineering*, *19*(1), 1–11.

Allen, T., Grant, R., Sullivan, M., Taraborrelli, L., Choppin, S., Spurr, J., & Haake, S. (2018). Recommendations for Measuring Tennis Racket Parameters. *Proceedings*, *2*(6), 263.

Allen, T., Haake, S., & Goodwill, S. (2009). Comparison of a Finite Element Model of a Tennis Racket to Experimental Data. *Sports Engineering*, *12*(2), 87–98.

Allen, T., Haake, S., & Goodwill, S. (2011a). Effect of tennis racket parameters on a simulated groundstroke. *Journal of Sports Sciences*, *29*(3), 311–325.

Allen, T., Haake, S., & Goodwill, S. (2011b). Effect of tennis racket parameters on a simulated groundstroke. *Journal of sports sciences*, *29*(3), 311–325.

Baker, J., & Putnam, C. (1979). Tennis racket and ball responses during impact under clamped and freestanding conditions. *Research Quarterly of the American Alliance for Health, Physical Education, Recreation and Dance*, *50*(2), 164–170.

Ball, K., & Best, R. (2011). Golf styles and centre of pressure patterns when using different golf clubs. *Journal of Sports Sciences*, *29*(6), 587–590.

Basheer, I., & Hajmeer, M. (2000). Artificial Neural Networks: Fundamentals, Computing, Design, and Application. *Journal of Microbiological Methods*.

Bishop, C. (1995). Neural networks for pattern recognition. *Journal of the American Statistical Association*, *92*, 482.

BOLA. (2017). BOLA. Retrieved from http://www.bola.co.uk/

References

Bower, R., & Cross, R. (2005). String tension effects on tennis ball rebound speed and accuracy during playing conditions. *Journal of Sports Sciences*, *23*(7), 765–771.

Bower, R., & Sinclair, P. (1999). Tennis racquet stiffness and string tension effects on rebound velocity and angle for an oblique impact. *Journal of Human Movement Studies*, (37), 271–286.

Bray, K., & Kerwin, D. (2006). Modeling the "run out" Thrown in Cricket. *The Engineering of Sport 6* (pp. 161–166). Springer.

Brody, H. (1979). Physics of the tennis racket I. *American Journal of Physics*, *47*(482), 482–487.

Brody, H. (1981). Physics of the tennis racket II. *American Journal of Physics*, *49*(482), 816–819.

Brody, H. (1985). The Moment of Inertia of a Tennis Racket. *The Physics Teacher*, *23*(4), 213–216.

Brody, H. (1997). The physics of tennis. III. The ball–racket interaction. *American Journal of Physics*, *65*(10), 981.

Brody, H., Cross, R., & Crawford, L. (2002). *The Physics and Technology of Tennis*. (H. Brody, R. Cross, & L. Crawford, Eds.) (1st ed.). Racquet Tech Pub.

Brody, H., & Roetert, P. (2004). Optimizing Ball and Racket Interaction. *Biomedical Engineering Principles in Sports* (pp. 183–206). New York: Springer-Science+Business Media.

Brownstein, M., Khodursky, A., Ben-Hur, A., & Guyon, I. (2003). Detecting Stable Clusters Using Principal Component Analysis. *Functional Genomics*, (1), 159–182.

Cadler, C., Holmes, J., & Mastny, L. (1987). Static and Dynamic Characteristics of Tennis String Performance. *Progs 1987 Sem Conference on Experimental Mechanics* (pp. 613–616). Houston.

References

Celebi, M., Kingravi, H., & Vela, P. (2013). A Comparative Study of Efficient Initialization Methods for the K-means Clustering Algorithm. *Expert Systems with Applications*, *40*(1), 200–210.

Chadefaux, D., Rao, G., Le Carrou, J., Berton, E., & Vigouroux, L. (2017). The effects of player grip on the dynamic behaviour of a tennis racket. *Journal of Sports Sciences*, *35*(12), 1155–1164. Routledge.

Choppin, S. (2008). *Modelling of Tennis Racket Impacts in 3D Using Elite Players*. University of Sheffield.

Choppin, S. (2013). An investigation into the power point in tennis. *Sports Engineering*, *16*(3).

Choppin, S., Goodwill, S., & Haake, S. (2010). Investigations into the effect of grip tightness on off-centre forehand strikes in tennis. *Proceedings of the Institution of Mechanical Engineers, Part P: Journal of Sports Engineering and Technology*, *224*, 249–257.

Choppin, S., Goodwill, S., & Haake, S. (2011). Impact characteristics of the ball and racket during play at the Wimbledon qualifying tournament. *Sports Engineering*, *13*(4), 163–170.

Choppin, S., Goodwill, S., Haake, S., & Miller, S. (2007a). 3D player testing at the Wimbledon Qualifying Tournament. *Tennis Science & Technology 3* (pp. 333–340). International Tennis Federation.

Choppin, S., Goodwill, S., Haake, S., & Miller, S. (2007b). 3D player testing results from the Wimbledon Qualifying Tournament. *Tennis Science & Technology 3* (pp. 341–348). London: International Tennis Federation.

Choppin, S., Goodwill, S., Haake, S., & Miller, S. (2008). Ball and Racket Movements Recorded at the 2006 Wimbledon Qualifying Tournament. *The Engineering of Sport 7* (1st ed., pp. 563–569). France: Springer.

De Cock, A., Willems, T., Witvrouw, E., Vanrenterghem, J., & De Clercq, D. (2006). A functional foot type classification with cluster analysis based on

References

plantar pressure distribution during jogging. *Gait and Posture, 23*(3), 339–347.

Coe, A. (2000). The Balance Between Technology and Tradition in Tennis. In S. J. Haake & A. Coe (Eds.), *Tennis Science & Technology 1* (pp. 3–40). London: International Tennis Federation.

Cottey, R. (2002). *The Modelling of Spin Generation with Particular Emphasis on Racket Ball Games*. Loughborough University.

Cross+Morse. (2017). Cross+Morse. Retrieved from http://www.cross-morse.co.uk

Cross, R. (1997). The dead spot of a tennis racket. *The American Journal of Physics*.

Cross, R. (1999). Impact of a ball with a bat or racket. *American Journal of Physics, 67*(8), 692.

Cross, R. (2000). Flexible beam analysis of the effects of string tension and frame stiffness on racket performance. *Sports Engineering, 3*(2), 111–122.

Cross, R. (2003a). Properties of Tennis Equipment: Balls that bite, rackets that don't vibrate and strings don't make any difference. *Tennis Science & Technology 2* (pp. 17–29). London: International Tennis Federation.

Cross, R. (2003b). Oblique impact of a tennis ball on the strings of a tennis racket. *Sports Engineering, 6*(4), 235–254.

Cross, R. (2010). The polar moment of inertia of striking implements. *Sports Technology, 3*(3), 215–219.

Cross, R., & Lindsey, C. (2005). *Technical Tennis* (1st ed.). Raquect Tech Publishing.

Cross, R., Lindsey, C., & Andruczyk, D. (2000). Laboratory testing of tennis strings. *Sports Engineering, 3*(4), 219–230.

References

Cross, R., & Nathan, A. (2009). Performance Versus Moment of Inertia of Sporting Implements. *Leisure/ Loisir*.

Dowlan, S., & Ball, K. (2007). Applications for Cluster Analysis in Sport Biomechanics. *Isbs*, 366–369.

Elliott, B. (1982). Tennis: the influence of grip tightness on reaction impulse and rebound velocity. *Medicine and science in sports and exercise*, *14*(5), 348–52.

Fields, A. (2009). *Discovering Statistics Using SPSS* (Third Edit.). SAGE Publications, Inc.

Goodwill, S. (2002). *The Dynamics of tennis ball impacts on tennis rackets*. University of Sheffield.

Goodwill, S., Capel-Davis, J., Haake, S., & Miller, S. (2007). Ball Spin Generation By Elite Players During Match Play. In S. Miller & J. Capel-Davis (Eds.), *Tennis Science & Technology 3* (pp. 349–356). London: International Tennis Federation.

Goodwill, S., Douglas, J., Miller, S., & Haake, S. (2006). Measuring ball spin off a tennis racket. *The Engineering of Sport 6* (Vol. 1, pp. 379–384). Springer.

Goodwill, S., & Haake, S. (2001). Spring damper model of an impact between a tennis ball and racket. *Proceedings of the Institution of Mechanical Engineers, Part C: Journal of Mechanical Engineering Science*, *215*(11), 1331–1341.

Goodwill, S., & Haake, S. (2003). Modelling of an impact between a tennis ball and racket. In S. Miller (Ed.), *Tennis Science & Technology 2* (pp. 79–86). London: International Tennis Federation.

Goodwill, S., & Haake, S. (2004). Ball Spin Generation for Oblique Impacts with a Tennis Racket. *Experimental Mechanics*, *44*(2), 195–206.

Goodwill, S., Haake, S., & Miller, S. (2007). Validation of the ITF Racket Power Machine. In J. Capel-Davis & S. Miller (Eds.), *Tennis Science &*

References

Technology 3 (1st ed., pp. 113–120). London: International Tennis Federation.

Haake, S. (2018). *Advantage Play*. Arena Sport.

Haake, S., Allen, T., Choppin, S., & Goodwill, S. (2007). The Evolution of the Tennis Racket and it's Effect on Serve Speed. *Tennis Science and Technology 3* (Vol. 1, pp. 257–271).

Haake, S., Allen, T., Jones, A., Spurr, J., & Goodwill, S. (2012). Effect of inter-string friction on tennis ball rebound. *Proceedings of the Institution of Mechanical Engineers, Part J: Journal of Engineering Tribology*, *226*(7), 626–635.

Haake, S., Carré, M., & Goodwill, S. (2003). The dynamic impact characteristics of tennis balls with tennis rackets. *Journal of Sports Sciences*, *21*(10), 839–850.

Haines, R. (1993). The Sporting Use of Polymers. *Shell Petrochemicals*, *22*.

Han, J., Kamber, M., & Pei, J. (2012). Cluster Analysis: Basic Concepts and Methods. *Data Mining: Concepts and Techniques*, 443–495.

Hatze, H. (1994). Impact Probability Distribution, Sweet Spot, and the Concept of an Effective Power Region in Tennis Rackets. *Journal of Applied Biomechanics*, *10*(1), 43–50.

Hatze, H. (1998). The Centre of Percussion of Tennis Rackets: A Concept of Limited Applicability. *Sports Engineering* (1st ed., pp. 17–25).

Head, H. (1975). Oversize Tennis Racket. United States.

ITF. (2017a). APPENDIX II: THE RACKET. *International Tennis Federation*. Retrieved September 3, 2017, from http://www.itftennis.com/technical/publications/rules/rackets/appendix-ii.aspx

ITF. (2017b). APPENDIX I: THE BALL. *International Tennis Federation*. Retrieved from

References

https://www.itftennis.com/technical/publications/rules/balls/appendix-i.aspx

ITF. (2017c). ITF Technical Department Web Resource. *Iternational Tennis Federation*. Retrieved August 27, 2017, from http://www.itftennis.com/technical/

ITF. (2018). History Of the Tennis Racket. Retrieved from https://www.itftennis.com/technical/rackets-and-strings/other/history.aspx

ITF. (2019). ITF Rules of Tennis 2019, 45.

Johnson, C., & McHugh, M. (2006). Performance demands of professional male tennis players. *British Journal of Sports Medicine*, *40*(8), 696–699.

Karamizadeh, S., Abdullah, S., Manaf, A., Zamani, M., & Hooman, A. (2013). An Overview of Principal Component Analysis. *Journal of Signal and Information Processing*, *04*(03), 173–175.

Kelley, J. (2011a). *Initial Report on the Sports Ball Spin Analysis Algorithm*.

Kelley, J. (2011b). *Measuring ball spin rates in match play tennis*. Sheffield Hallam University.

Kelley, J., Goodwill, S., Capel-Davis, J., & Haake, S. (2009). Ball Spin Generation at the 2007 Wimbledon Qualifying tournament. In M. Estivalet & P. Brisson (Eds.), *The Engineering of Sport 7* (pp. 571–578). Springer.

King, M., Kentel, B., & Mitchell, S. (2012). The Effects of Ball Impact Location and Grip Tightness on the Arm, Racquet and Ball for One-Handed Tennis Backhand Groundstrokes. *Journal of Biomechanics*, *45*(6), 1048–1052. Elsevier.

Knudson, D. (1991). Factors affecting force loading on the hand in the tennis forehand. *Journal of Sports Medicine and Physical Fitness*, *31*(4), 527–531.

Knudson, D. (2006). Biomechanics of the Forehand. *Biomechanical Principles of Tennis Technique: Using Science to Improve Your Strokes* (pp. 75–94). Raquect Tech Publishing.

References

Knudson, D., & Blackwell, J. (2005). Variability of impact kinematics and margin for error in the tennis forehand of advanced players. *Sports Engineering*, *8*(2), 75–80.

Knudson, D., & White, S. (1989). Forces in the hand in the tennis forehand drive; application of force sensing resistors. *International Journal of Sports …*, 324–331.

Kotze, J., Mitchell, S., & Rothberg, S. (2000). The Role of the Racket in High-Speed Tennis Serves. *Sports Engineering*.

Landau, S., Stahl, D., Everitt, B., & Leese, M. (2011). *Cluster Analysis* (5th Editio.). John Wiley & Sons, Ltd.

Leigh, D., & Lui, W. (1992). Dynamics of the interactions between ball, strings, and racket in tennis. *International Journal of Sport Biomechanics*, *8*(3), 181–206.

McMorris, T. (2014). *Acquisition and performance of sports skills. Wiley sport text series*.

Mertler, C., & Reinhart, R. (2016). *Advanced and Multivariate Statistical Methods. Advanced and Multivariate Statistical Methods*.

Miller, S. (2007). The Role of ITF Science & Technical in Evaluating and Regulating Tennis Equipment. In S. Miller & J. Capel-Davies (Eds.), *Tennis Science & Technology 3* (pp. 1–19). London: International Tennis Federation.

Miller, S., & Messner, S. (2003). On the Dynamic Coefficient of Restitution of Tennis Balls. In S. Miller (Ed.), *Tennis Science & Technology 2* (pp. 91–104). London: International Tennis Federation.

Mohsen G, Al-Fuqaha, A., Rayes, A., & Khan, B. (2010). Monte Carlo Simulation. *Network Modeling and Simulation* (pp. 69–96). Chichester, UK: John Wiley & Sons, Ltd.

Murray, N., & Hunfalvay, M. (2017). A Comparison of Visual Search Strategies

of Elite and Non-Elite Tennis Players Through Cluster Analysis. *Journal of Sports Sciences*, *35*(3), 241–246.

Nicolaides, A., Elliott, N., Kelley, J., Pinaffo, M., & Allen, T. (2013). Effect of string bed pattern on ball spin generation from a tennis racket. *Sports Engineering*, *16*(3), 181–188.

Papadopoulos, M., & Emmanouilidou, C. (2000). Kinematic Analysis of the Service Stroke in Tennis. *Tenis Science and Technology* (pp. 383–387). Blackwell Science Ltd.

Peebles, L., & Norris, B. (1998). *ADULTDATA, the handbook of adult anthropometric and strength measurements, data for design safety*. London: Department of Trade and Industry.

Phinyomark, A., Osis, S., Hettinga, B., & Ferber, R. (2015). Kinematic gait patterns in healthy runners: A hierarchical cluster analysis. *Journal of Biomechanics*.

Rayleigh, F. (1877). On the Irregular Flight of a Tennis-Ball. *Vortex Motion*, 14–17.

Rokach, L., & Maimon, O. (2005). Clustering methods. *The Data Mining and Knowledge Discovery Handbook* (pp. 321–352).

Savage, N. (2006). *Vibration Absorption in the Tennis Grip and the Effects on Racquet Dynamics*.

Seifert, L., & Davids, K. (2016). Ecological Dynamics : a theoretical framework for understanding sport performance , physical education and physical activity.

Seo, N., & Armstrong, T. (2009). Friction coefficients in a longitudinal direction between the finger pad and selected materials for different normal forces and curvatures. *Ergonomics*, *52*(5), 609–616.

Singh, K., Malik, D., & Sharma, N. (2011). Evolving Limitations in K-means Algorithm in Data Mining and their Removal. *IJCEM International Journal of*

References

Computational Engineering & Management ISSN, 12(April), 2230–7893.

Sissler, L. (2011). *Advanced Modelling and Design of a Tennis Ball.* Loughborough University.

Sissler, L., Jones, R., Leaney, P., & Harland, A. (2014). Viscoelastic modelling of tennis ball properties. *IOP Conference Series: Materials Science and Engineering* (Vol. 10).

Sperandei, S. (2014). Understanding Logistic Regression Analysis. *Biochemia Medica, 24*(1), 12–18.

Spurr, J. (2017). *Statistically Modelling Tennis Racket Impacts with Six Degrees of Freedom.* Sheffield Hallam University.

Spurr, J., & Downing, M. (2007). Good Vibrations: the Effect of Fundamental Frequency on Tennis. In S. Miller & J. Capel-Davis (Eds.), *Tennis Science & Technology 3* (1st ed., pp. 103–112). London: International Tennis Federation.

Spurr, J., Goodwill, S., Kelley, J., & Haake, S. (2014). Measuring the inertial properties of a tennis racket. *Procedia Engineering* (Vol. 72).

Taraborrelli, L., Grant, R., Sullivan, M., Choppin, S., Spurr, J., Haake, S., & Allen, T. (2019a). Materials Have Driven the Historical Development of the Tennis Racket. *Applied Sciences (Switzerland), 9*(20).

Taraborrelli, L., Grant, R., Sullivan, M., Choppin, S., Spurr, J., Haake, S., & Allen, T. (2019b). Recommendations for Estimating the Moments of Inertia of a Tennis Racket. *Sports Engineering, 22*(1), 1–9. Springer London.

Tate, R. (1992). *General Linear Model Applications.*

United States Tennis Association, & United States Lawn Tennis Association. (2004). Coaching Foundations. *Coaching Tennis Successfully* (2nd ed., pp. 1–19). Human Kinetics Publishers.

Whyld, N. (2004). *3D Image Reconstruction from a Stereo Camera Pair: Assessment of Calibration Techniques.* Sheffield.

References

Wold, S., Esbensen, K., & Geladi, P. (1987). Principal component analysis. *Chemometrics and Intelligent Laboratory Systems*, *2*(1–3), 37–52.

Xue, J., Lee, C., Wakeham, S., & Armstrong, R. (2011). Using principal components analysis (PCA) with cluster analysis to study the organic geochemistry of sinking particles in the ocean. *Organic Geochemistry*, *42*(4), 356–367. Elsevier Ltd.

A. Results of Inbound Playing (α) and Offset angles (β)

Resultant Inbound Velocity			α	β
V_x	V_y	V_z		
2.59	15.90	-28.49	-29.48	4.54
0.21	17.91	-33.03	-28.47	0.32
-1.31	15.30	-33.60	-24.56	-2.03
3.12	13.33	-35.76	-20.95	4.67
-1.67	16.20	-35.47	-24.66	-2.45
1.06	18.81	-33.66	-29.23	1.57
1.12	16.43	-32.11	-27.15	1.78
0.39	7.10	-32.35	12.40	0.67
0.30	14.28	-34.07	-22.75	0.47
1.45	15.51	-31.79	-26.10	2.35
7.95	-9.86	-25.73	26.21	16.10
1.03	15.49	-35.86	-23.41	1.51
-0.15	13.35	-33.98	-21.45	-0.24
-0.74	16.06	-33.60	-25.57	-1.14
-4.34	13.26	-37.26	-20.53	-6.26
-2.37	15.73	-35.68	-24.03	-3.48
-2.86	13.77	-37.49	-20.56	-4.10
-6.04	13.68	-38.66	-21.15	-8.38
2.52	7.28	-22.95	-18.56	5.98
1.44	11.80	-34.46	-19.03	2.26
1.41	11.60	-30.34	-21.07	2.49
5.45	-8.46	-32.81	-17.05	9.14
2.60	-8.84	-23.45	21.45	5.92
11.16	-10.08	-31.68	-25.39	18.56
-0.20	8.63	-31.92	-15.14	-0.35
-5.47	11.94	-28.55	-24.70	-10.02
-7.27	11.12	-31.10	-23.13	-12.41
10.94	-12.15	-28.56	-29.79	19.42
-2.63	10.24	-32.17	-18.19	-4.45
9.08	-8.02	-27.19	-24.02	17.76
-6.26	15.61	-30.16	-29.14	-10.44
-2.97	11.15	-30.97	-20.44	-5.16
-2.34	13.78	-32.33	-23.38	-3.81
9.06	-8.50	-24.27	-27.11	19.41
-1.82	11.13	-25.62	-23.76	-3.73
-0.49	9.40	-25.66	-20.14	-1.03
9.19	4.76	-23.69	23.60	20.82
19.15	-6.98	-26.87	-37.18	34.59
-4.82	17.23	-26.78	-33.74	-8.61

177

-4.27	11.14	-37.85	-17.50	-6.18
-6.85	15.00	-26.51	-31.89	-12.68
-1.84	14.06	-29.84	-25.42	-3.19
-5.23	13.46	-28.93	-26.52	-9.31
-8.86	10.40	-34.76	-21.46	-13.72
-7.79	12.62	-29.10	-27.01	-13.80
-9.38	-0.99	-28.95	18.05	-17.94
-7.84	8.60	-32.20	-19.87	-13.24
-4.55	7.96	-25.31	-19.91	-9.73
9.65	-7.60	-28.08	-23.63	18.35
-2.96	8.68	-31.96	-16.01	-5.11
-1.26	-13.68	-24.84	-28.90	-2.87
10.16	7.48	-24.31	-27.43	21.78
10.04	10.78	-35.28	-22.66	15.22
-4.14	-13.34	-32.18	-23.46	-6.78
-10.91	-16.70	-32.68	-31.40	-16.56
15.45	8.43	-32.33	-28.57	24.82
14.07	11.37	-27.17	-33.65	25.53
13.35	9.87	-33.31	-26.49	21.02
8.46	2.29	-31.44	-15.58	15.02
8.71	12.92	-31.89	-26.04	14.21
-3.17	12.87	-26.72	26.38	-6.10
11.25	10.66	-30.32	-27.08	19.29
14.27	-10.26	-35.45	-26.37	21.14
11.33	9.47	-33.15	-24.01	18.19
10.44	10.09	-39.80	-20.04	14.27
14.88	13.46	-35.98	-29.14	21.17
16.18	6.39	-32.62	-28.07	25.96
-2.20	13.82	-29.28	-25.55	-3.89
-0.36	-11.35	-30.91	20.17	-0.63

B. Selected Rackets for Testing

Racket Name:	Racket Label	Racket Mass (g)	Balance point (mm)	Head Length (mm)	Head Width (mm)	Strung Area (in^2)	Racket Length (mm)	Swingweight (RDC)	Twistweight (RDC)	Frame stiffness (RDC)
Hammer 1 Outer Edge	04-83	234	380	395	280	135	725	294	20	73
TT Viper	01-24	241	360	362	260	115	710	291	7	74
Metallix 10	06-219	244	353	370	275	124	695	256	12	66
DNX 1	06-5	247	360	352	266	115	705	283	12	69
YouTek Radical Lite	09-274	248	340	330	250	100	685	253	11	63
Hyper Hammer 2.6	01-10	252	360	370	270	115	710	298	10	78
Air Flow 1	07-235	255	347	330	250	100	685	258	10	74
Quad Flex 255	07-237	259	348	365	285	108	695	276	14	70
Head YouTek Five	10-286	260	357	340	264	107	695	291	14	72
Ki 15	06-100	263	345	340	255	105	700	289	14	69
Quad Flex 270	07-238	268	328	350	270	100	685	266	11	70
V-Con 20	03-79	268	360	360	260	117	700	307	7	68
V-Con 15	03-77	274	340	330	250	100	700	287	9	66
Aerogel 500	07-216	277	329	335	245	100	685	269	10	68
Hot Melt 500G	03-80	280	314	370	245	102	690	258	8	71
nCode Tour Two	06-223	283	340	330	235	95	695	296	11	63
MP-5i	01-9	283	360	363	260	98	696	310	11	67
Aerogel 400	06-215	286	333	335	245	100	690	289	12	69
Quad Flex 290	-07-239	289	316	355	265	98	685	279	4	65
RDS 003	06-225	293	322	330	250	100	695	280	12	67
Flexpoint Radical	05-84	298	328	325	240	98	682	299	9	63
Magnetic Pro-No.1 98	06-90	299	320	360	245	98	690	281	9	63
Microgel Extreme	07-236	300	315	325	260	100	690	268	12	65
TFeel 305	06-89	304	330	330	245	97	690	296	9	67
Quad Flex 305	07-240	308	320	345	265	95	685	298	10	61
Aerogel 300	07-228	309	305	330	240	98	685	270	10	62

More Control DB	**03-72**	**309**	**345**	**320**	**250**	**97**	**690**	**283**	**10**	**71**
Microgel Radical Pro	07-233	312	320	330	250	100	685	286	14	62
Pure Drive Roddick Plus	06-210	319	312	330	255	100	700	301	12	69
Aerogel 200	06-213	320	313	325	240	95	685	282	8	61
ITF Development	01-15	329	315	325	250	98	685	313	2	68
Microgel Prestige Mid	09-247	330	310	315	230	93	685	295	15	61
Pure Storm Team MP	06-212	332	332	330	255	103	685	284	13	68
Woofer Pure Drive + Team	01-41	335	310	330	255	100	700	291	3	71
DNX 10 Midplus Unbranded	06-11	338	320	325	232	98	705	339	12	60
RD Ti 50	01-8	330	298	243	243	95	690	286	8	54
nCode 61 Tour	06-99	352	316	320	243	95	686	329	1	64
Pro Staff Tour Classic	08-242	360	303	320	235	85	685	323	14	65
Pro Staff 6.0	02-46	365	318	305	220	85	690	353	7	66

C. Impact Positions and Relative Resultant Inbound Velocities Specific to Each Selected Racket

	Impact Position from Racket Butt (m)									
Racket Label:	Node Point		Impact 1		Impact 2		Impact 3		Impact 4	
	x	y	x	y	x	y	x	y	x	y
04-83	0.595	0	0.655	0	0.535	0	0.595	+0.060	0.595	-0.060
01-24	0.582	0	0.642	0	0.522	0	0.582	+0.060	0.582	-0.060
06-219	0.570	0	0.630	0	0.510	0	0.570	+0.060	0.570	-0.060
06-5	0.578	0	0.638	0	0.518	0	0.578	+0.060	0.578	-0.060
09-274	0.562	0	0.622	0	0.502	0	0.562	+0.060	0.562	-0.060
01-10	0.582	0	0.642	0	0.522	0	0.582	+0.060	0.582	-0.060
07-235	0.562	0	0.622	0	0.502	0	0.562	+0.060	0.562	-0.060
07-231	0.574	0	0.634	0	0.514	0	0.574	+0.060	0.574	-0.060
07-237	0.570	0	0.630	0	0.510	0	0.570	+0.060	0.570	-0.060
10-286	0.570	0	0.630	0	0.510	0	0.570	+0.060	0.570	-0.060
06-100	0.574	0	0.634	0	0.514	0	0.574	+0.060	0.574	-0.060
07-238	0.562	0	0.622	0	0.502	0	0.562	+0.060	0.562	-0.060
03-79	0.574	0	0.634	0	0.514	0	0.574	+0.060	0.574	-0.060
07-238	0.562	0	0.622	0	0.502	0	0.562	+0.060	0.562	-0.060
03-77	0.574	0	0.634	0	0.514	0	0.574	+0.060	0.574	-0.060
07-216	0.562	0	0.622	0	0.502	0	0.562	+0.060	0.562	-0.060
03-80	0.566	0	0.626	0	0.506	0	0.566	+0.060	0.566	-0.060
06-223	0.570	0	0.630	0	0.510	0	0.570	+0.060	0.570	-0.060
01-9	0.571	0	0.631	0	0.511	0	0.571	+0.060	0.571	-0.060
06-215	0.566	0	0.626	0	0.506	0	0.566	+0.060	0.566	-0.060
07-239	0.562	0	0.622	0	0.502	0	0.562	+0.060	0.562	-0.060
06-14	0.566	0	0.626	0	0.506	0	0.566	+0.060	0.566	-0.060
05-84	0.559	0	0.619	0	0.499	0	0.559	+0.060	0.559	-0.060
06-90	0.566	0	0.626	0	0.506	0	0.566	+0.060	0.566	-0.060
07-236	0.566	0	0.626	0	0.506	0	0.566	+0.060	0.566	-0.060
06-89	0.566	0	0.626	0	0.506	0	0.566	+0.060	0.566	-0.060
07-240	0.562	0	0.622	0	0.502	0	0.562	+0.060	0.562	-0.060
07-228	0.562	0	0.622	0	0.502	0	0.562	+0.060	0.562	-0.060
03-72	0.566	0	0.626	0	0.506	0	0.566	+0.060	0.566	-0.060
07-233	0.562	0	0.622	0	0.502	0	0.562	+0.060	0.562	-0.060
06-210	0.574	0	0.634	0	0.514	0	0.574	+0.060	0.574	-0.060
06-213	0.562	0	0.622	0	0.502	0	0.562	+0.060	0.562	-0.060
09-246	0.562	0	0.622	0	0.502	0	0.562	+0.060	0.562	-0.060
09-285	0.562	0	0.622	0	0.502	0	0.562	+0.060	0.562	-0.060
01-15	0.562	0	0.622	0	0.502	0	0.562	+0.060	0.562	-0.060
09-247	0.562	0	0.622	0	0.502	0	0.562	+0.060	0.562	-0.060
06-212	0.562	0	0.622	0	0.502	0	0.562	+0.060	0.562	-0.060
01-41	0.574	0	0.634	0	0.514	0	0.574	+0.060	0.574	-0.060
06-11	0.578	0	0.638	0	0.518	0	0.578	+0.060	0.578	-0.060
08-241	0.566	0	0.626	0	0.506	0	0.566	+0.060	0.566	-0.060
01-8	0.566	0	0.626	0	0.506	0	0.566	+0.060	0.566	-0.060
06-99	0.563	0	0.623	0	0.503	0	0.563	+0.060	0.563	-0.060
08-242	0.562	0	0.622	0	0.502	0	0.562	+0.060	0.562	-0.060
02-46	0.566	0	0.626	0	0.506	0	0.566	+0.060	0.566	-0.060

	Relative Resultant Inbound Ball Velocity									
Racket Label:	Slice Forehand					Topspin Forehand				
	Node point	Impact 1	Impact 2	Impact 3	Impact 4	Node point	Impact 1	Impact 2	Impact 3	Impact 4
04-83	36.0	36.4	35.7	36.3	35.7	29.7	30.1	29.4	29.5	29.9
01-24	36.1	36.5	35.8	36.4	35.8	29.7	30.2	29.4	29.5	29.9
06-219	36.0	36.5	35.7	36.3	35.7	29.7	30.1	29.4	29.5	29.9
06-5	36.0	36.5	35.7	36.3	35.7	29.7	30.1	29.4	29.5	29.9
09-274	36.1	36.5	35.8	36.4	35.8	29.7	30.2	29.4	29.5	29.9
01-10	36.1	36.5	35.8	36.4	35.8	29.7	30.2	29.4	29.5	29.9
07-235	36.0	36.4	35.7	36.3	35.7	29.7	30.1	29.4	29.5	29.9
07-231	36.1	36.6	35.8	36.4	35.8	29.8	30.2	29.4	29.6	30.0
07-237	36.1	36.5	35.8	36.4	35.8	29.7	30.2	29.4	29.5	29.9
10-286	36.0	36.4	35.7	36.3	35.7	29.7	30.1	29.3	29.5	29.9
06-100	36.1	36.6	35.8	36.4	35.8	29.8	30.2	29.4	29.6	30.0
07-238	36.1	36.6	35.8	36.4	35.8	29.8	30.3	29.5	29.6	30.0
03-79	36.0	36.4	35.7	36.3	35.7	29.7	30.1	29.3	29.5	29.9
07-238	36.1	36.6	35.8	36.4	35.8	29.8	30.3	29.5	29.6	30.0
03-77	36.1	36.6	35.8	36.4	35.8	29.8	30.3	29.5	29.6	30.0
07-216	36.1	36.6	35.8	36.4	35.8	29.8	30.2	29.4	29.6	30.0
03-80	36.3	36.8	35.9	36.6	36.0	29.9	30.4	29.6	29.7	30.1
06-223	36.1	36.6	35.8	36.4	35.8	29.8	30.2	29.4	29.6	30.0
01-9	36.0	36.4	35.7	36.3	35.7	29.7	30.1	29.3	29.5	29.9
06-215	36.1	36.6	35.8	36.4	35.8	29.8	30.2	29.4	29.6	30.0
07-239	36.2	36.7	35.9	36.5	35.9	29.9	30.3	29.5	29.7	30.1
06-14	36.2	36.7	35.9	36.5	35.9	29.9	30.3	29.5	29.7	30.1
05-84	36.1	36.6	35.8	36.4	35.8	29.8	30.2	29.4	29.6	30.0
06-90	36.2	36.7	35.9	36.5	35.9	29.9	30.3	29.5	29.7	30.1
07-236	36.3	36.8	35.9	36.6	36.0	29.9	30.4	29.5	29.7	30.1
06-89	36.1	36.6	35.8	36.5	35.8	29.8	30.3	29.5	29.6	30.0
07-240	36.2	36.7	35.8	36.5	35.9	29.9	30.3	29.5	29.7	30.1
07-228	36.3	36.8	35.9	36.6	36.0	30.0	30.4	29.6	29.8	30.2
03-72	36.1	36.5	35.7	36.4	35.7	29.7	30.2	29.4	29.5	29.9
07-233	36.2	36.7	35.8	36.5	35.9	29.9	30.3	29.5	29.7	30.1
06-210	36.3	36.9	35.9	36.6	36.0	30.0	30.5	29.6	29.8	30.2
06-213	36.2	36.7	35.9	36.5	35.9	29.9	30.4	29.5	29.7	30.1
09-246	36.2	36.7	35.9	36.5	35.9	29.9	30.4	29.5	29.7	30.1
09-285	36.3	36.9	35.9	36.6	36.0	30.0	30.5	29.6	29.8	30.2
01-15	36.2	36.7	35.9	36.5	35.9	29.9	30.4	29.5	29.7	30.1
09-247	36.3	36.8	35.9	36.6	36.0	29.9	30.4	29.6	29.7	30.1
06-212	36.1	36.6	35.8	36.4	35.8	29.8	30.2	29.4	29.6	30.0
01-41	36.4	36.9	36.0	36.7	36.1	30.0	30.5	29.6	29.8	30.2
06-11	36.3	36.8	35.9	36.6	36.0	30.0	30.4	29.6	29.8	30.2
08-241	36.1	36.6	35.8	36.4	35.8	29.8	30.2	29.4	29.6	30.0
01-8	36.4	36.9	36.0	36.7	36.1	30.0	30.5	29.6	29.8	30.2
06-99	36.2	36.7	35.9	36.5	35.9	29.9	30.4	29.5	29.7	30.1
08-242	36.3	36.8	35.9	36.6	36.0	30.0	30.5	29.6	29.8	30.2
02-46	36.2	36.7	35.9	36.5	35.9	29.9	30.4	29.5	29.7	30.1

D. Behavioural Cluster Results for Topspin Forehand

Table 36 - Topspin Behavioural Results for Cluster 1

Racket Label	Node Point				Impact Position 1				Impact Position 2				Impact Position 3				Impact Position 4			
	RS (RPM)	RPA (°)	ROA (°)	RRV (m/s)	RS (RPM)	RPA (°)	ROA (°)	RRV (m/s)	RS (RPM)	RPA (°)	ROA (°)	RRV (m/s)	RS (RPM)	RPA (°)	ROA (°)	RRV (m/s)	RS (RPM)	RPA (°)	ROA (°)	RRV (m/s)
07-216	1456	29	17	7.6	1454	51	3	7	1413	11	7	13	1631	39	17	7	1404	63	26	5
07-238	1426	29	16	8.3	1501	66	15	7	1491	13	9	11	1584	39	18	7	1354	65	24	6
07-235	1487	29	22	7.8	1302	47	-1	7	1413	15	9	12	1638	50	17	7	1326	75	21	7
08-242	1482	32	16	8.6	1319	48	-10	12	1246	19	10	11	1602	45	15	8	1383	78	11	8
07-233	1482	23	14	8.5	1315	57	-9	10	1268	10	7	13	1646	53	6	9	1340	78	14	7
06-225	1556	32	18	8.1	1282	62	-2	12	1250	21	9	12	1653	61	-2	12	1388	78	5	12
03-72	1574	31	15	8.9	1328	51	-7	11	1334	16	8	12	1647	66	5	9	1343	79	12	8
07-237	1530	32	15	8.5	1288	45	-12	12	1458	14	9	13	1599	70	-5	15	1414	75	5	12
Average	1499	30	17	8.3	1349	53	-3	10	1359	15	8	12	1625	53	9	9	1369	74	15	8
Standard Deviation	47	3	2	0.4	77	7	8	2	91	3	1	1	25	11	9	3	30	6	8	2

CLUSTER 1

Table 37 - Topspin Behavioural Results for Cluster 2

Racket Label	Node Point				Impact Position 1				Impact Position 2				Impact Position 3				Impact Position 4			
	RS (RPM)	RPA (°)	ROA (°)	RRV (m/s)	RS (RPM)	RPA (°)	ROA (°)	RRV (m/s)	RS (RPM)	RPA (°)	ROA (°)	RRV (m/s)	RS (RPM)	RPA (°)	ROA (°)	RRV (m/s)	RS (RPM)	RPA (°)	ROA (°)	RRV (m/s)
03-77	1537	42	12	8.9	1412	63	-6	13	1478	21	12	11	1655	42	-9	13	1389	44	-6	12
03-80	1539	52	15	7.7	1357	58	-9	11	1249	19	13	11	1723	41	0	12	1384	44	3	14
06-210	1617	29	17	9.5	1402	54	-9	12	1321	23	20	13	1624	43	10	10	1368	49	7	9
06-213	1477	30	11	8.8	1399	58	-12	14	1267	27	9	12	1598	53	-9	15	1378	47	-14	14
01-10	1474	32	12	8.9	1378	58	-12	14	1233	26	10	12	1669	52	-9	15	1403	51	-11	13
06-99	1460	23	12	8.7	1293	59	1	7	1218	24	1	13	1550	55	3	15	1388	49	17	7
05-84	1560	39	11	9.6	1388	49	9	11	1305	15	7	13	1561	41	17	8	1469	45	21	7
01-24	1511	40	11	8.5	1273	46	-6	11	1249	21	15	11	1567	44	-10	14	1290	38	-2	12
03-79	1572	35	14	9.2	1405	48	-2	12	1479	20	17	12	1705	51	-9	13	1498	41	1	12
01-9	1574	30	14	9.4	1430	48	-8	13	1389	17	14	12	1648	50	-8	14	1512	48	-4	14
09-274	1646	32	12	9.6	1321	48	-8	13	1456	18	14	13	1705	51	-7	13	1434	47	-6	14
Average	1542	35	13	9.0	1369	53	-6	12	1331	21	12	12	1637	48	-3	13	1410	46	1	12
Standard Deviation	57	8	2	0.5	49	6	6	2	97	4	5	1	59	5	9	2	61	4	10	3

CLUSTER 2

Table 38 - Topspin Behavioural Results for Cluster 3

Racket Label	Node Point				Impact Position 1				Impact Position 2				Impact Position 3				Impact Position 4			
	RS (RPM)	RPA (°)	ROA (°)	RRV (m/s)	RS (RPM)	RPA (°)	ROA (°)	RRV (m/s)	RS (RPM)	RPA (°)	ROA (°)	RRV (m/s)	RS (RPM)	RPA (°)	ROA (°)	RRV (m/s)	RS (RPM)	RPA (°)	ROA (°)	RRV (m/s)
02-46	1433	47	14	8.9	1314	51	-4	14	1225	17	10	12	1490	63	1	10	1326	47	-6	13
06-11	1536	44	13	9.6	1469	63	-7	13	1299	26	12	12	1514	55	-2	14	1301	55	-5	12
06-90	1549	37	23	8.6	1296	50	-12	12	1265	27	28	13	1630	52	19	8	1511	62	16	8
07-228	1561	47	10	9.8	1373	57	-6	8	1297	27	5	13	1625	45	20	7	1440	61	26	6
06-5	1694	51	2	10.3	1489	54	-10	12	1227	32	6	13	1706	51	-2	12	1550	52	-8	12
01-41	1583	45	15	8.6	1387	47	-7	12	1253	38	4	13	1500	53	-5	13	1314	56	-7	12
06-223	1553	41	14	9.2	1414	55	-10	12	1213	43	28	13	1649	51	-6	12	1546	43	-9	13
04-83	1475	41	12	13.3	1671	57	14	10	1269	32	7	12	1658	47	7	13	1394	46	-4	13
01-8	1617	40	20	8.0	1426	53	-7	10	1185	30	27	12	1531	47	12	8	1325	52	12	8
10-286	1649	38	15	9.1	1366	51	-11	14	1391	31	24	13	1662	45	-3	13	1409	46	-4	12
06-100	1507	43	13	8.2	1357	52	-12	12	1404	24	19	13	1645	48	-1	11	1431	46	0	11
Average	**1560**	**43**	**14**	**9.4**	**1415**	**54**	**-7**	**12**	**1275**	**30**	**15**	**13**	**1601**	**51**	**4**	**11**	**1413**	**51**	**1**	**11**
Standard Deviation	**72**	**4**	**5**	**1.4**	**98**	**4**	**7**	**2**	**66**	**7**	**9**	**0**	**73**	**5**	**9**	**2**	**88**	**6**	**11**	**2**

CLUSTER 3

Table 39 - Topspin Behavioural Results for Cluster 4

Racket Label	Node Point				Impact Position 1				Impact Position 2				Impact Position 3				Impact Position 4			
	RS (RPM)	RPA (°)	ROA (°)	RRV (m/s)	RS (RPM)	RPA (°)	ROA (°)	RRV (m/s)	RS (RPM)	RPA (°)	ROA (°)	RRV (m/s)	RS (RPM)	RPA (°)	ROA (°)	RRV (m/s)	RS (RPM)	RPA (°)	ROA (°)	RRV (m/s)
06-215	1593	47	9	11.2	1488	84	3	11	1329	29	6	14	1662	59	9	11	1566	69	6	11
07-239	1492	28	14	8.7	1460	77	1	8	1278	11	8	13	1603	42	16	8	1417	57	22	6
07-236	1557	47	12	11.1	1393	81	10	10	1282	29	10	13	1603	64	12	11	1360	74	7	10
06-89	1555	28	18	7.5	1333	82	-10	12	1298	12	9	13	1615	68	4	10	1434	63	7	9
07-240	1476	47	12	11.1	1303	81	10	10	1198	29	10	13	1656	64	12	11	1431	73	7	10
06-212	1478	30	16	10.1	1347	76	-8	13	1230	31	5	12	1588	50	18	8	1376	56	27	7
09-247	1504	35	13	10.6	1346	83	17	8	1296	19	7	13	1530	55	16	9	1356	56	17	9
01-15	1500	33	14	11.1	1374	75	20	9	1223	20	7	13	1557	43	15	9	1363	55	17	10
06-219	1653	33	25	7.1	1549	84	5	10	1306	15	16	11	1753	63	11	10	1415	58	15	9
Average	**1534**	**36**	**15**	**9.8**	**1399**	**80**	**5**	**10**	**1271**	**22**	**9**	**13**	**1618**	**56**	**12**	**10**	**1413**	**62**	**14**	**9**
Standard Deviation	**57**	**8**	**4**	**1.6**	**77**	**3**	**10**	**2**	**41**	**7**	**3**	**1**	**62**	**9**	**4**	**1**	**62**	**7**	**7**	**2**

CLUSTER 4

E. Behavioural Cluster Results for Slice Forehand

Table 40 - Slice Behavioural Results for Cluster 1

Racket Label	Node Point				Impact Position 1				Impact Position 2				Impact Position 3				Impact Position 4			
	RS (RPM)	RPA (°)	ROA (°)	RRV (m/s)	RS (RPM)	RPA (°)	ROA (°)	RRV (m/s)	RS (RPM)	RPA (°)	ROA (°)	RRV (m/s)	RS (RPM)	RPA (°)	ROA (°)	RRV (m/s)	RS (RPM)	RPA (°)	ROA (°)	RRV (m/s)
10-286	-1723	-37	16	11	-1614	-53	-2	12	-1506	-27	10	13	-1707	-54	1	18	-1419	-50	0	14
06-5	-1488	-39	10	11	-1593	-50	-7	16	-1513	-33	7	14	-1589	-53	-5	15	-1453	-54	-7	16
01-10	-1541	-40	10	11	-1676	-55	-9	15	-1481	-29	4	11	-1698	-48	-5	15	-1495	-49	-4	14
04-83	-1514	-42	9	11	-1647	-54	-6	14	-1336	-32	2	12	-1646	-53	-4	15	-1470	-50	-5	16
01-41	-1462	-36	17	10	-1698	-61	3	11	-1388	-27	8	12	-1726	-50	4	13	-1563	-55	3	12
06-90	-1529	-35	10	11	-1703	-60	13	9	-1491	-23	8	13	-1713	-50	14	10	-1604	-54	17	14
06-89	-1662	-34	11	11	-1592	-60	8	10	-1472	-24	7	13	-1700	-51	6	12	-1648	-50	6	11
07-236	-1526	-42	10	12	-1767	-58	6	11	-1488	-26	9	13	-1844	-49	7	12	-1531	-54	3	11
03-77	-1686	-37	16	11	-1709	-53	-1	13	-1522	-29	9	13	-1666	-49	0	14	-1513	-54	-6	15
06-215	-1617	-39	12	11	-1850	-57	-1	12	-1433	-29	5	14	-1775	-50	5	12	-1604	-55	3	12
06-219	-1564	-45	11	11	-1502	-62	2	11	-1562	-27	9	13	-1668	-56	10	10	-1519	-52	13	9
06-11	-1541	-33	15	11	-1593	-57	3	11	-1519	-29	9	13	-1745	-57	3	12	-1595	-57	-3	13
03-80	-1449	-47	11	11	-1767	-57	1	11	-1460	-28	8	12	-1775	-56	8	11	-1601	-59	7	10
Average	-1562	-39	12	11	-1670	-57	1	12	-1475	-28	7	13	-1712	-52	3	13	-1540	-53	2	13
Standard Deviation	82	4	3	0	90	3	6	2	58	3	2	1	62	3	6	2	67	3	7	2

CLUSTER 1

Table 41 - Slice Behavioural Results for Cluster 2

	Racket Label	Node Point				Impact Position 1				Impact Position 2				Impact Position 3				Impact Position 4			
		RS (RPM)	RPA (°)	ROA (°)	RRV (m/s)	RS (RPM)	RPA (°)	ROA (°)	RRV (m/s)	RS (RPM)	RPA (°)	ROA (°)	RRV (m/s)	RS (RPM)	RPA (°)	ROA (°)	RRV (m/s)	RS (RPM)	RPA (°)	ROA (°)	RRV (m/s)
CLUSTER 2	01-24	-1673	-54	-10	12	-1699	-52	8	10	-1394	-17	9	12	-1599	-48	9	12	-1619	-45	9	11
	03-79	-1738	-34	14	11	-1655	-51	7	11	-1552	-24	9	13	-1759	-49	6	11	-1516	-50	6	12
	01-9	-1481	-28	13	11	-1601	-50	14	9	-1674	-24	6	11	-1698	-45	8	11	-1661	-49	11	10
	01-15	-1536	-33	14	11	-1584	-56	15	9	-1514	-20	7	13	-1603	-48	16	10	-1671	-45	13	10
	06-223	-1598	-32	14	11	-1537	-55	12	9	-1469	-23	7	13	-1718	-44	12	10	-1559	-44	9	11
	06-210	-1550	-33	14	12	-1720	-58	6	13	-1497	-27	13	19	-1656	-43	12	11	-1548	-48	13	10
	07-237	-1663	-39	13	12	-1818	-59	3	11	-1619	-25	10	13	-1708	-46	13	11	-1569	-48	13	10
	Average	-1606	-36	10	11	-1659	-55	9	11	-1531	-23	9	14	-1677	-46	11	11	-1592	-47	11	11
	Standard Deviation	84	8	8	0	88	3	4	2	87	3	2	2	56	2	3	1	55	2	2	1

Table 42 - Slice Behavioural Results for Cluster 3

Racket Label	Node Point				Impact Position 1				Impact Position 2				Impact Position 3				Impact Position 4			
	RS (RPM)	RPA (°)	ROA (°)	RRV (m/s)	RS (RPM)	RPA (°)	ROA (°)	RRV (m/s)	RS (RPM)	RPA (°)	ROA (°)	RRV (m/s)	RS (RPM)	RPA (°)	ROA (°)	RRV (m/s)	RS (RPM)	RPA (°)	ROA (°)	RRV (m/s)
07-235	-1590	-39	14	11	-1681	-82	19	8	-1485	-24	8	13	-1620	-55	15	10	-1553	-61	17	8
09-274	-1504	-43	22	10	-1735	-65	13	9	-1490	-9	15	14	-1697	-63	21	9	-1509	-62	21	8
06-212	-1655	-38	17	11	-1721	-67	16	8	-1509	-22	9	13	-1719	-55	20	10	-1500	-55	18	8
07-238	-1583	-37	20	10	-1683	-70	16	8	-1446	-21	12	12	-1721	-55	22	9	-1695	-59	22	8
05-84	-1712	-31	14	11	-1882	-69	17	8	-1427	-18	7	13	-1733	-47	18	11	-1603	-60	16	9
07-228	-1469	-36	19	10	-1659	-67	14	8	-1407	-20	8	13	-1777	-55	19	9	-1540	-57	18	9
Average	-1586	-37	18	10	-1727	-70	16	8	-1461	-19	10	13	-1711	-55	19	10	-1567	-59	19	8
Standard Deviation	83	4	3	1	74	5	2	0	37	5	3	1	47	5	2	1	67	2	2	0

CLUSTER 3

Table 43 - Slice Behavioural Results for Cluster 4

Racket Label	Node Point				Impact Position 1				Impact Position 2				Impact Position 3				Impact Position 4			
	RS (RPM)	RPA (°)	ROA (°)	RRV (m/s)	RS (RPM)	RPA (°)	ROA (°)	RRV (m/s)	RS (RPM)	RPA (°)	ROA (°)	RRV (m/s)	RS (RPM)	RPA (°)	ROA (°)	RRV (m/s)	RS (RPM)	RPA (°)	ROA (°)	RRV (m/s)
07-216	-1680	-32	14	11	-1705	-62	16	8	-1618	-18	7	13	-1744	-48	18	9	-1479	-49	18	9
06-213	-1480	-31	15	10	-1703	-61	14	9	-1457	-21	9	13	-1632	-49	14	10	-1547	-51	13	10
06-100	-1800	-32	15	11	-1648	-59	16	9	-1712	-23	8	13	-1795	-47	14	10	-1596	-50	16	10
06.99	-1648	-30	15	11	-1669	-71	15	8	-1438	-17	7	13	-1704	-42	16	10	-1594	-49	14	9
07-240	-1734	-30	14	11	-1633	-68	13	8	-1587	-19	2	14	-1654	-44	9	12	-1552	-46	15	9
07-233	-1651	-35	15	12	-1734	-66	10	9	-1670	-26	6	15	-1733	-50	8	10	-1613	-47	10	10
07-239	-1544	-39	10	12	-1676	-66	16	9	-1545	-22	7	13	-1623	-50	12	10	-1542	-48	2	9
08-242	-1676	-40	19	10	-1805	-66	11	9	-1620	-23	8	13	-1708	-51	18	10	-1559	-55	15	9
01-8	-1575	-38	14	11	-1767	-65	10	9	-1582	-25	10	13	-1629	-51	13	10	-1548	-53	9	9
02-46	-1597	-43	11	10	-1566	-82	17	8	-1403	-16	7	13	-1643	-52	10	12	-1490	-54	3	10
09-247	-1616	-34	14	11	-1767	-63	14	9	-1533	-19	7	13	-1697	-54	16	9	-1612	-54	17	9
03-72	-1685	-35	16	11	-1572	-64	13	9	-1661	-22	7	13	-1805	-54	14	10	-1461	-51	9	10
06-225	-1660	-36	15	10	-1700	-64	14	9	-1514	-24	10	13	-1663	-52	9	11	-1516	-53	4	11
Average	-1642	-35	14	11	-1688	-66	14	9	-1564	-21	7	13	-1695	-50	13	10	-1547	-51	11	10
Standard Deviation	79	4	2	0	69	6	2	0	91	3	2	1	59	3	3	1	48	3	5	1

CLUSTER 4

F. Racket Properties of Each Cluster for Topspin Forehand

Cluster	Racket Label	Racket Mass (g)	Balance point (mm)	Head Length (mm)	Head Width (mm)	Strung Area (in^2)	Racket Length (mm)	Swingweight (RDC)	Twistweight (RDC)	Frame stiffness (RDC)
CLUSTER 1	07-216	277	329	335	245	100	685	269	10	68
	07-238	268	328	350	270	100	685	266	11	70
	07-235	255	347	330	250	100	685	258	10	74
	08-242	360	303	320	235	85	685	323	14	65
	07-233	312	320	330	250	100	685	286	14	62
	06-225	293	322	330	250	100	695	280	12	67
	03-72	309	345	320	250	97	690	283	10	71
	07-237	259	348	365	285	108	695	276	14	70
CLUSTER 2	03-77	274	340	330	250	100	700	287	9	66
	03-80	280	314	370	245	102	690	258	8	71
	06-210	319	312	330	255	100	700	301	12	69
	06-213	320	313	325	240	95	685	282	8	61
	01-10	252	360	370	270	115	710	298	10	78
	06-99	352	316	320	243	95	686	329	0	64
	05-84	298	328	325	240	98	682	299	9	63
	01-24	241	360	362	260	115	710	291	7	74
	03-79	268	360	360	260	117	700	307	7	68
	01-9	283	360	363	260	98	696	310	11	67
	09-274	330	310	315	230	93	685	295	11	61
CLUSTER 3	02-46	365	318	305	220	85	690	353	7	66
	06-11	338	320	325	232	98	705	339	12	60
	06-90	299	320	360	245	98	690	281	9	63
	07-228	309	305	330	240	98	685	270	10	62
	06-5	247	360	352	266	115	705	283	12	69
	01-41	335	310	330	255	100	700	291	3	71
	06-223	283	340	330	235	95	695	296	11	63
	04-83	234	380	395	280	135	725	294	20	73
	01-8	352	302	340	259	95	690	309	8	52
	10-286	260	357	340	264	107	695	291	14	72
	06-100	263	345	340	255	105	700	289	14	69
CLUSTER 4	06-215	286	333	335	245	100	690	289	12	69
	07-239	289	316	355	265	98	685	279	4	65
	07-236	300	315	325	260	100	690	268	12	65
	06-89	304	330	330	245	97	690	296	9	67
	07-240	308	320	345	265	95	685	298	10	61
	06-212	332	332	330	255	103	685	284	13	68
	09-247	330	310	315	230	93	685	295	15	61
	01-15	329	315	325	250	98	685	313	2	68
	06-219	244	353	370	275	124	695	256	12	66

G. Racket Properties of Each Cluster for Slice Forehand

Cluster	Racket Label	Racket Mass (g)	Balance point (mm)	Head Length (mm)	Head Width (mm)	Strung Area (in^2)	Racket Length (mm)	Swingw eight (RDC)	Twistw eight (RDC)	Frame stiffness (RDC)
CLUSTER 1	07-216	277	329	335	245	100	685	269	10	68
	06-213	320	313	325	240	95	685	282	8	61
	06-100	263	345	340	255	105	700	289	14	69
	06-99	352	316	338	268	90	686	329	1	64
	07-240	308	320	345	265	95	685	298	10	61
	07-233	312	320	330	250	100	685	286	14	62
	07-239	289	316	355	265	98	685	279	4	65
	08-242	360	303	320	235	85	685	323	14	65
	01-8	352	302	340	259	95	690	309	8	52
	02-46	365	318	305	220	85	690	353	7	66
	09-247	330	310	315	230	93	685	295	15	61
	03-72	309	345	320	250	97	690	283	10	71
	06-225	293	322	330	250	100	695	280	12	67
CLUSTER 2	07-235	255	347	330	250	100	685	258	10	74
	09-274	330	310	315	230	93	685	295	11	61
	06-212	332	332	330	255	103	685	284	13	68
	07-238	268	328	350	270	100	685	266	11	70
	05-84	298	328	325	240	98	682	299	9	63
	07-228	309	305	330	240	98	685	270	10	62
CLUSTER 3	01-24	241	360	362	260	115	710	291	7	74
	03-79	268	360	360	260	117	700	307	7	68
	01-9	283	360	363	260	98	696	310	11	67
	01-15	329	315	325	250	98	685	313	2	68
	06-223	283	340	330	235	95	695	296	11	63
	06-210	319	312	330	255	100	700	301	12	69
	07-237	259	348	365	285	108	695	276	14	70
CLUSTER 4	10-286	260	357	340	264	107	695	291	14	72
	06-5	247	360	352	266	115	705	283	12	69
	01-10	252	360	370	270	115	710	298	10	78
	04-83	234	380	395	280	135	725	294	20	73
	01-41	335	310	330	255	100	700	291	3	71
	06-90	299	320	360	245	98	690	281	9	63
	06-89	304	330	330	245	97	690	296	9	67
	07-236	300	315	325	260	100	690	268	12	65
	03-77	274	340	330	250	100	700	287	9	66
	06-215	286	333	335	245	100	690	289	12	69
	06-219	244	353	370	275	124	695	256	12	66
	06-11	338	320	325	232	98	705	339	12	60
	03-80	280	314	370	245	102	690	258	8	71